Probing the Role of Cell-Cell Interactions in Hepatic Ensembles

by

Amanda X. Chen

B.S., University of Rochester (2014)
M.Phil, University of Cambridge (2015)

Submitted to the Department of Biological Engineering
in partial fulfillment of the requirements for the degree of

Doctor of Philosophy in Biological Engineering

at the

MASSACHUSETTS INSTITUTE OF TECHNOLOGY

February 2021

Author .....
Department of Biological Engineering
January 5, 2021

Certified by .....
Sangeeta N. Bhatia, MD, PhD
John J. and Dorothy Wilson Professor of Health Science and Technology & Electrical Engineering and Computer Science, MIT
Thesis Supervisor

Certified by .....
Robert S. Langer
David H. Koch Institute Professor of Biological Engineering & Chemical Engineering, MIT
Thesis Supervisor

Accepted by .....
Katharina Ribbeck
Chair of the Graduate Program, Department of Biological Engineering, MIT

Probing the Role of Cell-Cell Interactions in Hepatic Ensembles

by

Amanda X. Chen

Submitted to the Department of Biological Engineering
on January 5, 2021, in partial fulfillment of the
requirements for the degree of
Doctor of Philosophy in Biological Engineering

Abstract

While organ transplantation is one of the greatest advances of modern medicine and provides immense therapeutic benefit to patients suffering from severe and fatal liver disease, donor tissue is scarce. Alternatives such as engineered cell-based therapies aim to restore tissue-specific functions of solid organs, but leave much to be desired. Key challenges hindering the translation of cell-based therapies relate to (1) cell sourcing, (2) graft scale-up, and (3) vascularization, all of which contribute to therapeutic performance.

The performance of an implantable graft is a function of the underlying cell-cell and cell-matrix interactions. These grafts typically consist of a multicellular ensemble in which combinations of epithelial, stromal, and immune cells give rise to physiologic function. Currently, precise, spatiotemporal control of these interactions is experimentally intractable. This thesis introduces a technique termed **CAMEO** (**C**ontrolled **A**poptosis in **M**ulticellular tissues for **E**ngineered **O**rganogenesis), in which we can non-invasively actuate the removal of a desired cell population from a pre-established multicellular ensemble. As an exemplar, we use CAMEO to study the contribution of supportive stromal cells to the phenotypic stability of primary human hepatocytes. 3D hepatic ensembles, in which stromal cells enhance phenotypic stability of spheroids, were found to rely only transiently on fibroblast interaction to support multiple axes of liver function, such as protein secretion and drug detoxification. Importantly, CAMEO revealed crucial cell-cell and cell-material interactions that occur in the first 24 hours of co-culture that drive the stabilization and enhancement of hepatic phenotype. Due to its modularity, we expect that CAMEO is extendable to other applications that are tied to the complexity of 3D tissues, including in vitro organoid models and in vivo integration of cell therapies. As such, we also employed CAMEO and our strategy of engineering-via-elimination in an implantable device containing both hepatic ensembles and engineered vasculature, and demonstrate our ability to engineer desired function and cell composition.

With an improved understanding of cell-cell interactions in vitro in hand, the next

step toward the clinic is to assess the performance of 3D hepatic ensembles in vivo. Here, we lay the groundwork for defining a final product lock for our hepatic cell therapies, and specifically explore the role of fibroblasts in in vivo integration, incorporate vasculature to meet the metabolic demands of scaled-up tissue grafts, and tune tissue microarchitecture to enhance engraftment, function, and persistence in vivo. Taken together, the efforts contained in this thesis represent a significant advance in tools and biology that enable clinical applications of tissue engineering and regenerative medicine.

Thesis Supervisor: Sangeeta N. Bhatia, MD, PhD
Title: John J. and Dorothy Wilson Professor of Health Science and Technology & Electrical Engineering and Computer Science, MIT

Thesis Supervisor: Robert S. Langer
Title: David H. Koch Institute Professor of Biological Engineering & Chemical Engineering, MIT

Acknowledgments

While the PhD dissertation is credited to me, it would be misguided to think that I prepared this body of work without consistent support and encouragement from dear friends, family, and colleagues. I made it here because many others paved the way for me, and encouraged me to keep trying when it was easier to give up or choose easier paths. I hope to showcase my gratitude for all of this effort by giving back to my scientific professional and academic communities, and hope to have a lasting impact through the development of new technologies in the healthcare, life science, and biotech spaces. In the following, I will highlight a select few that have been especially influential in my scientific journey (both before and during my tenure at MIT) – with the caveat that these mentions are by no means exhaustive.

To **Sangeeta.** There are too many things to thank you for. Thank you for cultivating a supportive lab environment and for helping me learn how to be more entrepreneurial and innovative in my thinking. The opportunities you bestowed upon me during my PhD taught me not just science, but also how to independently operate and run several interdisciplinary project teams. You believed in my ability to accomplish things far before I had the same confidence in myself – even if it took quite a lot of nudging and encouragement :) Without a doubt, I have evolved into a more rigorous scientist, a more adventurous thinker and doer, and a better human under your mentorship and guidance.

To **the real "dream team": LMRT admin.** How would our lab ever survive without all your efforts? We trainees are so spoiled to be under the care and mentorship of multiple superstars. **Heather**, our heroic lab director. In many ways, you were my lab "mom" and my "rock." The things that floated into my life during the PhD frequently derailed me, and I thank you many times over for always being there for putting me back on track. As you say, the PhD experience begets transformation like synaptic plasticity: in which the same starting cell material simply forms and reinforces useful pathways, and works around any barriers or inefficiencies. I now welcome challenges instead of balking at them. **Sue** - I already miss hanging out with you outside of Sangeeta's office before the Friday morning meetings. Thanks for always keeping things running smoothly, and for inviting us to your awesome rock concerts! One day I will also be cool enough to go to meditation retreats. To **Lian-Ee** - I have no idea how you handle it all! Thank you so much for keeping us all safe, compliant with EHS and DCM, and for making sure we always have all the supplies that we

need. These days, we all need a set of the "Life is Good" shirts that you so proudly sport on a daily basis. **Tarek** - even though I am not a "nano team" member, I always felt like I could reach out to you for support, and I cherish all the career-related advice that you shared with me! It was great to work together on some small projects for communication aspects of the Convergence Scholars program! Hope to keep in close touch with you all.

To **Bob, Katharina, and Alex**, my committee. When we formed the committee, it was meant to be a scientific sounding board. Which it was. But I also learned great tid-bits from each of you including: Bob's "I am 70 and I still am not sure what I am doing next with my life, so it's totally okay if you feel that way too," Katharina - for all your advice and care as my committee chair, and Alex especially for inspiring me with a god-like level of multi-tasking.

To **Chris and Jennifer**, my non-MIT scientific mentors. Thank you for creating and forming the 3D Organ Engineering space at the Wyss, and for encouraging us to dream of and pursue new avenues that continue to expand the capabilities of vascular engineering and 3D bioprinting.

To **Danielle and Michael**, from University of Rochester, which is the birthplace of "Amanda the Scientist." When I joined the lab during my sophomore year, I sort of knew what science was, but deinitely not what "research" was. In fact, **Danielle**, I called you Mrs. Benoit - not knowing that all professors have PhDs and are addressed as Prof/Dr. **Michael** - thank you for taking a chance on me as an undergrad. I made a lot of silly mistakes (including diluting solutions for cells with water... and lysing all my cells), yet you still encouraged me and helped me plan out my own independent research projects. You inspire me to challenge myself in multiple areas of life (not limited to science, but also including athletic feats).

To **Churchill, BSEG, and Whitaker**. I retroactively label this chapter of my life as the "social normalization phase," in which I learned I can do things besides go to lab and the library. I thank the W2 Boat Team (blades!), the members of the Winston Churchill Poker Group (spoons! JK, Lola Lo's), my housemates from Whittinghame, my labmates and peers at BSEG and CEB, and my co-fellows from the Whitaker International Fellows/Scholars program.

To **MIT**. These past five years have been a rollercoaster. They were hard, they were fun, but mostly they were hard. There are many to thank for preserving my sanity, including but not limited to: MIT Cycling Team (Em Chen - my "not" sister, Alex "hooked on" Klotz, Amy Ousterhout, Laura Treers), my MBB casing partners (Boyu Fan, Michael Kosowsky, Justin Berry, Eva Agapaki), the Johnny Harvard Poker Group ft. Harvard BBS, GSC HCA (Molly Bird, Shalini Gupta), my roommate (Ravi Kommajosyula - many fond memories of weekend runs around the Charles), 20.110 TA crew (especially Michael Birnbaum, who has been my sounding board past the end of our co-teaching days), BECL (Diana Chien, Prerna Bhargava), my students in HST.500 (who taught me a lot through their many R01 drafts, and tolerated our abrupt start to life on Zoom), and the 2015 BE PhD cohort (Isaac Rockafellow, Kyle Geiser, Beth Pearce, Noor Momin, Byong Kim, Erika DeBenedictis, Jared Kehe, Lauren Milling, Lauren Stopfer, Rob Wilson, Sheryl Wang, Charlie G. Rappazzo - I'm really only friends with you because of Lilly and Rory!, Amanda Facklam - Amanda dream team from taking class together...to teaching class together...to teaching me how to teach a class, Molly Bird - ever since we were zombies together during 1st year Halloween, Alex Triassi - especially for our genius branding with Qualified Match and being my running partner during thesis writing, Sarah Bening - my dear writing accountabili-buddy for the past and present and future).

To **Laszlo, Seda, and Robert**. I am so glad we met at the 2018 NIBR Hackathon. I would have never imagined that a 2-week program would bloom into a 2-year passion project exploring drug development and computational modeling. I look fondly at our many memories on the Rosenda chat, and am so proud that we had our work published in EBioMedicine. I am glad to have you all as mentors and role models.

To the 2020 "COVID class" of **Flagship Pioneering Fellows**, especially my dear friends Fuad and Lara. I am so glad to have experienced the summer with you all - it was a blessing against the backdrop of the ongoing pandemic. I wish us many more exciting years together of asking dogma-shattering "what if" questions - I know many of them will come to define the cutting edge of biotech in years to come.

To **Liver Bay, LMRT, and the CB Hep-Endo Team**. I am writing this section in short spurts as I clean out my samples and create an inventory for future trainees to use. Among the many fixed plates and frozen tubes, there is a lot of exciting science (even if they

were results we did not expect) and more importantly, the growth of deep friendships. I am happy to have spent my time in an interdisciplinary and translation-focused group - this challenged my mind to focus not just on the scientific perspective, but also constantly relate it to future impact. I am fortunate to have mentored two excellent undergraduate trainees, who each brought fresh perspectives to our lab: **Cydney** and **Emily**. I am proud that both are now at the beginnings of their respective PhD journeys. Liver Bay and Hep-Endo Team - we have traveled near (to nights in the microscope room or Ubers across town to each other's labs) and far (to conferences in other states) in our pursuit of building artificial livers. I find it difficult to capture all the scientific contributions of persons from these subgroups, and have attempted to detail this further in each Chapter of this dissertation. To close this section, I want to acknowledge **Greco**, my close collaborator and dear friend from Chris' lab. We first met at interview weekend of HST back in Spring of 2014, and I am lucky to have found myself on a project that led us to publish together! I'm sad you've moved away to NYC but I'll come visit soon! Lastly, to **Arnav**, otherwise better-described as my AC^2 counterpart). From our initial "meet" on GradCafe in 2013, to our official start as colleagues in 2015 (characterized by our constant flinging of ideas via paracrine communication channels, incl. iMessage, WhatsApp, Facebook Messenger, SnapChat, GChat, Instagram DMs, Signal, FaceTime, and recently, Zoom – and we're halfway to figuring out ESP), to enjoyment of tacos in Seaport or noods from Dakzen and 9Zaab. Honored to be Minister Chen in your backyard pandemic wedding and overly excited to continue to tackle society's challenges together.

To **Mom, Dad, and Eric**. Thank you for putting up with me and my ridiculous antics, especially during last 5 years of my PhD. Thank you for always reminding me to sleep and take care of myself. While we may not connect much on the experimental day-to-day of my life, the way I approach my work and personal connections are fueled by values you taught me as I was growing up: to be compassionate and kind, to be committed and excellent, and to chase my passions and curiosities. Thank you for giving me the foundation to go out into the world to try and do great things. Even though I've lived now ten years away from our our home in California, it is not easy to be far, and I am comforted that you are always just a text or phone call away. Thank you for sending me coffee and food and lots of cute pictures and Memoji recordings, especially while I was writing my dissertation. It continues to surprise me how you always seem to know exactly what I need (true ESP). I love you all and hope we can celebrate in person sometime soon.

Lastly, to myself and anyone else who is or was crippled by perfectionism: here's the most important thing I learned during my PhD:

"I wanted the answer, there is no answer"

- Chidi Anagonye, "The Good Place"

Thesis Committee Members

Katharina Ribbeck, PhD (Thesis Chair)

Hyman Career Development Professor, Biological Engineering

Massachusetts Institute of Technology

Sangeeta N. Bhatia, MD, PhD (Thesis Co-Supervisor)

John J. and Dorothy Wilson Professor, Electrical Engineering & Computer Science and Institute for Medical Engineering & Science

Massachusetts Institute of Technology

Robert S. Langer, PhD (Thesis Co-Supervisor)

David H. Koch (1962) Institute Professor, Biological Engineering and Chemical Engineering

Massachusetts Institute of Technology

Alex K. Shalek, PhD

Pfizer-Laubach Career Development Associate Professor, Chemistry and the Institute of Medical Engineering & Science

Massachusetts Institute of Technology

Contributions to the Field

**denotes first author or co-first author*

Primary Literature

1. **Amanda X Chen***, Arnav Chhabra, Hyun-Ho Greco Song, Heather E Fleming, Christopher S Chen, Sangeeta N Bhatia. "Controlled Apoptosis of Stromal Cells to Engineer Human Microlivers," ***Advanced Functional Materials*** (2020): 1910442.

Selected for Inside Front Cover

2. Robert Ietswaart*, Seda Arat*, **Amanda X Chen***, Saman Farahmand, Bumjun Kim, William DuMouchel, Duncan Armstrong, Alexander Fekete, Jeffrey J Sutherland, Laszlo Urban. "Machine Learning Guided Association of Adverse Drug Reactions with in vitro Target-Based Pharmacology," ***EBioMedicine*** (2020): 57: 102837.

2. Hyun-Ho Greco Song*, Alex Lammers, Subramanian Sundaram, Logan Rubio, **Amanda X. Chen**, Linqing Li, Jeroen Eyckmans, Sangeeta N Bhatia, Christopher S Chen. "Transient Support from Fibroblasts is Sufficient to Drive Functional Vascularization in Engineered Tissues." ***Advanced Functional Materials*** (2020): 2003777.

4. Kelly R Stevens*, Margaret A Scull, Vyas Ramanan, Chelsea L Fortin, Ritika R Chaturvedi, Kristin A Knouse, Jing W Xiao, Canny Fung, Teodelinda Mirabella, **Amanda X Chen**, Margaret G McCue, Michael T Yang, Heather E Fleming, Kwanghun Chung, Ype P De Jong, Christopher S Chen, Charles M Rice, Sangeeta N Bhatia. "In Situ Expansion of Engineered Human Liver Tissue in a Mouse Model of Chronic Liver Disease," ***Science Translational Medicine*** (2017): 9(399): eaah5505.

5. Lisa R Volpatti*, Alexander J Hanson, Jennifer M Schall, Jesse Dunietz, **Amanda X Chen**, Rohan Chitnis, Eric J Alm, Alison F Takemura, Diana M Chien, "Evaluating Peer Coaching in an Engineering Communication Lab: a Quantitative Assessment of Students' Revision Processes," ***American Society for Engineering Education*** (2020).

6. Carmen Unzu*, **Amanda X Chen***, Liliana Mancio Silva, Eric Zinn, Yanhe Wen, Cindy Zhu, Allegra Fieldsend, Julio Sanmiguel, Beatrice Bissig-Choisat, Karl-Dimiter Bissig, Ian Alexander, Sangeeta N Bhatia, Luk H Vandenberghe, "NGS-Based Multiplexed AAV Library Screening to Characterize Human Preclinical Liver Models," **In Preparation**.

Patents

1. Christopher Chen, Sangeeta Bhatia, Arnav Chhabra, **Amanda Chen**, Hyun-Ho Song. Tissue Fabrication By Selective Deletion Within a Multicellular Construct. U.S. Patent Application No. 16/953,002.

Secondary Literature

1. **Amanda X Chen***, Arnav Chhabra*, Heather E Fleming, Sangeeta N Bhatia, "Hepatic Tissue Engineering," in **Principles of Tissue Engineering**, Robert Lanza, Robert Langer, Jay Vacanti, Anthony Atala (eds.), Elsevier pp. 738-753. ISBN: 978-0-1282-1401-5 (2020).

2. Tiffany N Vo*, **Amanda X Chen**, Quinton B Smith, Arnav Chhabra, Sangeeta N Bhatia, "Integrated Technology for Liver Tissue Engineering," in **The Liver: Biology and Pathobiology**, Irwin M Arias, Harvey J Alter, James L Boyer, David E Cohen, David A Shafritz, Snorri S Thorgeirsson, Allan W Wolkoff (eds), John Wiley & Sons Ltd, pp. 1028-1035. ISBN: 978-1-1194-3682-9 (2020)

3. Arnav Chhabra*, **Amanda X Chen***, Keval N Vyas, Christopher S Chen, Sangeeta N Bhatia, "Satellite Cell Transplantation," **In Preparation**.

Selected Oral Presentations

1. **Amanda X Chen*** et al. "New Tools for Stabilizing Functional Hepatic Phenotype in Tissue Engineered Microlivers for Cell-Based Liver Therapies." **Gordon Research Seminar & Gordon Research Conference**, Andover: Signal Transduction in Engineering Extracellular Matrices, New Hampshire, July 22, 2018

Gordon Research Seminar Discussion Leader

2. **Amanda X Chen*** et al. "A 'Suicide Switch' to Improve Models of Human Tissue Engineered Microlivers." **Biomedical Engineering Society Annual Meeting**, Atlanta, Georgia, October 19, 2018.

3. **Amanda X Chen***, Sebastien GM Uzel* et al. "Liver Engineering via Programmable Multicellular Control and Assembly." **Wyss Institute 11th Annual Retreat**, Boston, Massachusetts, November 22, 2019.

4. **Amanda X Chen*** & Sangeeta N Bhatia. "Engineering Tissues via Elimination: Tales of the Liver." **Virtual Seminars in Biomedical Science**, Virtual, September 10, 2020.

Invited Speaker

5. **Amanda X Chen*** et al. "Controlled Apoptosis of Stromal Cells to Engineer Human Microlivers." **Biomedical Engineering Society Annual Meeting**, Virtual, October 14, 2020.

Contents

List of Figures

List of Tables

Chapter 1

INTRODUCTION

1.1 Challenges in Organ Transplantation

Organ and tissue transplantation is one of the great advances of modern medicine and can save the lives of patients affected by terminal organ failure. Progress over the past few decades reflects advancements not only with surgical techniques and protocols that control graft rejection but also in policies for organ allocation and distribution (**Figure 1-1**). However, the growing demand for organ transplants is unlikely to be met without disruptive technologies that more drastically expand the donor pool. In this dissertation, we present work that contributes to the development of cell-based therapies as an alternative to donor transplantation, and specifically focus on cell-based therapies that are designed for heterotopic transplantation sites. These sites not only decouple the implant from the diseased microenvironment, but also provide highly vascularized beds for improved engraftment and integration. As these implants are remotely located (relative to the orthotopic site) yet share a common goal with the parent organ, we refer to them as **satellite cell therapies**. Additionally, satellite cell therapies support bidirectional interactions with the host organ as well as other tissue compartments, and thus pose an interesting opportunity for precision engineering to control the underlying interactome and biology. Broadly, beyond expansion of the transplantable graft pool in countries that support a high capacity of organ donation (such as the United States and Spain), we also envision that satellite cell therapies may compensate for extremely low donor rates in countries such as China, Japan, and Israel, where legal, cultural, financial, and/or religious barriers prohibit direct transplantation.

In this dissertation, we will first discuss the history and current clinical status for transplantation of solid organs, and then focus specifically on the liver as an exemplar. We will overview the current state of liver therapies in the clinic, and review in vitro and in vivo models that have been and will be useful for the development of cell-based therapies to address serious liver disease. We will then discuss components that may comprise a cell-based therapy, including cells and extracellular matrix, which are known to drive phenotypic stability of the parenchyma, as well as the formation of functional structures such as the vasculature and biliary network. Lastly, we will discuss overarching design criteria for such satellite cell therapies, including considerations for various anatomic sites for transplantation and readouts that are compatible with non-invasive assessment of liver-specific function. Lastly, we will close the introduction with a brief overview of the scope of the work contained in this thesis.

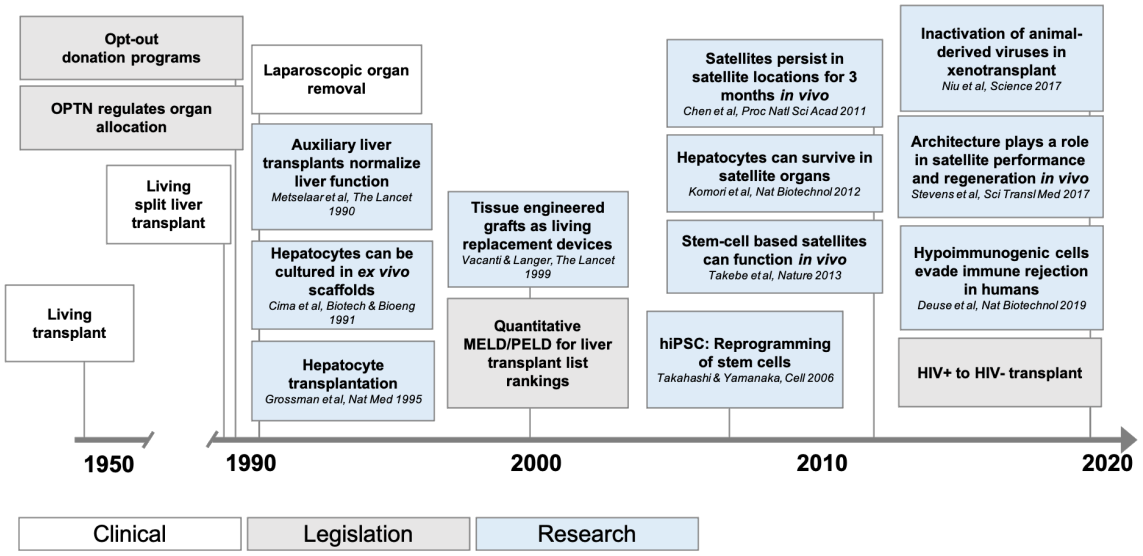

Figure 1-1: **Timeline of milestones in organ transplantation and engineered tissue therapies.** Advances in surgical techniques and immunosuppression have enabled transplantation of full and split organs (white). Bioethics-driven paradigms for organ allocation and distribution as well as advances in management of viral infection have greatly impacted the ability to fairly allocate donor organs for patients in need (grey). Seminal works in cell therapy and regenerative medicine lay the groundwork for satellite cell-based therapies (blue). Content adapted from work in preparation. Featured references: [179, 48, 93, 289, 264, 40, 141, 266, 198, 256, 56].

1.1.1 Past Advances in Transplantation

Currently, there are approximately 111,400 patients on the waitlist for organ transplants, with the vast majority of candidates waiting for a kidney (94,900), liver (12,500), heart (3,500), simultaneous kidney-pancreas (1,700) or lung (1,200) transplants in the US [196]. While efforts coordinated by UNOS have steadily improved transplant numbers over the years (in 2019, 23,402 kidney, 8,896 liver, 3,552 heart, 872 simultaneous kidney-pancreas, 2,714 lung transplants), an increased demand for donor organs and tissues continues to grow as a result of the declining health status of the general population. The ongoing obesity and diabetes epidemics increase the need for kidney and liver transplants, which represent the two most needed organ pools.

In the past, improvements to the clinical impact of organ transplantation have primarily been driven by refinement of surgical technique and organ preservation/transportation, formalization of organ procurement of distribution, improvement to technology for preservation and transportation of harvested organs, and development of pharmacologics and biologics for controlling transplant rejection. Formally, policies and frameworks that ensure the equitable procurement and distribution of organs are regulated by the Organ Procurement and Transplantation Network (OPTN). Importantly, these efforts and advances have optimized usage of a limited donor pool. We envision that these principles and frameworks, discussed in detail below, can also be used as a framework for fair distribution of engineered cellular therapies.

1.1.2 Surgical Techniques and Biopreservation

Techniques established for other surgical procedures formed the basis of methodologies for surgical implantation of organ transplants. Through attempts both in animals and the first transplants in humans, methods were refined to enable multi-organ retrieval from living and deceased donors that reduced ischemic injury and subsequent graft damage, which are reviewed in depth elsewhere [25]. Notably, liver transplants are particularly challenging, requiring careful handling of the vascular and biliary networks for successful anastomosis. Harvest from living donors is expectedly more challenging, and is associated with premature graft loss [74] but improved by using less invasive techniques such as laparoscopic retrieval of the kidney. In tandem, protocols to ensure the quality of donor grafts were developed to en-

able preservation and transport before transplantation, and are reviewed in depth elsewhere [96]. The understanding of biopreservation continues to evolve over time, as illustrated by the recent clinical validation of normothermic machine perfusion of liver transplants as a superior preservation method over the prior standard of static cold storage [121]).

1.1.3 Transplant Allocation and Distribution

Allocation of organs in a fair, ethical way that is immune to political and socioeconomic overtones is essential for fair allocation and reduction of both waitlist and post-transplant mortality. While living donors are most likely to agree to a direct donation to a relative, new strategies that enable paired exchange and domino chains have increased the occurence of donations that would otherwise be impossible due to donor-recipient incompatibility [186].

Identification of ideal organ recipients requires an organ-specific approach. For the liver, the evidence-based MELD/PELD (Model for End-Stage Liver Disease / Pediatric End-Stage Liver Disease) score, which is based on lab tests and adjustments based on clinical data, has been shown to successfully predict pre-transplant mortality, though the diverse etiologies of end stage liver disease constitute a challenge for rare diseases [167, 298]. For the kidney, the KDPI (Kidney Donor Profile Index) multivariate model reflecting both clinical biomarkers and patient demographics is used to determine kidney allocation [218].

Recently, there have been instances of transplants using expanded criteria donors, including organs that test positive for viral pathogens such as HIV, hepatitis B and hepatitis C [29]. A more refined framework for stratifying the quality of grafts to ensure optimal donor-recipient matching will be required as the donor pool continues to expand via these avenues.

1.1.4 Immunosuppression

Immunocompatibility for allogeneic and xenogeneic grafts constitutes a major challenge in organ transplantation. Donor-recipient compatibility to screen for acute rejection of a graft in part can be addressed by established tests for serotyping, tissue typing, and cross matching. Besides autologous grafts, all transplants currently require maintenance with immunosuppressant drugs. Broadly, immunosuppressive drug regimens have been designed to inhibit both proliferative and cytotoxic effects of the innate and humoral arms of the

immune system, and have been reviewed in depth elsewhere [47]. Notably, the discovery of the immunophilin binding agent, cyclosporin, was critical to the inception of the field of transplantation. However, the use of systemic immunosuppressants for life-long maintenance of donor grafts also puts the recipient at risk for opportunistic infection, dysregulated metabolism, and emergence of neoplasms (e.g. from reduced immunosurveillance, transfer of malignant cells, infection with oncogenic viruses) [47]. Current research efforts focus on approaches to enable local immunosuppression or create universally tolerated grafts via precision engineering [102, 85, 279, 222, 56]. As an example, operational tolerance and donor-specific unresponsiveness has been achieved preclinically with T regulatory cells, as well as simultaneous bone marrow transplant for kidney graft recipients [250]. For cell therapies that use allo- and/or xeno- cell sources, such developments in local immunosuppression are directly relevant and useful.

Taken together, the described innovations for utilizing a limited donor pool have positively impacted the clinical reach of transplantation, and will synergize robustly with incoming engineered cell therapies, which have the potential to directly can address the supply shortage.

1.2 Liver Disease Burden

In this body of work, we focus specifically on the liver as an example of a metabolic, solid organ with a large, unaddressed disease burden. Fatal liver disease accounts for approximately 2 million deaths annually worldwide and has steadily increasing rates over the years [184]. Liver failure can be divided into three major categories: a) acute liver failure (ALF), which presents as a rapid loss of liver function in patients without pre-existing liver disease, b) chronic liver disease due to metabolic dysfunction, and c) chronic liver failure accompanied by tissue remodeling and scarring.

ALF is a rare syndrome with an annual incidence of less than 10 cases per million people in the developed world. In the United States, approximately 2,000 cases of ALF are diagnosed each year [192]. It commonly develops in healthy adults in their 30s. Patients with ALF usually present with abnormal liver biochemistry, coagulopathy and encephalopathy. The causes vary geographically. Damage due to drug exposure (e.g. acetaminophen) is the most common cause in the West, while in large parts of the East, viruses (e.g. Hepatitis A

and E) are the most prominent cause of ALF [3]. Clinically, ALF can be subdivided based on the period of time between the appearance of jaundice and onset of hepatic encephalopathy. Data from O'Grady et al. proposed the following classification: hyperacute for periods between 0 and 7 days, acute for periods between 7 and 28 days and subacute for periods between 4 and 12 weeks [203]. In hyperacute cases, the cause is usually acetaminophen toxicity or viral infection. Subacute cases that evolve slowly often result from idiosyncratic drug-induced liver injury. Even though patients with a subacute presentation have less coagulopathy and encephalopathy, paradoxically they have a consistently worse medical outcome than those with a more rapid onset of the disease [17].

Chronic liver disease develops on the background of a constant injurious insult, either resulting from a metabolic disorder or a number of etiologies that lead to widespread tissue remodeling and pathologic deposition of extracellular matrix. Inborn liver-based errors of metabolism are life-threatening conditions caused by genetic defects in single enzymes or transporters and lead to blockade of a specific metabolic pathway. While they can be accompanied by progressive fibrosis and cirrhosis, such as in the case of α 1-antitrypsin ZZ deficiency, hemochromatosis, Wilson's disease and hereditary tyrosinemia [20], the liver parenchyma often remains intact. Some examples of metabolic disorders with an intact parenchyma include hypercholesterolemia, Crigler-Najjar syndrome, ornithine carbamylase deficiency, organic aciduria and hyperoxaluria [243]. In a biopsy, the lack of parenchymal destruction often leads to a delayed diagnosis, exposing the patient to sequelae. In all cases of liver disease, the lack of FDA-approved non-invasive biomarkers makes it challenging to diagnose and treat liver diseases.

Chronic liver disease occurs in the setting of non-alcoholic fatty liver disease (NAFLD). NAFLD is marked by hepatic steatosis and is related to the presence of metabolic syndrome in association with obesity, diabetes and/or arterial hypertension [63]. A subset of NAFLD patients will develop signs of non-alcoholic steatohepatitis (NASH), a more severe condition associated with lobular inflammation and hepatocellular ballooning, and can lead to fibrosis and cirrhosis [73]. In NAFLD, the liver is unable to utilize carbohydrates and fatty acids properly, leading to toxic over-accumulation of lipid species. These metabolites induce cellular stress, injury and death, which predisposes the liver to sequelae such as cirrhosis and hepatocellular carcinoma [43].

In the United States, the number of NAFLD cases is projected to expand from 83.1

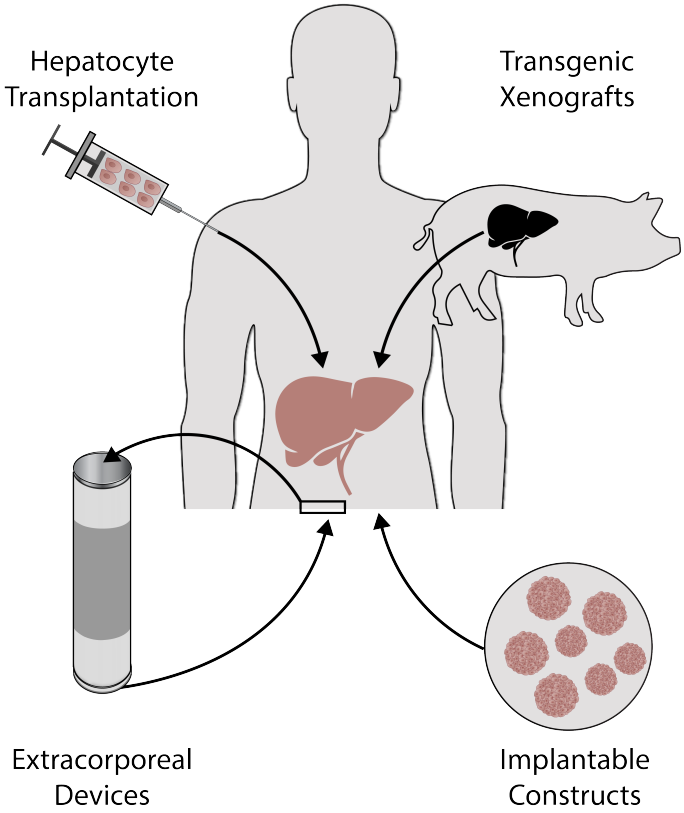

Figure 1-2: **Cell-based therapies for liver disease.** A variety of cell-based therapies have been designed to address liver disease. Hepatocytes can be transplanted directly or implanted as implantable constructs. Extracorporeal devices perfuse a patient's blood or plasma through bioreactors. Genetically modified large animals can be used for xenotranplantation. Adapted from [146].

million in 2015 (26% of the population) to 100.9 million by 2030 (28% of the population) [70]. An increasing percentage of these cases is projected to be classified as NASH, rising from 20% to 27% of adults with NAFLD during this interval [70]. While diagnosing NASH at an early stage remains a challenge, multiplexed protease-activated nanosensors have demonstrated utility in monitoring NASH progression and treatment response in a 3,5-diethylcarbonyl-1,4-dihydrocollidine (DDC) model of fibrosis in mice. With further development, these non-invasive readouts can be used to diagnose disease.

1.3 Current State of Liver Therapies

In order to mitigate the clinical burden of liver disease, several therapeutic strategies have been undertaken (**Figure 1-2**).

1.3.1 Extracorporeal Liver Support Devices

Liver failure is associated with abnormal accumulation of numerous endogenous substances such as bilirubin, ammonia, free fatty acids and proinflammatory cytokines [36]. Extracorporeal liver support devices have been developed to detoxify the blood and plasma in order to bridge patients to liver transplantation or allow the native liver to recover from injury. Artificial liver (AL) devices use non-living components for detoxification, such as membrane separation or sorbents to selectively remove toxins, but have limited clinical use because they do not replace the synthetic and metabolic roles of the liver [36]. Bioartificial liver (BAL) devices, on the other hand, contain a cell-housing bioreactor that aims to provide the detoxification and synthetic functions of the liver and are an ongoing topic of clinical investigation. Current versions are either based on hollow fiber cartridges [69, 51, 226] or on perfused three-dimensional (3D) matrices [290]. BALs, just like other hepatocyte-based therapies, face many challenges, such as the lack of readily available functional cell sources and the loss of cell viability and phenotype during the treatment process.

1.3.2 Biopharmaceuticals

In the setting of acute liver failure, N-Acetyl Cysteine (NAC) is FDA-approved to reduce the extent of liver injury after acetaminophen overdose [166]. In the setting of chronic liver disease, however, most of the FDA-approved therapies are for Hepatitis A, B and C. A detailed listing can be found in **Table 1.1**.

Table 1.1: FDA-Approved Therapies for Liver Disease

Drug Name	**Year Approved**	**Indication(s)**	**Mechanism**

Heplisav-B	2017	Hepatitis B	Combines hepatitis B surface antigen with a proprietary Toll-like Receptor 9 agonist to enhance the immune response
Mavyret	2017	HCV genotype 1-6	Fixed-dose combination of glecaprevir, a hepatitis C virus (HCV) NS3/4A protease inhibitor, and pibrentasvir, an HCV NS5A inhibitor
Vosevi	2017	Hepatitis C	Fixed-dose combination of sofosbuvir, a hepatitis C virus (HCV) nucleotide analog NS5B polymerase inhibitor, velpatasvir, an HCV NS5A inhibitor, and voxilaprevir, an HCV NS3/4A protease inhibitor
Ocaliva	2016	Primary biliary cholangitis	Farnesoid X receptor (FXR) agonist
Zepatier	2016	HCV genotype 1 or 4	Fixed-dose combination product containing elbasvir, a hepatitis C virus (HCV) NS5A inhibitor, and grazoprevir, an HCV NS3/4A protease inhibitor
Cholbam	2015	Bile acid synthesis and peroxisomal disorders	Primary bile acid synthesized from cholesterol in the liver

Daklinza	2015	HCV genotype 3	Inhibitor of NS5A, a nonstructural protein encoded by HCV
Technivie	2015	HCV genotype 4	Fixed-dose combination of ombitasvir, a hepatitis C virus NS5A inhibitor, paritaprevir, a hepatitis C virus NS3/4A protease inhibitor, and ritonavir, a CYP3A inhibitor
Olysio	2013	Hepatitis C	Small molecule orally active inhibitor of the NS3/4A protease of hepatitis C virus
Sovaldi	2013	Hepatitis C	Inhibitor of the HCV NS5B RNA-dependent RNA polymerase
Incivek	2011	HCV genotype 1	Inhibitor of the HCV NS3/4A serine protease
Victrelis	2011	HCV genotype 1	Inhibitor of the hepatitis C virus non-structural protein 3 (NS3) serine protease
Viread	2008	Hepatitis B	Oral nucleotide analogue DNA polymerase inhibitor
Tyzeka	2006	Hepatitis B	Inhibitor of HBV DNA polymerase
Baraclude	2005	Chronic hepatitis B with evidence of active viral replication	Small-molecule guanosine nucleoside analog with selective activity against hepatitis B virus (HBV) polymerase

Hepsera	2002	Chronic hepatitis B with evidence of active viral replication	Inhibitor of HBV DNA polymerase
Pegasys	2002	Chronic hepatitis C with compensated liver disease	Binds to and activates human type 1 interferon receptors
Peg-intron	2001	Chronic Hepatitis C	Binds to and activates human type 1 interferon receptors
Ribavarin	2001	Chronic Hepatitis C	Synthetic nucleoside analog with antiviral activity
Twinrix	2001	Hepatitis A and B	Recombinant vaccine

While a few treatments have shown moderate efficacy, there are currently no biopharmaceuticals that are approved for NAFLD, NASH or cirrhosis. Glitazones, for example, upregulate adiponectin, an adipokine with anti-steatogenic and insulin-sensitizing properties [225]. Vitamin E, an antioxidant, can prevent liver injury by blocking apoptotic pathways and protecting against oxidative stress [225]. Despite clinical studies of a large number of therapeutic candidates, no single agent or combination has shown improvement to liver-related morbidity and mortality in patients with NASH. Until a drug is FDA-approved for NASH indications, lifestyle modifications and optimizing metabolic risk factors are the best medical treatment options for these patients.

1.3.3 Liver Transplantation

The first attempt at human liver transplantation took place at the University of Colorado on March 1, 1963 but turned out to be unsuccessful [254]. Based on the pioneering work of Thomas Starzl, the first extended survival of a human recipient after liver transplantation

(LT) was achieved on July 23, 1967 with a 19-month-old female patient with hepatocellular carcinoma who survived 13 months before succumbing to metastatic disease [253]. After the initial success of the surgery, advancements were made to improve donor organ quality, recipient selection, operative and perioperative management, immunosuppression and infectious complications. These advancements have made orthotopic liver transplantation the primary treatment for end-stage liver disease and certain cancers. These transplants have 1-year patient survival rates over 80% [306]. However, many challenges remain, including donor organ shortages, recipients with more advanced disease at transplant, a growing need for re-transplantation, and adverse effects associated with long-term immunosuppression. To overcome a growing imbalance between the supply and demand of donor livers, transplant centers have developed strategies to expand the donor pool. These strategies include live donor liver transplantation [72], split-liver transplantation [33], and extended criteria for donor livers [274]. Despite all these efforts, the number of liver transplants has not increased in the last decade.

An alternative to human liver transplantation is xenotransplantation, though it has been clinically intractable due to concerns about immunological rejection and zoonotic pathogen transfer. With the advent of accessible genetic engineering technologies to circumvent the aforementioned challenges, the breeding efficiency of animals can be leveraged to mass-produce tissue for human organ transplants. Niu et al. applied CRISPR-Cas9 to inactivate all 62 copies of porcine endogenous retroviruses, thus paving the way for pig-to-human transplants [198]. Relatedly, Längin et al. genetically engineered porcine heart xenografts and demonstrated long-term pig-to-baboon orthotopic transplantation [145].

1.3.4 Hepatocyte Transplantation

Given the several drawbacks of LTs, alternative strategies have been pursued. A potential alternative to liver transplantation is allogeneic hepatocyte transplantation (HT). Transplanted cells can provide the missing or impaired hepatic function once engrafted. Given their synthetic and metabolic capabilities, mature hepatocytes are the primary candidates for liver cell transplantations. HT offers several advantages over LT. It is less invasive and can be performed repeatedly to meet metabolic requirements. Furthermore, multiple patients can be treated with a single dissociated donor tissue, and harvested cells can be

cryopreserved for later use on an as-needed basis.

The first experimental attempt of HT was done in 1976 to treat an animal model for Crigler-Najjar syndrome type I [175]. Along with other observations, it led to the first transplant of autologous hepatocytes in 10 patients with liver cirrhosis in 1992 in Japan [181]. Since then, reports have been published on more than 100 patients with liver disease treated by HT worldwide [77]. Human HT has resulted in partial correction of a number of liver diseases including urea cycle disorders [108], factor VII deficiency [58], glycogen storage disease type 1 [191], infantile Refsum's disease [244], phenylketonuria [59], severe infantile oxalosis [13] and acute liver failure [22]. HT faces several limitations: limited supply of high quality mature hepatocytes, freeze-thaw damage due to cryopreservation, poor cellular engraftment (estimated to be from 0.1 to 0.3% of host liver mass in mice after infusion of 3 - 5% of the total recipient liver cells) [77] and allogeneic rejection.

Clinically, the most widely used administration route for HT is through the portal vein or one of its branches. Hepatocytes traverse the sinusoidal vasculature and create transient occlusions. The occlusions lead to vascular permeabilization which allows transplanted cells to reach the liver parenchyma [59]. The number of cells that are injected intraportally and subsequently engraft is a function of portal pressure and liver architecture. Thus, other administration routes have been explored for patients with cirrhosis who have high portal pressures due to fibrosis.

In animal studies, hepatocytes transplanted into the spleen proliferate for extended periods of time and display normal hepatic function. The spleen has been shown to be well-suited for hepatocyte engraftment because it functions as a vascular filter and provides an immediate blood supply [77]. The peritoneal cavity represents an attractive administration route as it is easily accessible and can house a large number of cells. Due to cell number requirements associated with metabolic compensation, it has been used in patients with acute liver failure [262]. As an alternative to the portal vein, spleen and peritoneum, the lymph node (LN) has also been shown to demonstrate engraftment of donor hepatocytes [107, 141]. While this strategy has not been utilized in the clinic yet, the preclinical data is promising.

1.3.5 Current Clinical Trials

Several pathways have been implicated in the biology and pathogenesis of NAFLD development: insulin resistance, lipotoxicity, oxidative stress, altered immune/cytokine/mitochondrial functioning, and apoptosis. New therapeutic modalities are being developed to target many of these pathways. For a detailed overview of NAFLD-targeted drugs that are currently in the clinical trial pipeline, please refer to Younossi et al. [304].

1.4 In Vitro Models of the Liver

To build high-fidelity cellular models and therapies, components of the native liver microenvironment must be incorporated (**Figure 1-3**). The liver's highly organized structure is key to its role as a complex tissue supporting myriad synthetic and metabolic functions. In addition to hepatocytes, the main parenchyma of the liver, there are several non-parenchymal cell types such as liver sinusoidal endothelial cells (LSECs), Kupffer cells, cholangiocytes and stellate cells. In each lobule of the liver, an array of parallel hepatocyte cords are sandwiched between the sinusoid, carrying circulating blood, and the bile duct, carrying hepatocyte-secreted bile acids. Notably, this arrangement dictates a unique set of architecturally-driven cell-cell and cell-matrix cues, which give rise to liver-specific phenotypes. Gradients of physicochemical stimuli along the sinusoid drive zonal phenotypes with disparate metabolic and synthetic functional profiles [82]. Interrupting the natural order of cell arrangement in the liver is directly connected with diseases discussed in **Section 1.2**. In this book chapter we will primarily focus on human platforms, which are biologically distinct from animal-derived cell models of the liver that are reviewed more in depth elsewhere [84].

1.4.1 Two-Dimensional Liver Culture

Hepatocytes are responsible for more than 500 metabolic and synthetic functions of the human body, often categorized broadly as protein synthesis and secretion, detoxification, bile synthesis and nitrogen metabolism. Primary hepatocytes quickly lose their phenotype and function after a few days in traditional monolayer culture and require a collagen-coated surface for adherence and survival [20]. In contrast, when primary human hepatocytes are cultured between two layers of collagen gel (i.e. sandwich culture configuration), they retain

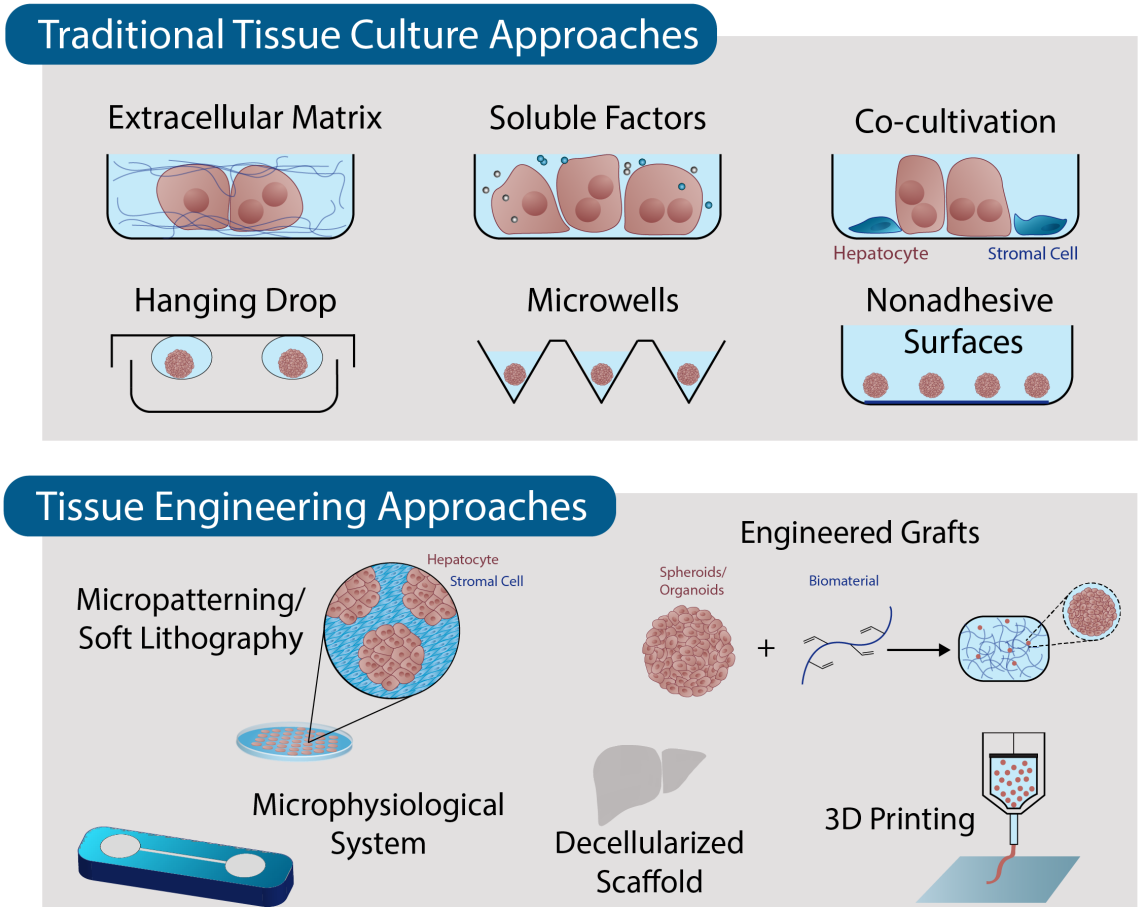

Figure 1-3: **Advances in hepatic tissue engineering.** Traditional tissue culture approaches such as addition of extracellular matrix, soluble factors, co-cultivation with supporting cell types, hanging drop, microwell molding, and non-adhesive surfaces have enabled the early study of hepatocyte phenotype in vitro in both 2D and 3D cultures. The advent of technologies from disciplines such as chemical engineering and electrical engineering has led to a new level of control for hepatic tissue cultures, such as micropatterning to template cell interactions, microphysiological systems to study the impact of bioactive perfusate, polymeric biomaterials for constructing 3D cell-laden grafts, perfusion technologies for decellularization/recellularization strategies, and 3D printing for scalable engineering of cellular grafts. Adapted from [146].

viability, polarity and many axes of relevant metabolic and synthetic function [263, 67]. Guguen-Guillouzo et al. found that a random co-culture with a liver epithelial cell line was sufficient to support hepatic albumin secretion, suggesting the importance of heterotypic cell interactions for long-term ex vivo culture [94]. Bale et al. demonstrated that other non-parenchymal liver cells can better recapitulate hepatic response to inflammatory stimuli, through higher-order intercellular interactions captured in a multicellular platform [8]. It

was later discovered that a micropatterned architecture consisting of hepatocyte-filled islands surrounded by a non-biomimetic cell type, mouse fibroblasts, can also stabilize hepatocytes, suggesting the existence of conserved co-culture signals across species. These micropatterned co-cultures (MPCCs) enable the study of drug-induced liver injury (DILI) and hepatotropic pathogen infection for several weeks in vitro [170, 129, 128]. Furthermore, Davidson et al. added hepatic stellate cells to the traditional MPCC to create an in vitro model of NASH [52].

Despite the utility of 2D hepatic cultures in screening assays, a wealth of literature suggests that they are dissimilar to hepatocytes in vivo. Specifically, 2D formats, even with overlaid collagen matrix, are more flattened than their native cuboidal architecture. On a subcellular level, this translates to major differences in cytoarchitecture, which is linked to aberrant polarization and non-physiological behavior [305, 159]. Griffith and Swartz have described the improved presentation of relevant biochemical and mechanical cues in 3D cultures, typically cell-laden hydrogels, compared to traditional 2D cultures [89].

1.4.2 Three-Dimensional Liver Constructs

Commonly, 3D hepatic cultures consist of primary cell or induced pluripotent stem cell (iPSC)-derived spheroid and organoid cultures, which are typically embedded in ECM-based hydrogels [156]. Spheroids and organoids can be manufactured using a variety of techniques, such as microwell mold-based technologies, which offer a high degree of composition and size control, but are difficult to scale. Spinning flasks and bioreactors can produce large populations of spheroids, though they are typically non-uniform in size and function. Bell et al. showed that primary human hepatic spheroids fabricated and cultured in microwell plates serve as useful models of hepatotoxicity and multiple liver pathologies [16].

Toward transplantable cell therapies, Stevens et al. used microwell molds to create 3D hepatic spheroid co-cultures of primary human hepatocytes and fibroblasts, which can be embedded in agarose, fibrin or polyethylene glycol hydrogel scaffolds. The resulting tissue constructs support hepatic function in vitro and in vivo after ectopic transplantation into the peritoneal cavity [257]. Furthermore, Stevens et al. demonstrated that implanting a tissue seed, consisting of hepatic aggregates and vascular cords, into an FRNG (fumarylacetoacetate hydrolase-deficient (Fah-/-), recombinase activating gene-deficient (Rag1-/-), non-

obese diabetes (NOD), interleukin-2 receptor γ chain-deficient (Il2rγ-null)) mouse model of hereditary tyrosinemia leads to a 50-fold expansion in serum human albumin and formation of perfusable vessels after 80 days of cycled exposure to regenerative stimuli [256]. Relatedly, Takebe et al. constructed liver buds consisting of iPSC-derived hepatocyte-like cells, mesenchymal stem cells, and human umbilical vein endothelial cells; mesenteric transplantation of these human liver buds resulted in vascularization and rescued a lethal TK-NOG mouse model of liver injury [266].

To create clinically-viable engineered liver constructs, cell sourcing (discussed further in **Section 1.6**) and clinical-scale manufacturing of organoids and spheroids must be addressed. Toward this end, Takebe et al. constructed a large-scale liver bud microwell culture platform, enabling the formation of 108 liver buds [267].

1.4.3 Physiological Microfluidic Models of Liver

Despite improvements to in vitro liver platforms as model systems and implants, static cultures lack physiologically-relevant dynamic components. The native liver's dynamic physiology arises from blood circulation and multi-organ crosstalk. Thus, to improve biological fidelity, many have attempted to create microfluidic models of the liver [114]. By leveraging techniques from the semiconductor manufacturing industry like soft lithography, groups have fabricated microphysiological systems with pre-formed channels to allow for perfusion of nutrients and to aid in waste removal [87, 19, 115, 133, 135, 242]. These so-called liver-on-chip platforms allow for the study of biochemical and mechanical cues such as growth factor gradients and shear stress. Lee et al. demonstrated that the presence of human stellate cells and application of shear via flow enabled formation of stable hepatic spheroids on chip [151]. Furthermore, by linking microfluidic channels between multiple tissue models, multi-organ phenomena such as drug metabolite toxicity and disease progression can be captured in vitro, which is not possible in traditional cultures [238, 68, 91].

1.4.4 Drug Development Applications

Even though disease modeling in liver-on-a-chip devices is in its early stages, one area where the field has made significant headway is in studying drug metabolism. The pharmaceutical pipeline is clogged by drugs that pass the pre-clinical (in vitro and animal testing) phase but

fail after several years of human trials. Approximately 90% of the drugs that make it to human trials fall under this category and end up costing pharmaceutical companies hundreds of millions of dollars per drug. For drug studies, in particular, animal models are often not predictive of human outcomes, due to species-specific drug metabolism pathways such as those regulated by cytochrome P450 enzymes. Additionally, given their ability to integrate multiple organ systems, liver-on-a-chip systems have been shown to more faithfully model human ADME/TOX and capture adverse drug reactions. These physiologically coupled devices have predicted the formation of toxic metabolites by the liver, which have downstream deleterious effects on other organ systems. For example, Viravaidya et al. characterized the conversion of naphthalene into its toxic metabolite with a liver-lung-fat tissue chip, in which they observed depleted glutathione levels in the downstream lung chamber caused by accumulated compounds in the fat chamber [291]. Coupling organ systems offers preclinical analysis of ADME/TOX and of cancer drug metabolism [45, 273], which is typically limited to animal models.

1.4.5 Controlling 3D Architecture and Cellular Organization

Another approach to improving the functionality of tissue-engineered constructs is to more closely mimic in vivo microarchitecture by generating scaffolds with a highly defined material and cellular architecture, which would provide better control over the 3D environment at the microscale.

A range of rapid prototyping and patterning strategies have been developed for polymers using multiple modes of assembly including fabrication using heat, light, adhesives, or molding, and these techniques have been extensively reviewed elsewhere [281]. For example, 3D printing with adhesives combined with particulate leaching has been utilized to generate porous PLGA scaffolds for hepatocyte attachment [136], and microstructured ceramic [211] and silicon scaffolds [122, 200] have been proposed as platforms for hepatocyte culture. Furthermore, molding and microsyringe deposition have been demonstrated to be robust methods for fabricating specified 3D PLGA structures towards the integration into implantable systems [292].

Microfabrication techniques have similarly been employed for the generation of patterned cellular hydrogel constructs. For instance, microfluidic molding has been used to form bi-

ological gels containing cells into various patterns [270]. In addition, syringe deposition in conjunction with micropositioning was recently illustrated as a means to generate patterned gelatin hydrogels containing hepatocytes [294]. Patterning of synthetic hydrogel systems has also recently been explored. Specifically, the photopolymerization property of PEG hydrogels enables the adaptation of photolithographic techniques to generate patterned hydrogel networks. In this process, patterned masks printed on transparencies act to localize the UV (ultraviolet) exposure of the pre-polymer solution, and thus, dictate the structure of the resultant hydrogel. The major advantages of photolithography-based techniques for patterning of hydrogel structures are its simplicity and flexibility. Photopatterning has been employed to surface pattern biological factors [100], produce hydrogel structures with a range of sizes and shapes [219, 14], as well as build multilayer cellular networks [161, 271]. Consequently, hydrogel photopatterning technology is ideally suited for the regulation of scaffold architecture at the multiple length scales required for implantable hepatocellular constructs. As a demonstration of these capabilities, photopatterning of PEG hydrogels was utilized to generate hepatocyte and fibroblast co-culture hydrogels with a defined 3D branched network, resulting in improved hepatocyte viability and functions under perfusion [282]. More recently, a 'bottom-up' approach for fabricating multicellular tissue constructs utilizing DNA-templated assembly of 3D cell-laden hydrogel microtissues demonstrates robust patterning of cellular hydrogel constructs containing numerous cell types [153]. Also, the additional combination of photopatterning with dielectrophoresis-mediated cell patterning enabled the construction of hepatocellular hydrogel structures organized at the cellular scale. Overall, the ability to dictate scaffold architecture coupled with other advances in scaffold material properties, chemistries, and the incorporation of bioactive elements (discussed further in **Section 1.7**) will serve as the foundation for the future development of improved tissue-engineered liver constructs that can be customized spatially, physically, and chemically.

1.5 In Vivo Models

While there have been impressive advances in cell culture models of the human liver, experimental animal models still play an important role in the effort to engineer liver therapies. Commonly performed surgeries such as bile duct ligation and partial hepatectomy are ex-

perimentally tractable models of acute liver injury, yet they are of little clinical relevance. Drug-induced (e.g. carbon tetrachloride, acetaminophen, or thioacetamide) hepatotoxicity to induce necrotic lesions is more recapitulative of human pathophysiology, but the phenotype is difficult to reproduce [205]. Additionally, modeling chronic liver injury in animal models is problematic because they tend to rapidly correct severe hepatic damage after a few days, which is not representative of human disease progression and resolution [78]. In order to model a human-like context for liver injuries, it is necessary to develop improved, controlled models of human liver injury. Such animal models can be useful for the evaluation of human liver biology and the preclinical performance of candidate therapies and drugs [92, 269]. To accomplish this, human hepatocytes can be transplanted orthotopically in immunocompromised mice with no liver injury via injection of a cell solution, and are useful for modeling human-specific drug metabolism, liver injury, and hepatotropic infections. However, on average, hepatocyte transplantation exhibits poor levels of engraftment (10-30%) [98]. Transplanted hepatocytes have the ability to expand preferentially if the host is compromised by injury or genetic modification. The first genetically engineered mouse model to demonstrate this was the Alb-uPA mouse, which carries a uroplasminogen activator under an albumin promoter, causing liver injury and failure [220]. Aiming to improve on the Alb-uPA system, a transgenic model of hereditary tyrosinemia I was developed, in which a genetic knockout of FAH leads to the hepatotoxic accumulation of fumarylacetoacetate [6]. FAH knockout mouse injury initiation and duration can be controlled through the administration of a small molecule drug, 2-(2-nitro-3-trifluoro-methylbenzoyl)-1,3-cyclohexanedione; NTBC) in the drinking water. Another inducible model called TK-NOG, which expresses thymidine kinase under an albumin promoter, causes hepatocyte ablation following activation by ganciclovir treatment [103]. In the AFC8 injury model, induction by the small molecule AP20187 drives caspase-8-initiated apoptosis of hepatocytes modified to express FK506 under an albumin promoter [23]. For all of the above models, engraftment rates surpassing 70% have been observed. A classical study in parabiotic rats in the 1960's revealed that hepatic injury results in the expression of systemic, soluble signals that have the potential to drive liver regeneration [32]. Despite decades of research, the complex signaling cascade driving liver regeneration is still not well understood, but has found utility in ectopic humanized mouse models. Chronic liver injury often presents with high portal pressures, which can reduce engraftment levels during an orthotopic transplantation. Thus,

transplantation to ectopic sites is clinically attractive. Ectopic grafts that anastomose to the host vasculature can interact with regenerative stimuli from the host liver, causing expansion and proliferation of the transplanted human hepatocytes. Initially, ectopic transplantation was demonstrated in the lymph node [141] and spleen [213], and later in the subcutaneous space and mesenteric fat-pad, both of which offer ease of accessibility for manipulation and non-invasive imaging [256, 266, 40]. Taken together, the range of liver injury animal models are an essential tool for studying various perturbations to normal liver biology and building implantable tissue constructs to address acute and chronic liver failure. The field is just beginning to uncover mechanisms that control liver regeneration in various disease and injury contexts. The discovery of new soluble regenerative signals will be central to advancing therapies that have the potential to improve the supply of donor tissue.

1.6 Cell Sourcing

1.6.1 Cell Number Requirements

The development of cell-based therapies poses myriad challenges, partially stemming from the scale of the liver. An adult human liver is estimated to possess 241 billion hepatocytes, 24 billion stellate cells and 96 billion Kupffer cells [21]. Sourcing such enormous cell numbers using current technologies is not feasible.

However, many human hepatocyte transplantation studies suggest that clinical intervention is possible with a fewer number of cells, and offer critical insights to help us determine minimum cell numbers. In a review, Fisher and Strom cataloged 78 different human hepatocyte transplantation studies, detailing both the input cell number and a qualitative description of functionality [77]. Correlating these, we can broadly surmise that to correct inborn errors of metabolism, at least 1-10 billion hepatocytes are needed. However, for acute liver failure, that number grows to 5-20 billion cells. For liver cirrhosis, hepatocyte transplantations have largely been unsuccessful (discussed further in **Section 1.3.4**); therefore, it is unclear what the cellular requirements for cirrhosis are. While injection of hepatocytes is not the same as implantation within a scaffold, these studies serve as useful inputs into more complex physiological models.

In order to get us closer to these numbers, many different cell sources have been explored.

1.6.2 Immortalized Cell Lines

Immortalized hepatocyte cell lines can be derived from liver tumor tissue or directly from primary hepatocytes in vitro. The prominent lines utilized today are HepG2, derived from hepatocellular carcinoma, HepaRG [97], a human bipotential progenitor cell line, C3A, derived from HepG2s, and Huh7, derived from liver tumor [42]. Several other fetal and adult hepatic cell lines have also been established, typically using a combination of viral oncogenes and the human telomerase reverse transcriptase (hTERT) protein [283]. However, these cell lines lack the full functional capacity of primary adult hepatocytes and there is a risk that oncogenic factors could be transmitted to the patient, limiting their use as a cell source for transplantation therapies.

1.6.3 Primary Cells

Unlike immortalized lines, primary human hepatocytes (PHHs) can provide a whole host of human liver-specific function. PHHs, however, are limited in supply and their phenotype is difficult to maintain in vitro. Many methods have been developed for maintaining long-term functionality of hepatocytes through the use of a variety of configurations and biomaterial constructs, which are further discussed in **Section 1.4**. Due to limitations in the supply of mature human hepatocytes, many groups have attempted to promote the expansion and proliferation of PHHs in vitro. Peng et al. have shown that TNFα promotes the expansion of hepatocytes in 3D cultures and enables serial passaging and long-term culture for more than 6 months [209]. In a similarly notable study, Hu et al. identified an optimal cell culture cocktail consisting of B27 supplement (without vitamin A), R-spondin, CHIR99021 (a Wnt agonist), NAC, nicotinamide, gastrin, EGF, TGFα, FGF7, FGF10, HGF, and TGFβ inhibitor (A83-01) and ROCK inhibitor that led to long-term 3D organoid culture of PHHs [110].

1.6.4 Fetal and Adult Progenitors

Given their ability to differentiate into diverse lineages both in vitro and in vivo, iPSC and human embryonic stem cell (hESC) cultures can also be utilized to generate hepatocyte-like cells (HLCs). Various differentiation protocols have been applied to these cultures to yield cell populations that exhibit some phenotypic and functional characteristics of hepatocytes

[87, 237, 88, 34, 248]. These populations are termed HLCs because of their expression of fetal proteins and fetal-like cytochrome P450 profiles [230]. While they are distinct from mature adult hepatocytes, HLCs can still serve as a potential cell source in very specific contexts.

In addition to pluripotent cells, bipotential progenitor cells can also serve as a source for hepatocytes. Huch et al. delineated conditions that allow for long-term expansion of adult bile duct-derived $EpCAM^+$ bipotential progenitor cells from the human liver [113]. The expanded cell population attained using their protocol is stable at the chromosomal level and can be converted into functional HLCs in vitro and in vivo [113].

1.6.5 Reprogrammed Hepatocytes

HLCs can also be generated using direct reprogramming of mature cell types. For example, several groups have demonstrated the feasibility of reprogramming fibroblasts into HLCs without a pluripotent intermediate [308, 111, 65]. Cheng et al. demonstrated that a combination of nuclear factors can stimulate conversion of hepatoma cells to HLCs [42]. These findings raise the future possibility of deriving human HLCs directly from another adult cell type.

1.7 ECM for Cell Therapies

The ECM of the liver provides a structural scaffold with bioactive cues that modulate hepatic function and promote vascularization. Collagen and fibronectin are the major structural components of the liver ECM. Along with other non-structural proteins, these components participate in integrin-mediated signaling between cells and their surrounding matrix. Hepatocytes are sensitive to their ECM, and it has been demonstrated that the presence of abnormal amounts and/or types of ECM components correlates with the onset and progression of liver fibrosis [296].

ECM scaffolds for hepatic tissue engineering are useful for constructing 3D tissue models and as a delivery vehicle for implants. Polymeric biomaterial hydrogels gained popularity as an engineering tool for recapitulating a physiologically-relevant 3D tissue niche. Aside from creating a permissive environment for hepatocyte survival and growth, ECM scaffolds for hepatic tissue engineering also enable the formation of biliary and vascular networks,

which will be further discussed in **Section 1.8**. Broadly speaking, ECM scaffolds can be constructed using synthetic and/or naturally-derived polymers.

1.7.1 Natural Scaffold Chemistry and Modifications

A wide range of natural biomaterial polymers spanning polysaccharides (e.g. dextran, chitosan), peptides (e.g. collagen, fibrin), decellularized ECM (dECM) and composites of these have been employed as hepatic tissue engineering scaffolds [156, 257, 256, 83, 217, 232, 31, 71, 126, 288]. The advantages of biologically-derived materials include their biocompatibility, naturally occurring cell adhesive moieties, and, in the case of decellularization, native architectural presentation of extracellular matrix molecules. However, naturally-derived biomaterials have several barriers to use in the clinic, primarily due to lot-to-lot variability and xenogeneic origin.

The choice of material determines the physicochemical and biological properties of the scaffold. For example, early efforts in developing implantable hepatic constructs utilized collagen-coated dextran microcarriers that enabled hepatocyte attachment since hepatocytes are known to be anchorage-dependent cells. The intraperitoneal transplantation of these hepatocyte-attached microcarriers resulted in successful replacement of liver functions in two different rodent models of genetic liver disorders [55]. Subsequently, collagen-coated or peptide-modified cellulose [137, 126], gelatin [272], and gelatin-chitosan composite [155] microcarrier chemistries have also been explored for their capacity to promote hepatocyte attachment. On the other hand, materials that are poorly cell adhesive like alginate [83] have been exploited for their utility in promoting hepatocyte-hepatocyte aggregation (i.e. spheroid formation) and phenotypic stabilization within these scaffolds. Collectively, the size of engineered tissues created by these approaches is limited by oxygen and nutrient diffusion to only a few hundred microns in thickness.

To address this constraint, recent work has sought to use decellularized whole organ tissue as a matrix for liver tissue engineering. The decellularization process utilizes perfusion-based technologies to remove cells from donor tissues but preserve the structural and functional characteristics of the native underlying tissue. Recent advances in decellularization protocols have yielded scaffolds with native liver ECM composition, growth factor presentation, vascular structure, and biliary network architecture [10, 249, 177]. To date, seeding protocols

have achieved up to 95% efficiency of recellularization with relevant cell populations (e.g. hepatocytes, vascular cells, bipotent hepatic progenitors); resulting re-cellularized grafts exhibited liver-specific function and survival after transplantation in rodents [201, 288, 10]. Furthermore, cell-laden, xeno-derived decellularized ECM (dECM) scaffolds are compatible with immunocompetent animal models [177]. However, given the shortage of donor tissue, the wide use of dECM scaffolds is unlikely.

1.7.2 Synthetic Scaffold Chemistry

In contrast to biologically-derived material systems, synthetic materials enable precisely customized architecture (porosity and topography), mechanical and chemical properties, and degradation modality and kinetics, which are known to drive cell behavior. Synthetic materials that have been explored for liver tissue engineering include poly(L-lactic acid) (PLLA), poly(D,L-lactide-co-glycolide) (PLGA), poly(ϵ -caprolactone) (PCL), and poly(ethylene glycol) (PEG) [40, 46, 48, 188, 187, 120, 282, 287]. Polyesters like PLLA and PLGA are the most common synthetic polymers utilized in the generation of porous tissue-engineering constructs. These materials are biocompatible, biodegradable, and have been used as scaffolds for hepatocyte transplantation [188, 241]. A key advantage of PLGA is the potential to finely tune its degradation time due to differences in susceptibility to hydrolysis of the ester groups of its monomeric components (lactic acid and glycolic acid). However, the accumulation of hydrolytic degradation products has been shown to produce an acidic environment within the scaffold which initiates peptide degradation and stimulates inflammation, which may affect hepatocyte function [109]. Consequently, as alternatives to macroporous scaffold systems, approaches aimed at the efficient and homogeneous encapsulation of hepatocytes within a fully 3D structure have been explored. In particular, hydrogels that exhibit high water content and thus similar mechanical properties to tissues are widely utilized for various tissue-engineering applications including hepatocellular platforms. Synthetic, PEG-based hydrogels have been increasingly utilized in liver tissue-engineering applications due to their high water content, hydrophilicity, resistance to protein adsorption, biocompatibility, ease of chemical modification, and the ability to be polymerized in the presence of cells, thereby enabling the fabrication of 3D networks with uniform cellular distribution [210]. PEG-based hydrogels have been used for the encapsulation of diverse cell types, including immortalized

and primary hepatocytes and hepatoblastoma cell lines [40, 282, 287]. The encapsulation of primary hepatocytes requires distinct material modifications (e.g. 10% w/v polyethylene glycol (PEG) hydrogel, inclusion of RGD adhesive motifs) as detailed below, as well as, analogous to 2D co-culture systems, the inclusion of non-parenchymal supporting cell types such as fibroblasts and endothelial cells [287].

1.7.3 Modifications in Scaffold Chemistry

The relatively inert nature of synthetic scaffolds allows for the controlled incorporation of chemical/polymer moieties or biologically active factors to regulate different aspects of cellular function. Chemical modifications like oxygen plasma treatment or alkali hydrolysis of PLGA [104, 194], or the incorporation of polymers like poly(vinyl alcohol) (PVA) or poly(N-p-vinylbenzyl-4-O-β-D-galactopyranosyl-D-glucoamide) (PVLA) into poly(lactic-co-glycolic acid) (PLGA) or poly-l-lactide acid (PLLA) scaffolds [188, 125, 149] have improved hepatocyte adhesion by modulating the hydrophilicity of the scaffold surface [37]. Biological factors may include whole biomolecules or short bioactive peptides. Whole biomolecules are typically incorporated by non-specific adsorption of extracellular matrix molecules such as collagen, laminin or fibronectin [104, 75] and covalent conjugation of sugar molecules such as heparin [99, 134], galactose [46, 208], lactose [99] or fructose [154] or growth factors such as EGF [176]. Alternatively, short bioadhesive peptides that interact with cell surface integrin receptors have been extensively utilized to promote hepatocyte attachment in synthetic scaffolds. For example, conjugation of the RGD peptide to PLLA has been shown to enhance hepatocyte attachment [35], whereas RGD modification significantly improved the stability of long-term hepatocyte function in PEG hydrogels [40, 287]. The additional incorporation of adhesive peptides that bind other integrins may serve as a way to further modulate and enhance hepatocyte function within synthetic polymer substrates. Moreover, Stevens et al. demonstrated that integration of matrix metalloproteinase-sensitive peptide sequences into hydrogel networks as degradable linkages has been shown to enable cell-mediated remodeling of the hydrogel [255].

The capacity to modify biomaterial scaffold chemistry through the introduction of biologically active factors will likely enable the finely tuned regulation of cell function and interactions with host tissues important for implantable systems.

1.7.4 Porosity

A common feature of many implantable tissue engineering approaches is the use of porous scaffolds that provide mechanical support, often in conjunction with cues for growth and morphogenesis. Collagen sponges, various alginate and chitosan composites and PLGA are the most commonly used porous scaffolds for hepatocyte culture, and are generally synthesized using freeze-dry or gas-foaming techniques. Pore size has been found to regulate cell spreading and cell-cell interactions, both of which can influence hepatocyte functions [217], and may also influence angiogenesis and tissue ingrowth [199]. Porous, acellular scaffolds are normally seeded using gravity or centrifugal forces, capillary action, convective flow, or through cellular recruitment with chemokines, but hepatocyte seeding is generally heterogeneous in these scaffolds [300, 150].

1.8 Vascular and Biliary Tissue Engineering

Beyond compatibility with hepatic cell types, scaffolds should also be conducive to vasculature formation. Relying on vascularization by the host is not sufficient for large tissue constructs required for the clinic, because cells that are not near capillary structures ($>$ 150 – 200 μm) are at a risk for necrosis after a matter of hours due to a lack of oxygen, nutrient availability and waste transport. In this section, we discuss composite approaches toward building scalable, vascularized constructs.

1.8.1 Vascular Engineering

Approaches to engineering vessels can generally be categorized as bottom-up induction of vascular assembly and top-down fabrication of vascular conduits [245]. Bottom-up vascular engineering approaches are built upon the idea of neovascularization, or new vessel formation. Vessel formation can occur by angiogenic sprouting, the formation of vessels branching off of an existing blood vessel, or vasculogenesis, the self-assembly of single endothelial cells or progenitor cells into lumenized vessels. Despite the ability of single vascular cells to coalesce to enable self-assembly, vasculogenesis is accelerated by co-culture with supporting stromal cells, such as fibroblasts, mesenchymal stem cells and pericytes [245, 265, 54]. Studies exploring angiogenesis and sprouting events suggest that chemical gradients, fluid-driven

shear stress, and a hypoxia are key players in vessel formation [185, 247, 79, 206].

Top-down fabrication approaches dictate geometry and architecture, rather than driving self-assembly. Polymer molding using microetched silicon has been shown to generate extensive channel networks with capillary dimensions, though it is not amenable to high-throughput manufacturing [28]. While direct printing of cells can be cytotoxic, 3D printing has become a popular approach for fabricating hollow channels that enable vascular cell seeding. The challenge lies in using this approach to build patent capillary beds, which are 5-10 μm in diameter. While 2-photon polymerization has an impressively high feature size resolution at 100 nm, the tradeoff between build volume (i.e. building constructs large enough for clinical impact), build speed (i.e. impacting manufacturability) and printer resolution renders it inappropriate for most applications in tissue engineering. Alternate printers using direct-ink writing (DIW) of viscoelastic materials have emerged as a powerful tool for fabrication of patterned hydrogel constructs. DIW can achieve minimum feature size resolutions from 1 to 250 µm, depending the ink 'building block' size [280]. However, DIW printing requires yield-stress fluid inks with restrictive viscosities (102-106 mPa·s), such that they fluidize under stress but regain the original shear elastic modulus after printing [280]. Kolesky et al. demonstrated that DIW and fugitive inks were useful for multi-material printing as well as construction of thick (>1 cm), vascularized tissues [140, 139]. Miller et al. demonstrate the use of thermal microextrusion approach to create sacrificial sugar glass lattices that can be embedded in various cell-laden biomaterials, evacuated and subsequently lined with vascular cells [180].

Taken together, self-assembly-driven formation of a capillary bed can be combined with printing of larger vessels to enable the fabrication of a fully vascularized tissue construct. Song et al. used 3D printing to create curved vascular channels using a fugitive ink [247]. The vascular cells lining the channel were able to degrade the surrounding hydrogel matrix and undergo sprouting when exposed to angiogenic factors. They further demonstrated that the curvature and complexity of printed vasculature impacted the extent of sprouting, which will be an important consideration for vessel patterning in future clinical applications [247].

1.8.2 Host Integration

For vascularized constructs to survive after implantation, the engineered vessels must anastomose with the host vasculature. To date, the exact mechanism that drives integration with the host is not well understood [245]. A number of studies have elucidated the contribution of cytokines important in angiogenesis and recruitment of host vasculature in implant constructs, such as VEGF [241], basic fibroblast growth factor (bFGF) [148], and vascular endothelial growth factor (VEGF) in combination with platelet-derived growth factor (PDGF) [221]. Furthermore, preimplantation of VEGF releasing alginate scaffolds prior to hepatocyte seeding was demonstrated to enhance capillary density and improve engraftment [127]. Additionally, while building an artificial liver tissue construct, Stevens et al. demonstrated that the co-implantation of parallel endothelial cell cords with primary human hepatocyte and fibroblast spheroids led to better hepatic performance and survival when compared to an implant with non-patterned endothelial cells, suggesting that there may be an optimal templated endothelial geometry that enables vascularization and host integration in vivo [256]. Surgical anastomosis poses an alternative to biologically-driven anastomosis, though this approach requires invasive surgery and access to suture-able vessels both in the graft and in the host. Strategies to incorporate vasculature into engineered constructs include the microfabrication of vascular units with accompanying surgical anastomosis during implantation [122, 90].

In addition to interactions with the vasculature, integration with other aspects of host tissue will constitute important future design parameters. For instance, incorporation of hydrolytic or protease-sensitive domains into hepatocellular hydrogel constructs could enable the degradation of these systems following implantation [255]. Of note, liver regeneration proceeds in conjunction with a distinctive array of remodeling processes such as protease expression and extracellular matrix deposition. Interfacing with these features could provide a mechanism for the efficient integration of implantable constructs. Similarly to whole liver or cell transplantation, the host immune response following the transplant of tissue-engineered constructs is also a major consideration. Immunosuppressive treatments will likely play an important role in initial therapies, although stem cell-based approaches hold the promise of implantable systems with autologous cells. Furthermore, harnessing the liver's unique ability to induce antigen-specific tolerance [215] could potentially represent

another means for improving the acceptance of engineered grafts.

1.8.3 Biliary Network Engineering

Importantly, future iterations of hepatic grafts should include a biliary system, which is responsible for excretory functions. In a similar vein, we envision that a combination of 'top down' manufacturing, such as the aforementioned technologies for generating patent vascular conduits, and 'bottom up' approaches, which could involve leveraging biological phenomena that drive biliary morphogenesis, will be useful for building a biliary network.

The biliary tree is a complex, 3D network of tubular conduits of various sizes and properties. The liver contains an intrahepatic compartment that is lined by biliary epithelial cells, termed cholangiocytes, that aid in the modification and removal of hepatocyte-secreted bile. Even though the blood vessel fabrication approaches delineated above have not yet been applied to engineering bile networks for implantable liver constructs, advancements in cholangiocyte sourcing methods have made it feasible. Sampaziotis et al. identified a protocol for directed differentiation of human iPSCs into cholangiocyte-like cells [223]. In 2017, the same group provided the first proof-of-concept study to reconstruct the gallbladder wall and repair the biliary epithelium using human primary cholangiocytes expanded in vitro [224]. Furthermore, current studies are focused on the development of in vitro models which exhibit biliary morphogenesis and recapitulate appropriate polarization and bile canaliculi organization [260, 118, 5], as well as platforms for the engineering of artificial bile duct structures [182, 64].

1.9 Engineered Cell Therapies as Satellite Transplants

In this review, we present engineered cell therapies as an alternative to donor-harvested organs and tissues, and focus on solid organs that require transplantation of functional cells or engineered cell-laden grafts. There are multiple tissues that fit this description, including the liver, which performs over 500 complex, metabolic functions [20], and the pancreas, which imparts tight control of glucose homeostasis via exocrine secretions. Importantly, satellite cell therapies have specific utility in use cases in which a remote functional unit of cells can address host deficiency. We envision that these cell-based therapies can act as a bridge to transplant or as a long-lasting, synthetic organ.

Cell therapies can be engineered using autologous cell sources such as induced pluripotent stem cells (iPSCs) or cadaveric donors. Additionally, cell sources may be xeno-derived, especially considering recent progress toward immunocompatibility through engineered cross-matching and removal of pathogenic, zoonotic viruses [198]. Availability of cells and the capacity for expansion and self-renewal is key for sustaining these cell therapies, and are current topics of preclinical research. There is clinical precedent for the success of engraftment of allogeneic cells; for example, transplantation of donor islet cells led to a 50% reduction in dependence on exogenous administration of insulin in patients with diabetes [204, 105].

1.9.1 Success Criteria

Early iterations of engineered cell therapies were simplistic in nature and consisted of injections of dissociated cell mixtures (and were discussed further in **Section 1.3.4**). While success through initial attempts was promising, research in the field of regenerative medicine strongly suggests that long-term integration and function of an engineered graft is closley tied to rationally-designed cell structures and scaffolds. Here we define three success criteria for engineered cell therapies as life-saving artificial organs:

1. **Engraftment:** which entails the successful initial survival and integration of cells or a cell-laden construct with the host, which in some instances will involve morphogenetic processes such as vasculogenesis and angiogenesis, or surgically-assisted anastomoses,

2. **Function:** which describes the capacity of the transplanted cells to carry out organ-specific function and response (such as drug metabolism and protein synthesis of the liver, or glucose-sensing and insulin production of the pancreas), and

3. **Persistence:** which captures the propensity for the artificial graft to sustain function and integration over a long period of time, such that it may compensate or replace the function of a missing or diseased organ, without being compromised by immune attack.

1.9.2 Anatomic Sites for Transplantation

The success of engineered cell therapies in the clinic has been in part impaired by the limited exploration of heterotopic transplantation sites. While most organ transplants are performed at the orthotopic site, this is not ideal because a diseased host organ is often inhospitable to engraftment (e.g. elevated portal hypertension, cirrhosis, or fibrosis of the liver). Thus, assessment of satellite locations for heterotopic transplant is of great clinical interest. Importantly, there is precedent for tissue function in heterotopic locations in normal biology [106, 57], disease settings such as malignant cancers [240], clinical procedures such as auxiliary liver transplantation [15], direct injection of donor cells [213, 107, 141], and engineered cell therapies in the preclinical space [256, 256, 40, 266].

As alluded to in **Section 1.3.4**, satellite cell therapies benefit from the choice of a hospitable, heterotopic location, from which they can provide compensatory organ-specific function for the damaged and/or diseased host organ. Importantly, heterotopic transplantation sites represent key differences in local microenvironment, including oxygen tension, nutrient supply, blood supply and pre-existing microvasculature, and immune surveillance. Engineered cell therapies may consist of artificial scaffolds that leverage and/or compensate for any aspects of the local environment, such as through provision of cues that promote vasculogensis or angiogenesis in the case of insufficient native vascular supply. Anatomic locations and delivery options that are amenable to implantation and engraftment include intravenous delivery, subcutaneous injection, renal subcapsular implantation, lymph node implantation, and intraperitoneal implantation in the mesentery or omentum. Furthermore, other factors also affect the choice of anatomic site for a satellite cell therapy, including the local immune environment, surgical accessibility in the case of need for removal to ensure safety, and compatibility with accommodating a growing cell mass [57]

1.10 New Readouts for Liver Function

As new technologies for creating liver therapies and preclinical models become more complex and widespread, real time, longitudinal, noninvasive, and more scalable readouts are needed for evaluation. Advances in and integration of disparate fields have enabled new sensors for monitoring long-term function, assessing therapeutic efficacy, and elucidating biology. For longitudinal and real time monitoring, imaging modalities such as magnetic

resonance spectroscopy, bioluminescence imaging, and radioactive labeling provide ways to gauge liver status and metabolic function noninvasively over time. In addition to traditional blood protein measurements using host biomarkers, nanotechnology also has enabled new ways to diagnose liver disease. For example, nano-sized synthetic protease-sensitive activity markers have successfully been employed to noninvasively detect liver fibrosis with high signal-to-noise ratio using urinary detection [144]. For evaluation and elucidating biology, soft epidermal electronics or electronically integrated tissues provide ways to analyze tissue characteristics and augment existing function. Electrochemical sensors, force-sensitive cantilevers, and electrosensitive materials have been integrated within tissue culture platforms and benchtop organ-on-chip systems or engineered artificial tissues to track cell signaling [307]. Although preliminary in many ways, these new readouts can help improve translation of therapies, refine non-human experimental models, and ultimately bridge the gap between in vitro data and clinical translation.

1.11 Outlook

Traditionally, hepatic tissue engineering research has focused on designing the microenvironment to support a stable hepatic phenotype. As concomitant advances in pluripotent cell research and polymer chemistry have been actualized, new cell sources and extracellular matrices have been added to the pipeline. This interdisciplinary synergy has been the driving force behind the development of tissue engineered grafts with long-term survival and growth. In order to inch closer to the regenerative medicine north star of an ex vivo engineered graft that can serve as a replacement for the native organ, there are several areas to consider for improvement: a) vascularization of thick, dense grafts through a combination of self-assembly and bioprinting, b) engineering of the hepatic graft to prevent immune rejection in allogeneic and xenogeneic settings, c) improved understanding of metabolic and cellular requirements of various liver diseases, d) development of scalable, renewable cell sources that do not compromise the functional capabilities of cells, e) leveraging of animal injury models as bioreactors for cell sourcing, and f) upscaling of grafts in a manner that is compatible with the FDA's Good Manufacturing Practice (GMP) standards.

1.12 Thesis Scope & Organization

The lack of clinically viable options (including but not limited to donor organs, cell transplantation, extracorporeal devices, and implantable cell-laden constructs) to sufficiently treat patients with serious liver diseases is our main motivation pursuing the development of satellite cell therapies. While there are several challenges associated with the clinical translation of these technologies, this thesis focuses more deeply on building precise engineering methods to control and study the underlying cell-cell interactions, which we showed to reveal new insights into 2D liver models, 3D tissue constructs, and implanted satellite grafts in small animal models.

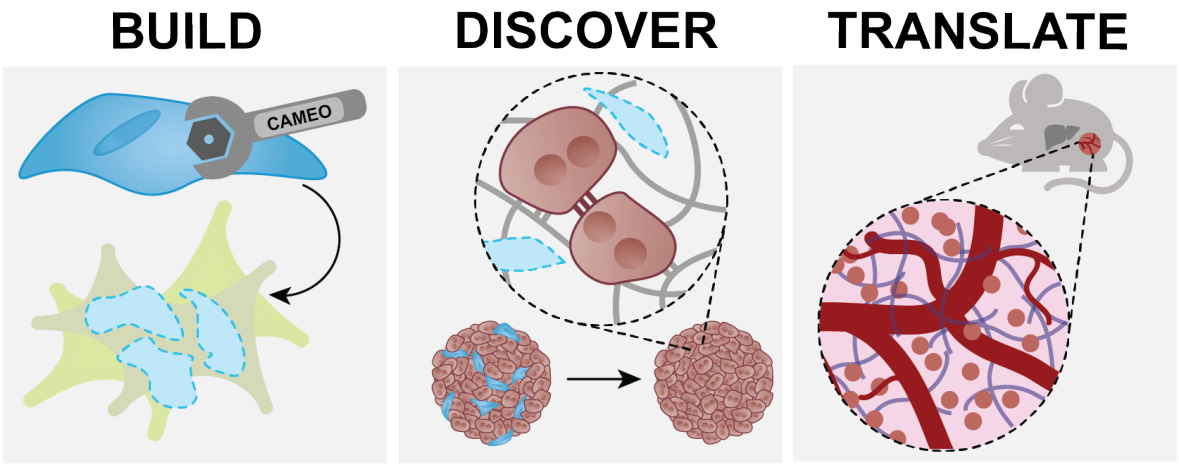

Figure 1-4: **Thesis Overview.** This thesis broadly encompasses three phases. **BUILD**: Designing a molecular tool to control cell-cell interactions in a way that enables organogenesis (left). **DISCOVER**: Applying such a tool to unlock new biology in 3D hepatic ensembles, which act as organ building blocks of satellite cell therapies (middle). **TRANSLATE**: Addressing several challenges related to optimization and testing of satellite cell therapies in vivo (right). Unpublished.

This thesis can be bucketed into three thrusts as shown in **Figure 1-4**. Our work is summarized below in brief overview and expanded upon in dedicated Chapters in this document:

Aim 1: BUILD

We have created a synthetic biology-driven tool (termed **CAMEO**, **C**ontrolled **A**poptosis in **M**ulticellular tissues for **E**ngineered **O**rganogenesis) that enables precise control of cell-cell interactions toward the end goal of engineering organogenesis. This tool is broadly

applicable to all avenues of tissue engineering. Here, we study 2D hepatocyte-fibroblast co-cultures as an exemplar, and find that our results corroborate the existing literature describing related hepatocyte-fibroblast systems.

Aim 2: DISCOVER

We then employed CAMEO to investigate cell-cell interactions in 3D hepatocyte-fibroblast ensembles, which was previously experimentally intractable. We discover that primary human hepatocytes do not require sustained fibroblast co-culture for long-term phenotype stability in vitro. Furthermore, we elucidate key drivers of phenotypic stabilization in our 3D hepatic ensembles.

Aim 3: TRANSLATE

In this Aim, we describe an approach for using our hepatic organ building blocks as the functional unit in satellite cell therapies. Here, we pursue several collaborative efforts in order to manufacture pre-vascularized grafts and highly-dense grafts. We also discuss considerations for further development of satellite cell therapies.

Future Perspectives

Lastly, we close this thesis with a discussion of new avenues both outside of and within tissue engineering that are enabled by our CAMEO technology. In this Chapter, we also provide additional commentary on considerations for applying satellite cell therapies to diseased animal models.

1.13 Lay Summary

1.14 Acknowledgements

The content of this Chapter was produced across multiple stand-alone pieces of work including two book chapters (published) and one review paper (in preparation) by myself and co-authors **Dr. Tiffany Vo**, **Dr. Arnav Chhabra**, **Dr. Quinton Smith**, **Keval Vyas**, **Dr. Heather E Fleming**, **Dr. Christopher Chen**, and **Dr. Sangeeta Bhatia**.

Chapter 2

BUILD: Development of a Non-Invasive Tool for Probing Intercellular Communication

2.1 Introduction

Three-dimensional (3D) tissue engineered models have evolved to encompass a range of applications spanning therapeutic cell-based therapies to in vitro organoid models. In all use cases, recapitulation of physiologic functions and native tissue behavior is key to studying and harnessing complex, tissue-specific phenomena in normal and pathophysiological states [165, 268, 207, 24, 284, 27, 197]. Across these systems, it is experimentally difficult to decouple the dynamic contributions of homotypic and heterotypic cell-cell interactions, cell-matrix interactions, soluble bioactive factors, chemical cues, and mechanical stimuli. Many existing approaches were designed to decipher these interactions, including tunable hydrogel systems [165, 276]; controlled manipulation via magnetic, fluidic, optical, electrical, mechanical, and intermolecular forces [278, 301]; and time-lapse microscopy for tracking cell fate and cellular rearrangement [38, 110, 227]. However, the contribution of cell-cell interactions remains difficult to disentangle, especially in engineered tissues with high cellular diversity.

2.1.1 Manipulation of Cell-Cell Interactions

For the liver, the inclusion of hepatocytes, which comprise the parenchymal compartment, has been shown to be required to address numerous liver-specific synthetic and metabolic functions [20]. However, it is well known that primary hepatocytes rapidly lose viability and function upon isolation from their native microenvironment, thereby presenting an inherent challenge for creating bioengineered liver tissue. A body of work has established that the provision of heterotypic and homotypic cell-cell interactions are of particular importance in engineered livers, including 3D stem cell-derived and primary tissue-derived ensembles. Specifically, we and others have shown that co-culture with stromal cells derived from the liver or elsewhere can enhance phenotypic stability of primary hepatocytes in a biomaterial context, though whether this enhancement of hepatocyte function and longevity derives from ongoing, direct cell-cell interaction, or a more transient, even indirect mechanism is not comprehensively understood [18, 84, 95]. Multiple groups have demonstrated that the interactions between various species of hepatocytes (including human, rat, monkey, and dog) and 3T3-J2 murine fibroblasts significantly enhance the long-term phenotypic stability of hepatocytes in vitro and in vivo [40, 131, 257, 256, 286, 9, 157]. Some evidence points toward contributions from cell-cell contacts and cell-secreted matrix molecules (e.g. T-cadherin, decorin, E-cadherin, liver-regulating protein) [131, 86, 101, 130]. Relatedly, we previously executed a high-throughput screen which identified stromal gene products that impact hepatocyte function in vitro [233, 234]. However, these phenomena are poorly studied in both 2D and 3D tissue structures since dynamic and precise manipulation of established complex, multicellular cultures is experimentally challenging.

In 2D, Hui et al. previously engineered a mechanical tool that enables user-defined control of cell-cell interactions in both time and space, and demonstrated its utility in studying the temporal dynamics of hepatocyte-fibroblast interactions [116, 117]. Specifically, Hui et al. engineered a micromachined silicon substrate (hereby referred to as micromechanical combs) consisting of interdigitating fingers that could move together and apart (**Figure 2-1**). In the studies, primary hepatocytes and fibroblasts were cultured on a set of combs, and the substrates were manipulated during the duration of culture to prescribe temporal control of cell-cell interactions. Importantly, precise control of cell-cell interactions after initiation of co-culture is otherwise experimentally challenging and in most cases, intractable.

In further studies, micromechanical combs were also used to study the interactions of liver sinusoidal endothelial cells, hepatocytes, and fibroblasts [169].

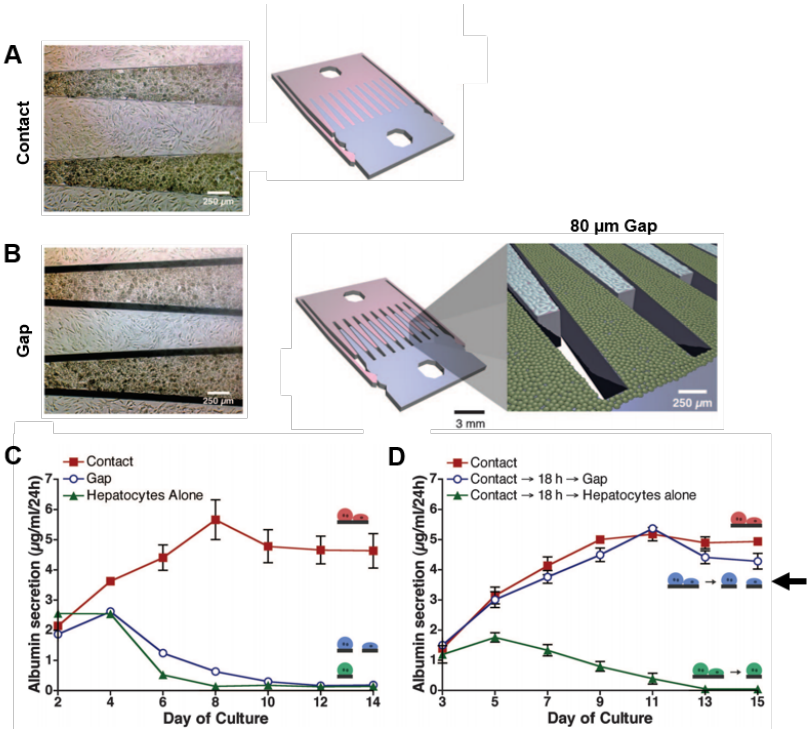

Figure 2-1: **Temporal dynamics of hepatocyte-fibroblast interactions in 2D micromechanical chip co-cultures.** (A) Micromechanical combs enable μm-resolution cell positioning, enabling both Contact Mode, in which comb fingers are locked together in contact, and (B) Gap Mode, in which comb fingers are slightly separated by an 80 μm gap. (A and B) Zoom-in of bright-field images of hepatocytes (darker cells) and fibroblasts (lighter cells) cultured on comb fingers (left; scale bar = 250 μm) and schematic of full micromechanical substrate platform (right). (C) Contact between hepatocyte and fibroblast combs was required to maintain albumin secretion over a 2 week period (red square = Contact Mode; blue circle = Gap Mode; green triangle = hepatocytes alone). (D) After an initial 18-hour period of Contact Mode, long-term culture in Gap Mode, which allows diffusion of paracrine signals, sustained albumin secretion for the remainder of the 2 week period (blue circle; **arrow**). In contrast, complete removal of fibroblasts led to deterioration of albumin secretion (green triangle). Adapted from [116].

The micromechanical combs were designed to snap together in Contact Mode (in which hepatocytes and fibroblasts were cultured in direct contact; **Figure 2-1**A) or in Gap Mode (in which hepatocytes and fibroblasts were cultured in across an 80 μm gap, allowing for only paracrine signal exchange between the two cell populations; **Figure 2-1**B). Similar to previous work, it was found that initial juxtacrine interactions between hepatocytes and

fibroblasts in Contact Mode (**Figure 2-1**C, red) were essential for supporting liver-specific function such as the secretion of albumin; in contrast, hepatocytes that were either cultured initially in Gap Mode (**Figure 2-1**B, blue) or alone (**Figure 2-1**B, green) were not able to sustain liver-specific function. Interestingly, Hui et al. demonstrated that the maintenance of liver-specific phenotype and viability could be mediated by an initial Contact Mode priming of 18 hours, followed by followed by sustained paracrine interactions with fibroblasts in Gap Mode (**Figure 2-1**C, blue). These findings highlight that there are spatiotemporal nuances in the role that fibroblasts play in maintaining hepatocytes [116, 117].

2.1.2 Design Criteria

While this platform enables precise, user-defined control of cell-cell interactions and opens the door to decoupling the contribution of molecular interactions over space and time, the micromechanical combs system is limited to 2D cultures consisting of 2 distinct cell populations cultured on rigid, silicon substrates. In order to enable matched studies in other 2D configurations as well as in 3D formats, we engineered a new method as defined by the following desired design criteria:

- Non-invasive, on-demand manipulation, enabling compatibility with complex architectures and 3D microenvironments
- Minimal side effects
- Short time scale of manipulation
- Maximum and complete separation of cell populations

Taking each criteria above into account, we identified suicide genes as the ideal candidate for tool building and development. Suicide genes can be installed genetically in a cell, and upon activation, causes the suicide gene-bearing cell to undergo apoptosis. Common suicide genes include herpes simplex virus thymidine kinase (HSV-TK) triggered by ganciclovir (GCV), Fas ligand activation, activation of caspase proteins via inducible dimerization (including caspase, 3, 8, 9), deamination of 5-fluorocytosine prodrug via cytosine deaminase to produce toxic 5-fluororacil, and induction of p53 tumor suppressor.

At current, suicide genes are widely used in clinical applications for cancer, either in order to (1) introduce a suicide gene into cancer cells to maximize lethality upon induction

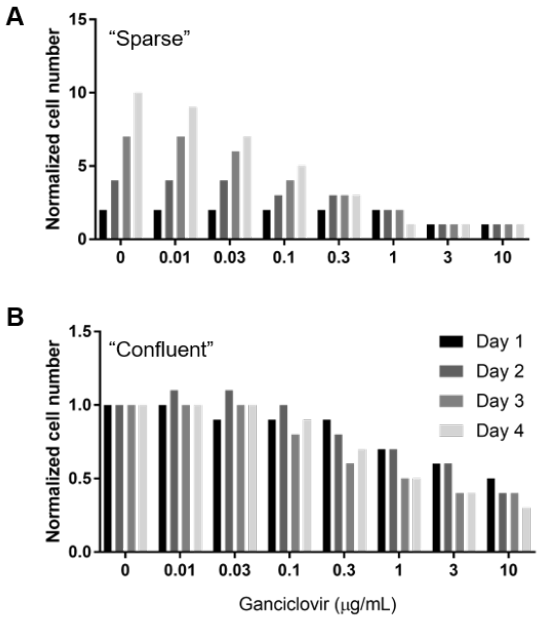

Figure 2-2: **HSV-TK/GCV suicide switch activation is sensitive to cell division** (A) Cells bearing HSV-TK were seeded at (A) 3,000/cm^2 or (B) 30,000/cm^2 and treated with a concentration between 0 to 10 μg/mL ganciclovir. Cell number was quantified and normalized to day 0, non-treated cells for 4 days post-dose. (Unpublished, data courtesy of Arnout Schepers)

[251] or (2) as a safety switch for infusions of Chimeric Antigen Receptor T-cell therapies, which are designed to kill cancer cells but may require elimination if hyper-activation leads to cytokine release syndrome [26]. In our application, we utilize suicide genes as a method to remove a select population of cells from a co-culture. Most suicide genes are triggered by small molecule drugs, which enables non-invasive and on-demand activation by adding the drug to cell culture media, or infusing a patient with the drug. We also expect that apoptosis will have minimal side effects, since apoptosis is a normal form of programmed cell death that is required during development and maintenance of homeostasis. With certain suicide genes, activation of the switch can lead to apoptosis in less than 3 to 4 hours, and subsequently reduces and decays a cell into fragments called apoptotic bodies, which are then eliminated by macrophages. Empirically, we found that the use of HSV-TK was sensitive to the rate of cell division (**Figure 2-2**), likely because the mechanism of cell killing depends on the blockage of DNA elongation, which causes toxicity upon replication. In contrast, other suicide switches may be deployed on shorter timescales and are independent

of proliferative state, such as those that rely on triggering initiator caspase proteins. Lastly, it is possible to engineer and enrich for a suicide gene-bearing cell population using traditional molecular approaches such as FACS or negative selection media, which is necessary in order to manipulate an entire or defined subset of a cell population.

As we will demonstrate through this Chapter, we addressed all the above design criteria using a cell line bearing the suicide gene inducible caspase-9 (iCasp9). Using this tool, we introduce a technique termed **CAMEO** (**C**ontrolled **A**poptosis in **M**ulticellular tissues for **E**ngineered **O**rganogenesis), in which a genetically-modified cell population can be induced to undergo apoptosis-driven elimination from a multicellular tissue construct. We implemented CAMEO and demonstrated non-invasive, rapid manipulation of established co-cultures in order to explore the phenotypic stability of both 2D (**Chapter 2**) and 3D (**Chapter 3**) hepatic ensembles. We envision that access to the CAMEO method will also impact the field of organoid science, in which stromal feeder layers are conventionally used to promote stem cell renewal and maintenance.

2.2 Results & Discussion

2.2.1 Activation of Suicide Gene-Expressing Fibroblasts Led to Uniform Elimination by Apoptosis

We sought to design a cell line that could undergo quick, complete removal using a non-invasive trigger. We employed iCasp9, which is activated by treatment with a small molecule chemical inducer of dimerization (CID; also known as rapalog, an analog of rapamycin) and leads to subsequent cell death through the intrinsic apoptosis pathway (**Figure 2-3**) [60, 81, 258].

The safety and efficacy of the iCasp9 transgene and CID have previously been shown in vitro and in vivo in animals and humans [60, 81, 258]. We used a lentivirus to transduce 3T3-J2 murine fibroblasts ('J2'), shown previously to support primary human hepatocyte function in both 2D and 3D platforms [18, 129, 152], with a bicistronic expression cassette encoding iCasp9 and GFP genes, and used FACS to enrich the infected population for the 15% highest-expressing GFP^+ cells. Previous users of this construct have demonstrated tight correspondence between the expression of the reporter (GFP) and target protein (iCasp9)

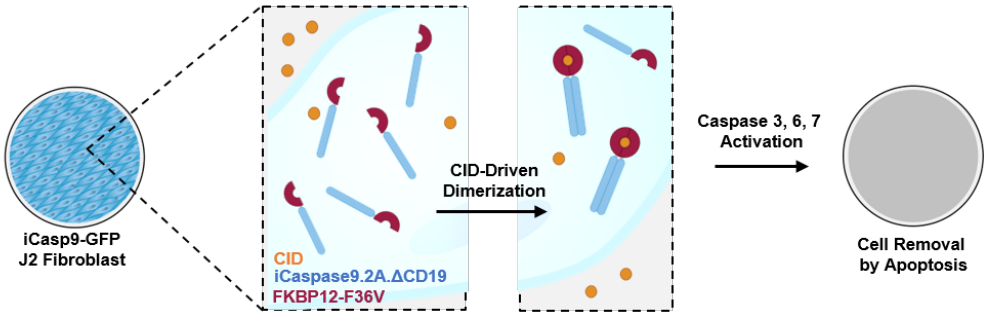

Figure 2-3: **Schematic for CAMEO: Controlled Apoptosis in Multicellular Tissues for Engineered Organogenesis.** 3T3-J2 fibroblasts bearing an iCasp9 suicide gene were treated with CID to induce iCasp9 dimerization, leading to apoptosis and elimination of the cells from culture. Adapted from [41].

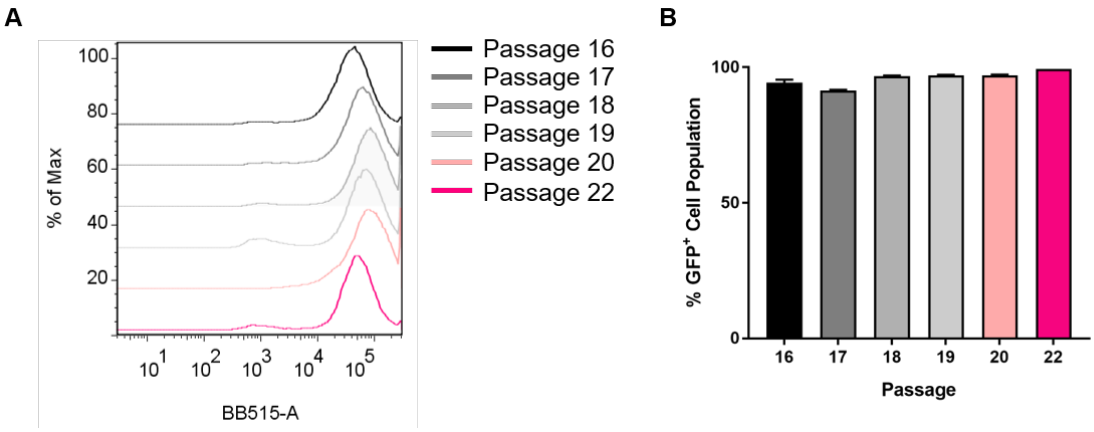

Figure 2-4: **iCasp9-GFP J2s maintain stable expression of transgenes.** (A) iCasp9-GFP J2s were analyzed by flow cytometry and (B) percentage of GFP$^+$ population was quantified for 7 passages. Adapted from [41].

[258]. However, bicistronic vectors with internal ribosome entry sites (IRES) have well-documented differences between the expression of the cap-dependent first gene (iCasp9) and the IRES-dependent second gene (GFP). Mizuguchi et al. showed that the second gene is often only expressed at a level that is equivalent to 20-50% of that of the first gene, as measured by protein activity [183]. In either case, our strategy for cell selection and purification (by sorting for the second gene, GFP) will either yield a 1:1 expression or a 2- to 5-fold higher expression of iCasp9 than GFP. By flow cytometry analysis, we confirmed that the GFP+ cell population appeared homogeneous for at least 7 passages, and the population remained >97% GFP$^+$ even at passage 20 (**Figure 2-4**). Taken together, this analysis suggests that the iCasp9-GFP J2 cell line was robustly modified and maintains

persistent transgene expression for a range of passages that extend beyond the usage for experiments in this work.

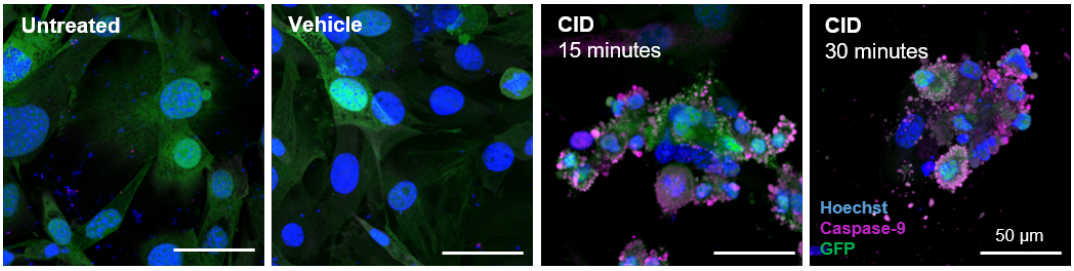

Figure 2-5: **iCasp9-GFP J2s are activated by CID.** CID-induced dimerization of iCasp9 unimers was detectable by immunofluorescence imaging. Cells were stained for caspase-9 (magenta) and counterstained with Hoechst to detect cell nuclei (scale bar = 50 μm). Adapted from [41].

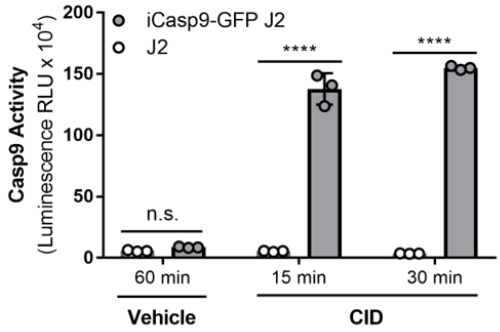

Figure 2-6: **iCasp9-GFP J2s underwent CID-induced activation of Casp9 activity.** CID treatment induced activation of caspase-9 cleavage activity (****$p<0.0001$ vs. time-matched, dose-matched J2s, n=3). Adapted from [41].

After GFP$^+$ J2 fibroblasts were exposed to CID, iCasp9 dimers were detected by staining with a caspase-9 antibody, confirming the expression of the bicistronic iCasp9-IRES-GFP vector (**Figure 2-5**). Compared to wild-type J2s, iCasp9-GFP J2s underwent significantly increased caspase-9 cleavage at 15 (16-fold) and 30 (18-fold) minutes after CID dosing (**Figure 2-6**).

To confirm that CID-triggered caspase-9 activation led to apoptosis, unfixed cells were stained with Annexin V, which binds to an early indicator of apoptosis, and SYTOX, a general marker of cell death, and analyzed by flow cytometry. The proportion of iCasp9-GFP J2s undergoing apoptosis increased in a time-dependent manner within the first hour after CID treatment (**Figure 2-7**). Lastly, we observed that CID-treated iCasp9-GFP J2s were

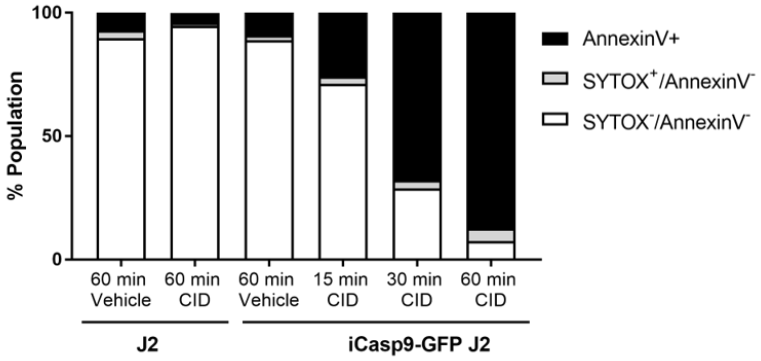

Figure 2-7: **CID-treated iCasp9-GFP J2s underwent apoptotic activity.** iCasp9-GFP J2s were treated with vehicle or CID and harvested at 1,5, 30, or 60 minutes post-treatment. Cells were stained with Annexin V (apoptosis marker) or SYTOX (general cell death marker) and analyzed by flow cytometry to quantify the extent of apoptotic activity (n=100,000 events). Adapted from [41].

efficiently removed from culture by 1 hour after exposure (**Figure 2-8**, <1% by cell viability for ATP). Prior studies using similar inducible iCasp9-based switches have observed similar time frames for rapid onset of apoptotic activity and subsequent cell death. Specifically, Straathof et al. created a similar transgenic population of human T cells and used FACS to sort for a population of GFP^{hi} cells. They observed apoptotic characteristics within 14 hours of dosing (and did not examine earlier timepoints), eventually leading to 99% of deletion [60]. Marin et al. observed an apoptotic phenotype (as measured by Annexin V, a marker of apoptosis) within 30 minutes after CID dosing [172], which corroborates our observation of the quick onset of apoptotic activity (**Figure 2-7**). Lastly, Di Stasi et al. observed in vivo elimination of up to 90% of their transgenic cell population within 30 minutes after dosing patients that were previously infused with iCasp9-expressing T cells [60]. Taken together, these results demonstrate that an iCasp9-bearing population of J2s could be treated with CID to quickly and efficiently eliminate them from culture by activating the apoptotic pathway.

2.2.2 2D Hepatic Ensembles are Compatible with CAMEO

Recapitulation of cues from the native hepatic microenvironment, including from cells, ECM, and soluble factors, has been found to lead to phenotypic rescue of primary hepatocytes as well as prolongation of longevity and function [84, 40, 287]. In our system, the incorpo-

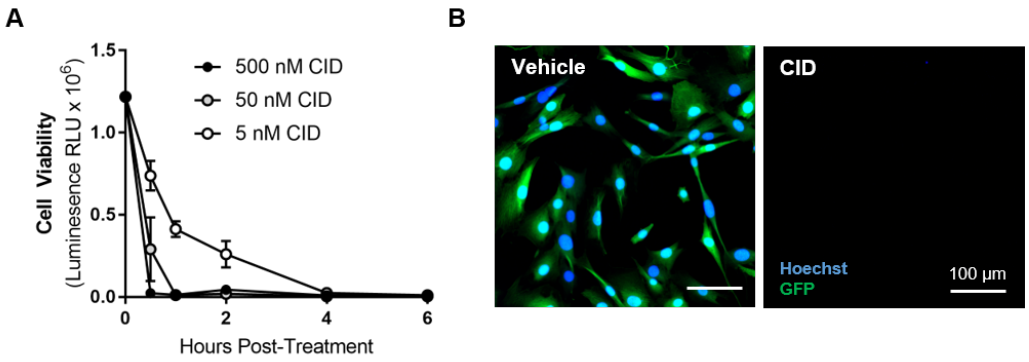

Figure 2-8: **CID-treated iCasp9-GFP-J2s were removed from culture after apoptosis.** (A) iCasp9-GFP J2s were treated with 5, 50, or 500 nM CID and viability was measured at 0.5, 1, 2, 4, and 6 hours post-treatment. (B) 24 hours after treatment, iCasp9-GFP J2s were not detected by immunofluorescence. Adapted from [41].

ration of J2 fibroblasts enhanced phenotypic stability of hepatocytes [116, 129, 152]. To study this phenomenon, we previously engineered an actuatable 2D platform to enable the manipulation of established co-cultures. Using this platform, the dependency of hepatocytes on fibroblasts was interrogated in 2D; it was found that despite an initial priming phase of direct cell-cell contact with fibroblasts, primary human hepatocytes did not maintain phenotypic stability if fibroblast juxtacrine and paracrine support were both removed [116]. We hypothesized that CAMEO-driven removal of fibroblast support would also be disruptive to hepatocyte culture in 2D. As a first step to test this hypothesis, we cultured primary human hepatocytes and J2 fibroblasts in a micropatterned co-culture (MPCC), in which we corroborated our past findings [129] that hepatocyte phenotypic stability is enhanced by J2 co-culture (**Figure 2-9**A). iCasp9-GFP J2 and J2 fibroblasts both provided support of multiple axes of liver function, including synthesis of albumin protein (**Figure 2-9**B), production of urea as a byproduct of nitrogen metabolism (**Figure 2-9**C), and expression of drug metabolism-related enzymes (**Figure 2-9**D), suggesting that genetic modification of J2s did not abrogate their capability to support hepatocytes. Throughout this work, we make use of the aforementioned readouts as a representative and stringent panel of readouts for the assessment of hepatocyte function.

Furthermore, hepatocyte albumin production was not abrogated if MPCCs were cultured with conditioned 'apoptotic' medium, suggesting that at least one axis of liver-specific function was not affected by exposure to neighboring apoptotic cells (Figure 2-10). Altogether,

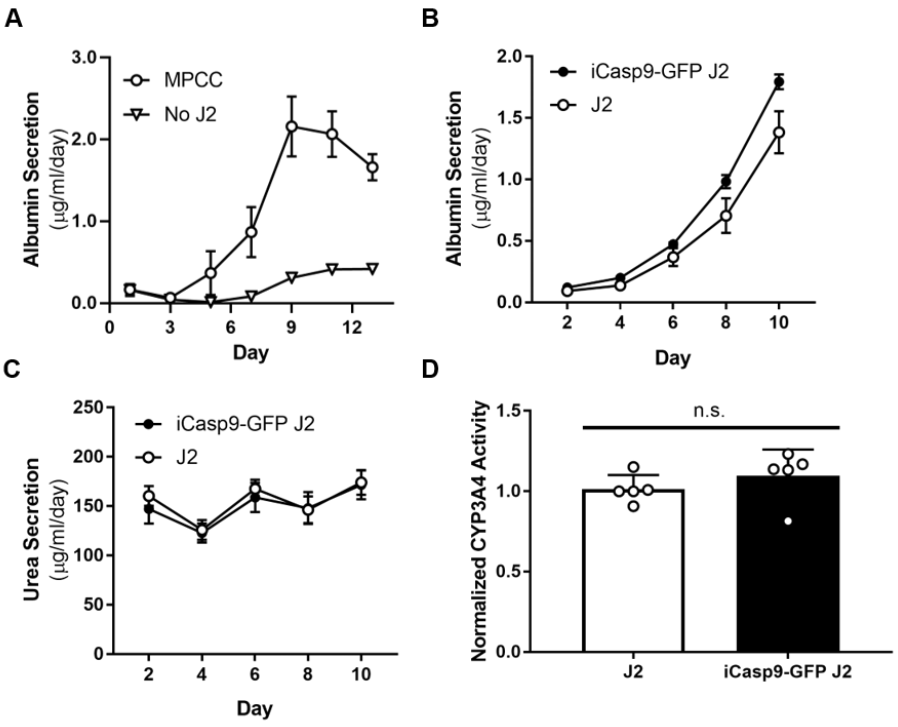

Figure 2-9: **PHH cultured in 2D MPCC format are supported by iCasp9-GFP J2 fibroblasts** MPCCs or pure hepatocytes were assayed for albumin secretion rate (A, n=3). MPCCs containing wild-type and modified J2s were assayed for albumin secretion rate (B, n=6), urea secretion rate (C, n=6), and basal expression of CYP3A4 (D, n=5, day 10). Adapted from [41].

these data suggest that CID-driven removal of stromal cells by apoptosis is a compatible system for probing phenotypic stability of hepatocytes in MPCCs.

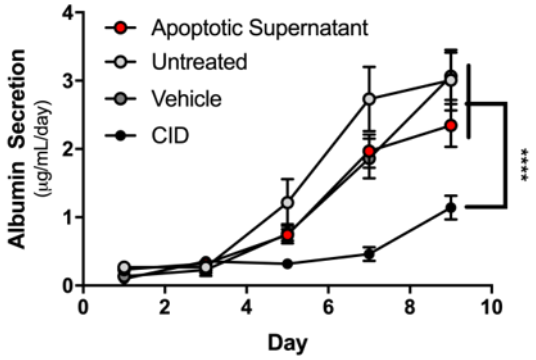

Figure 2-10: **PHH cultured in 2D MPCC format are not de-stabilized by treatment with media enriched with apoptotic cell fragments**. MPCCs were treated with conditioned apoptotic media, vehicle, CID or untreated and assayed for albumin secretion rate (n=4, ****$p<0.0001$ vs. CID).. Adapted from [41].

2.2.3 CID is not Acutely Toxic to 2D Hepatic Ensembles

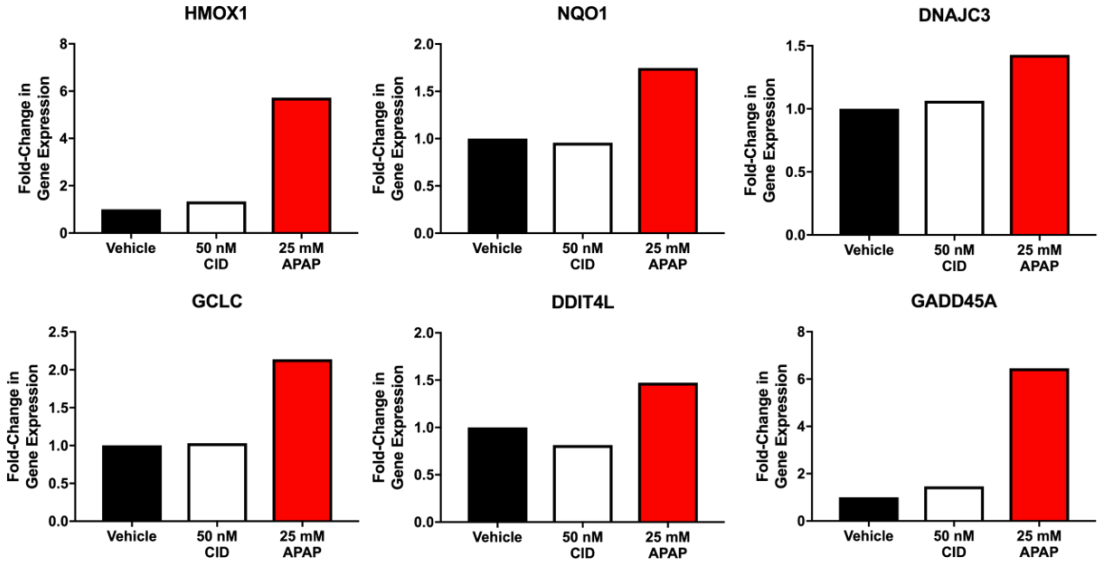

Figure 2-11: **CID does not have potent hepatotoxic or stress-related effects on primary human hepatocytes** Expression of genes (fold-change over vehicle control) associated with cellular stress and hepatic disease (n=2). Adapted from [41].

In addition to negligible effects of apoptotic cells in 2D hepatic ensembles, suggesting the lack of any apparent toxicity to co-cultured primary human hepatocytes, we also assessed specific hepatic markers for liver-specific damage by quantifying gene expression of a panel broadly related to hepatotoxicity and cellular stress. We treated 2D MPCCs with vehicle (as a negative control), CID (as the experimental condition) and acetaminophen (as the positive control, "APAP"; 25 mM).

We found a 1.3- and 5.7- fold increase in hemeoxygenase-1 (HMOX1) expression in CID- and APAP-treated MPCCs, which is expected because elevation of plasma HMOX1 is a marker of APAP-induced hepatotoxicity [80]. Relatedly, NADPH quinone oxidoreductase 1 (NQO1) underwent a 0.96- and 1.75- fold change in CID- and APAP-treated cultures compared to vehicle controls, respectively. NQO1 upregulation has been specifically described in human liver in response to APAP-induced hepatotoxicity and other disease states such as primary biliary cirrhosis [1]. We also evaluated expression of DnaJ Heat Shock Protein Family (Hsp40) Member C3 (DNAJC3), which is a known marker of endoplasmic reticulum stress, and has been shown to cause apoptosis of beta cells in vitro and in patient samples [160, 147]. We observed a 1.06- and 1.43-fold increase in DNAJC3 expression in CID- and

APAP-treated MPCCs compared to vehicle-treated cultures, respectively.

Broadly, we also compared the upregulation of several genes associated with cellular stress and DNA damage across various disease and injury contexts, including hepatocellular carcinoma [143, 88, 277]. We found upregulation of glutamate cysteine ligase catalytic subunit (GCLC; 1.03- and 2.14-fold), DNA damage inducible transcript 4 (DDIT4; 0.81- and 1.47-fold), growth arrest and DNA damage 45-alpha (GADD45A; 1.46- and 6.46-fold) in CID- and APAP-treated MPCCs compared to vehicle treated controls, respectively. Taken together, only very modest changes in injury-associated gene expression were observed in CID-treated MPCCs compared to more robust upregulation of these same transcripts in APAP-treated positive controls. We interpret this data to suggest that exposure to CID does not induce high levels of acute toxicity in primary human hepatocytes.

We next sought to eliminate inducible apoptosis gene-bearing cells in a multicellular culture, by treating iCasp9-GFP J2-bearing MPCCs with CID (**Figure 2-12**A). CID-dosed MPCCs displayed selective removal of the iCasp9-GFP J2 population (**Figure 2-12**B-C), whereas unmodified J2s plated in MPCCs were unaffected by CID exposure (data not shown).

2.2.4 2D Hepatic Ensembles Depend on the Sustained Presence of Stromal Cells

To query the dependence of hepatocytes on fibroblasts with CAMEO, we deleted fibroblasts from MPCCs by CID treatment at various time points and assessed the albumin production rate as a surrogate marker of phenotypic stability. We observed that the deletion of stromal cells resulted in loss of hepatocyte phenotypic stability at early (day 1), intermediate (day 3), and late (day 7) time points (**Figure 2-13**). Taken together, these data suggest that the function of primary human hepatocytes is heavily reliant on stromal support in this 2D MPCC configuration, which is consistent with our past 2D studies [116, 129].

2.3 Conclusion

In this work, we leverage an inducible apoptosis switch to study the temporal role of fibroblasts in the maintenance of phenotypic stability of hepatic tissue engineered models.

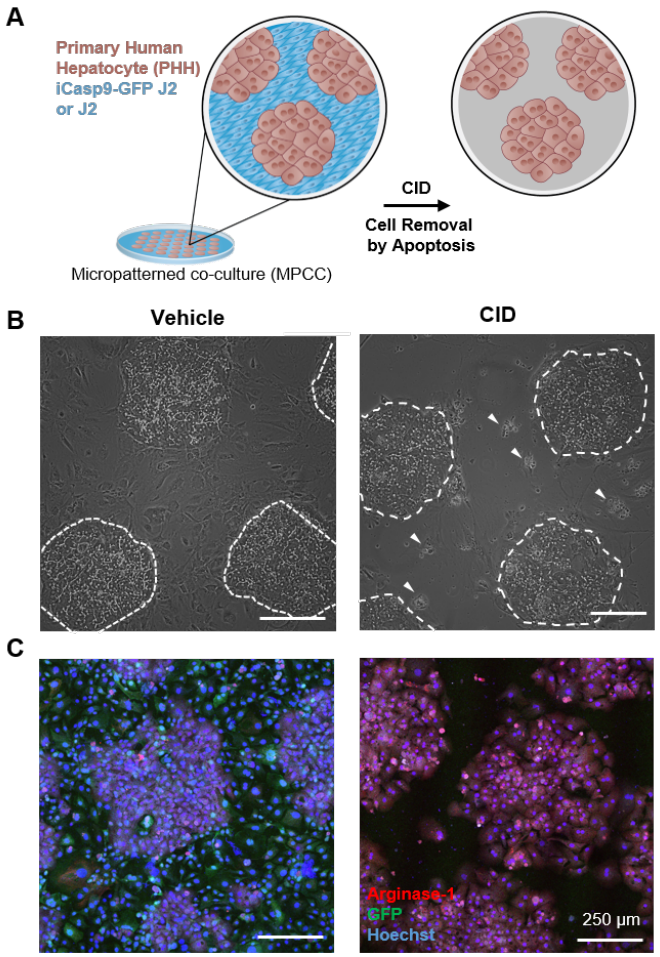

Figure 2-12: **CID treatment led to selective removal of iCasp9-bearing cells from 2D MPCCs** (A) MPCCs comprised of primary human hepatocytes (brown) and iCasp9-GFP J2 or wild-type J2 fibroblasts (blue) were treated with CID to remove iCasp9-GFP J2s by apoptosis. (B) Vehicle- or CID-treated MPCCs were visualized using brightfield microscopy or (C) stained and visualized by immunofluorescence imaging (scale bar = 250 μm). Adapted from [41].

Specifically, we engineered the 3T3-J2 mouse fibroblast line to constitutively express a caspase-9-driven apoptotic switch and used it to query the temporal dependence of primary human hepatocytes on stromal support. Previously, inducible caspase-9 has been deployed as a safety measure for engineered cell therapies (e.g. adoptive T cell therapy, engineered cell therapy, mesenchymal cell therapy) across a range of applications (e.g. regeneration, anti-cancer) [60, 81, 258].

Recently, inducible apoptosis gene-engineered stromal cells were used to probe the contribution of cancer-associated fibroblasts to metastatic potential in vivo [235]. In this work,

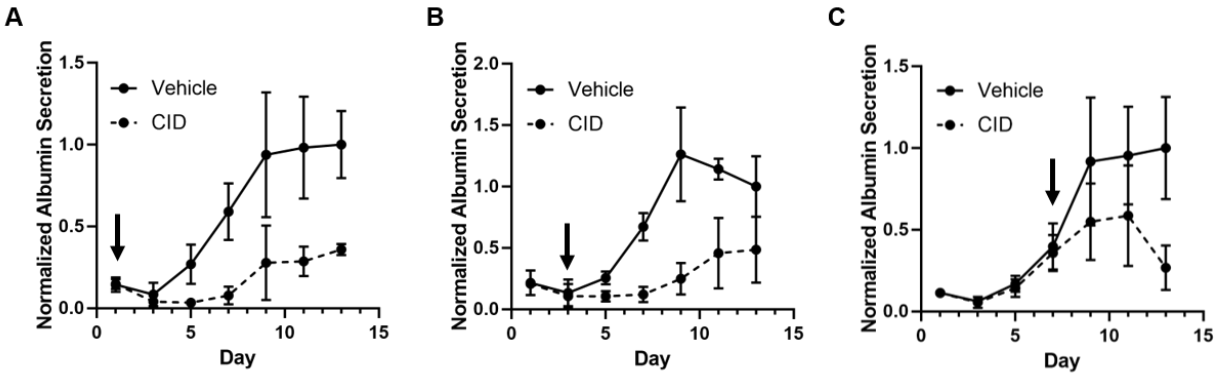

Figure 2-13: **2D MPCC cultures depend on the sustained presence of stromal cells** MPCCs were treated with CID at day 1 (A), 3 (B), or 7 (C) after initiating co-culture and assayed for albumin secretion rate (n=5, normalized to day 13, arrows indicate CID dose day). Adapted from [41].

we demonstrate a new use case for inducible apoptosis genes as tools for tissue engineering. Here, we show that iCasp9-bearing fibroblasts are amenable to quick, efficient, and robust removal. We show that iCasp9-bearing cells can be specifically and efficiently removed from 2D co-cultures. Using CAMEO, we demonstrate that fibroblasts enable significant enhancement of the phenotypic stability of hepatocytes in 2D MPCCs, which is consistent with our previous findings in a related 2D model [116].

2.4 Methods

2.4.1 Cell Culture

Primary cryopreserved human hepatocytes (Lot ZGF, 33-year-old, Caucasian, male; BioreclamationIVT) were maintained in high-glucose Dulbecco's modified Eagle's medium (DMEM) with 4.5 g/L glucose (CellGro) containing 10% (v/v) fetal bovine serum (FBS) (Gibco), 1% (v/v) ITS supplement (insulin, transferrin, sodium selenite; BD Biosciences), glucagon (70 ng/mL), dexamethasone (0.04 µg/mL), 0.015 M HEPES, and 1% (v/v) penicillin-streptomycin (Invitrogen). 3T3-J2 murine fibroblasts were a kind gift provided by Howard Green (Harvard Medical School) and were cultured in DMEM with 4.5 g/L glucose, 10% bovine serum, and 1% (v/v) penicillin-streptomycin.

2.4.2 Micropatterned Co-Cultures

Micropatterned co-cultures (MPCC) were fabricated as described previously [129, 170]. Briefly, collagen was adsorbed in each well of a 96 well plate (glass bottom), and then patterned using an elastomeric polydimethysiloxane mold and oxygen plasma gas ablation. Human hepatocytes were thawed and seeded (70k/well) on the collagen islands (500 µm with 1,200 µm center-to-center spacing). Adhered hepatocytes (10k/well) were allowed to spread overnight before fibroblasts were seeded for co-culture (7k/well).

2.4.3 Cell Line Generation and Validation

J2s were lentivirally transduced using the 3rd generation lentiviral system with an iCasp9-IRES-GFP plasmid (gift from David Spencer, Addgene; #15567 pMSCV-F-del Casp9.IRES.GFP; cloned in-house to a lentivirus plasmid backbone with an SFFV promoter) [258]. Briefly, plasmids were co-transfected into HEK-293T cells with pVSVG, pRSV-REV, and pMDLg/pRRE using the calcium phosphate transfection method. Assembled viruses were collected in the culture supernatant after 48 hours and precipitated using PEG-IT (SBI), resuspended in PBS, and stored at -80°C. To transfect J2s, virus was added to growth media and cultured overnight. iCasp9-GFP J2s were purified (top 15% of cell population; GFP) by FACS (FACSAria II, BD Biosciences). iCasp9-GFP J2 fibroblasts at passage 22 were grown at confluence for 2 weeks to mimic experimental culture conditions, without a decrease in the percentage of the cell population with positive GFP expression (Figure 2-4). iCasp9-GFP J2s were plated in monolayer and dosed with ethanol vehicle or CID (B/B homodimerizer, AP20187; rapalog; Takara/ClonTech) at a concentration of 50 nM (1:10,000 dilution) unless otherwise noted in the text. Cultures were then assayed for cell viability using the CellTiter-Glo® Luminescent Cell Viability Assay (Promega), for caspase-9 activation using the CaspGLOW™ Fluorescein Active Caspase-9 Staining Kit (Thermo Fisher Scientific) and Caspase-Glo®9 Assay Systems (Promega), or stained with the Pacific Blue™ Annexin V/SYTOX™ AADvanced™ Apoptosis Kit (Thermo Fisher) to identify apoptotic cells by flow cytometry (>100,000 cells analyzed per condition).

2.4.4 CID Treatment

MPCCs were dosed with 50 nM CID (1:10,000 dilution of stock prepared in ethanol) for all co-culture experiments.

2.4.5 Biochemical Assays

Spent supernatant was collected from cultures every other day and stored at -20°C. Human albumin was quantified using an enzyme-linked immunosorbent assay using a sheep anti-rat albumin antibody (ELISA) (Bethyl Laboratories) and 3,3',5,5'-tetramethylbenzidine (TMB, Thermo Fisher). Urea concentration was measured using a colorimetric (diacetylmonoxime) assay with acid and heat (Stanbio Labs). CYP3A4 activity was assessed with the luminogenic P450-Glo^{TM} CYP450 assay kit (Promega) for nonlytic assays using cultured cells. Cultures were pre-treated with 25 µM rifampin or 1:1000 DMSO vehicle control prepared in hepatocyte maintenance media for 72 hours (daily replenishment) where indicated.

2.4.6 Immunofluorescence Imaging

For immunostaining of cellular constructs, tissues were fixed in 4% paraformaldehyde. For identification of primary human hepatocytes, tissues were incubated with primary antibody against human arginase-1 (rabbit, 1:400; Sigma-Aldrich) followed by Alexa Fluor® 546-conjugated rabbit anti-human secondary antibody (1:1000; Life Technologies). Alternatively, hepatocytes were visualized by pre-labeling with 1 μM CellTracker Deep Red (Thermo Fisher) for 20 minutes at 37°C. Nuclei were stained with Hoechst (1:2000).

2.4.7 Imaging

Fiji was used to uniformly adjust brightness/ contrast, pseudocolor, and merge images. A Nikon Ti-E inverted epifluorescent microscope was used to capture brightfield and fluorescence images.

2.4.8 Statistical Analysis

All data are expressed as mean ± standard deviation and/or visualized as dot plots (n = 2-6 as indicated). Statistical significance ($\alpha = 0.05$) was determined using the appropriate

statistical test (unpaired 2-tailed t-test, 1-way ANOVA, 2-way ANOVA), and followed by multiple comparisons testing (Tukey's post hoc test) (GraphPad).

2.5 Acknowledgements

Dr. Arnav Chhabra and **Dr. Hyun-Ho Greco Song** were crucial thought and experimental partners for this project, which is now captured in two published manuscripts as well as a patent co-authored by **Prof. Sangeeta Bhatia** and **Prof. Christopher Chen**.

This work would not be possible without assistance from **Glenn Paradis**, **Michael Jennings**, **Michele Griffin**, **Jeffrey Wyckoff**, and **Eliza Vasile** of the Flow Cytometry and Imaging cores of the Koch Institute Swanson Biotechnology Center. I will always remember the "kid in a candy shop" reaction I had in 2014 during PhD interview weekend, when I walked into the Koch Institute and was given a tour of all the Core Facilities and their very dedicated technical staff. Their constant efforts to keep the cores running and provide valuable scientific input are key reasons why the Koch Institute is asscoiated with scientific excellence. I am incredibly lucky to have been a part of this supportive, intellectually-engaging community.

The late **Howard Green** of Harvard Medical School provided the 3T3-J2 fibroblast cell line as a kind gift. **Wilson Wong** of Boston University was crucial to discussions surrounding the feasibility of this work as well as brainstorming for next steps and optimization.

This work was supported in part by the NIH (R01 EB008396, R01 EB000262, UG3 EB017103), Koch Institute Support (core) Grant P30-CA14051 from the National Cancer Institute, the National Science Foundation Cellular Metamaterials Engineering Research Center, and the Boston University Biological Design Center.

Chapter 3

DISCOVER: New Insights into Cell-Cell Interactions of Engineered Hepatic Ensembles

3.1 Introduction

In the previous Chapter, we introduced CAMEO as a synthetic biology-driven technology for enabling user-controlled, precise manipulation of cell-cell interactions. We demonstrated the utility of this technology by probing the importance of cell-cell interactions in 2D hepatic ensembles consisting of hepatocyte-fibroblast co-cultures in a micropatterned 96-well culture. We found that hepatocytes require sustained presence of fibroblasts for long-term phenotypic stability, which corroborates past work by Hui et al. in which an actuatable micromechanical comb system was used to probe a similar hepatocyte-fibroblast co-culture [116, 117].

The true utility of the CAMEO technology extends beyond use cases with complex 2D architectures, such as the micropatterned co-culture described in the previous chapter, which consists of hepatocyte "islands" surrounded by fibroblasts. We envisioned that CAMEO can also address use cases in 3D multicellular cultures. In this Chapter, we lay the groundwork for applying CAMEO to 3D hepatic ensembles, and demonstrate its ability to elucidate new mechanistic information that describes the dynamic underlying cell-cell interactions that drive phenotypic stability.

Here, we cultured 3D hepatic ensembles, which consist of hepatocyte-fibroblast spheroids in fibrin hydrogel scaffolds. This culture system was originally described by Stevens et al. and highlights the importance of microscale organization within cellular compartments in 3D engineered tissues, as well as the inclusion of supportive stromal cells for both in vitro performance and in vivo persistence in the context of an implanted engineered graft [257, 256].

3.2 Results & Discussion

3.2.1 Optimization of CAMEO for 3D Hepatic Ensembles

In order to adapt the CAMEO technology to use cases involving 3D microenvironments, we first assessed the ability of CID to drive cell apoptosis on short time frames. Subsequently, we also tuned the aggregation speed of hepatocyte-fibroblast spheroids in accordance with findings from Hui et al., in which a crucial "switch" in hepatocyte-fibroblast dependence occured after 18 hours of co-culture [116].

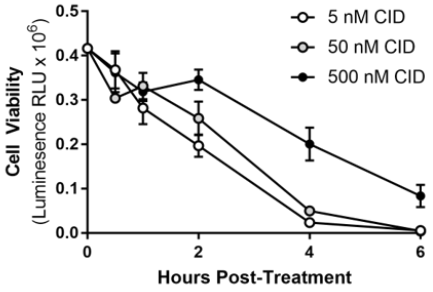

Figure 3-1: **CID quickly deletes iCasp9-bearing fibroblasts.** iCasp9-GFP fibroblasts were encapsulated in fibrin hydrogels and treated with CID, then assayed for viability (n=3). Adapted from [41].

First, we sought to confirm the effectiveness of CID treatment for the elimination of iCasp9-GFP fibroblasts embedded in a hydrogel. We encapsulated iCasp9-GFP fibroblasts in a fibrin hydrogel and treated with CID, and found that fibroblast viability was undetectable by 6 hours (**Figure 3-1**). Our observation of cell killing time in 3D was approximately 6x (1 hour vs. 6 hours) longer than our findings in 2D (**Figure 2-8**). We hypothesize that altered cellular cue presentation in 2D vs. 3D, which has been reviewed in depth elsewhere

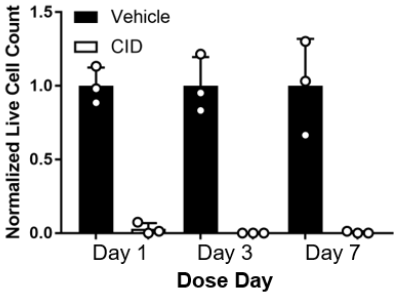

Figure 3-2: **iCasp9-GFP fibroblasts are robustly deleted from culture.** iCasp9-GFP fibroblasts were encapsulated in fibrin hydrogels and treated with CID at day 1, 3, or 7 after encapsulation. Number of cells (by nuclei count) present in the culture at day 21 were quantified for 3 representative fields of view per sample. Adapted from [41].

.

[7], may lead to increased resistance to apoptosis in 3D. Other potential contributors could be a reduction in effective CID concentration, as we prepared 50 nM CID in hepatocyte growth medium for both 2D (100 μL volume of supernatant) and 3D (100 μL volume of supernatant, effectively "diluted" by 2-fold when applied to a 100 μL cell-laden hydrogel) cultures; however, a 10-fold increase in the CID concentration (i.e. 5 vs. 50 nM CID, **Figure 3-1**) did not compensate for the killing kinetics, suggesting that a 1:1 correction of CID concentration is not able to speed up cell killing speed. We also do not expect that diffusion limitation would greatly hinder the transport of CID small molecule peneration into our 3D cultures.

In the future, we may employ CAMEO in epithelial cells; relatedly, more sophisiticated cell populations such as hepatocytes, the expression of hepatic efflux pumps - which are known to be upregulated in 3D - regularly eliminate xenobiotics, and could also act on CID [84]. Additionally, cell-matrix interacitons lead to the activation of focal adhesion kinase, which need to be cleaved by the caspase family before the onset of apoptotic activity [297, 2]. Furthermore, in 3D epithelial systems, it has been shown that polarized structures can drive protection of cultured cells against apoptosis, compared to cultures with non-polarized structures [295].

In this study, we selected the CID concentration for our studies that would lead to near-complete killing of fibroblasts in each of our 2D and 3D hepatic ensemble systems. Future investigation can further explore the cell-cell and cell-matrix interactions that control the

onset of apoptosis, as well as the kinetics of apoptotic activity, and may contributed toward engineered control of cell killing speed.

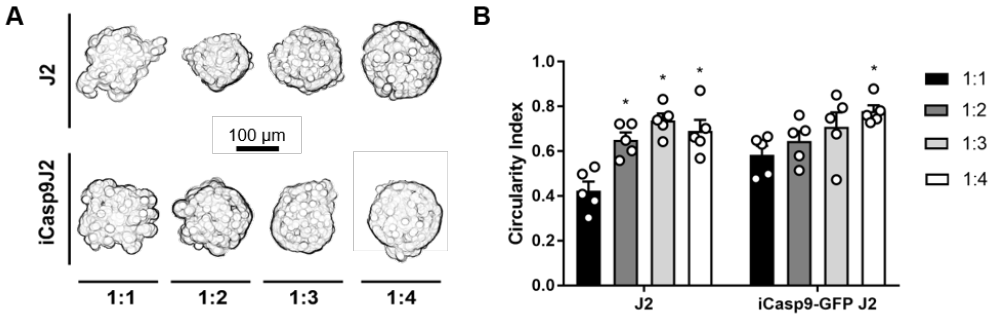

Figure 3-3: **Spheroid compaction kinetics were accelerated by increasing fibroblast:hepatocyte ratio.** (A) Hepatocytes and fibroblasts were cultured in microwells at an increasing fibroblast:hepatocyte ratio (1:1 to 1:4; with 500k hepatocytes in each sample) and imaged at 24 hours post-seeding. (B) Images were quantified for circularity as a measure of compaction (n=5, *p<0.05 vs. stromal cell-matched 1:1 spheroids). Adapted from [41].

.

Furthermore, we assessed the robustness of cell-killing by performing a long-term experiment in our 3D hydrogel environment. We cultured iCasp9-GFP fibroblasts embedded in fibrin hydrogels, treated with 50 nM CID, and then observed cultures for cell regrowth over a time period of 3 weeks (to match functional experiments described later in this Chapter). We observed either negligible or undetectable cell growth in multiple fields of view of the fixed samples at the endpoint (**Figure 3-2**). Notably, fibroblasts were not growth-arrested prior to culture, suggesting that lack of regrowth is either due to complete removal of fibroblasts, or a remnant quiescent population.

In our prior work, we found that phenotypic stability and longevity of primary hepatocytes cultured as 3D microtissues were transiently supported by pre-aggregation to increase homotypic cell-cell interactions, and were further enhanced upon inclusion of J2 fibroblasts [152]. Thus, here we incorporate iCasp9-GFP J2 fibroblasts into these 3D hepatic ensembles, which were fabricated by plating primary human hepatocytes and fibroblasts in microwells in order to facilitate physical cell-cell contacts, as previously described [257, 256]. Optimal overnight aggregation into stable spheroids was achieved by increasing the amount of fibroblasts co-seeded in the microwells (**Figure 3-3**). We also attempted to accelerate aggregation by increasing the number of hepatocytes per microwell and did not observe any appreciable

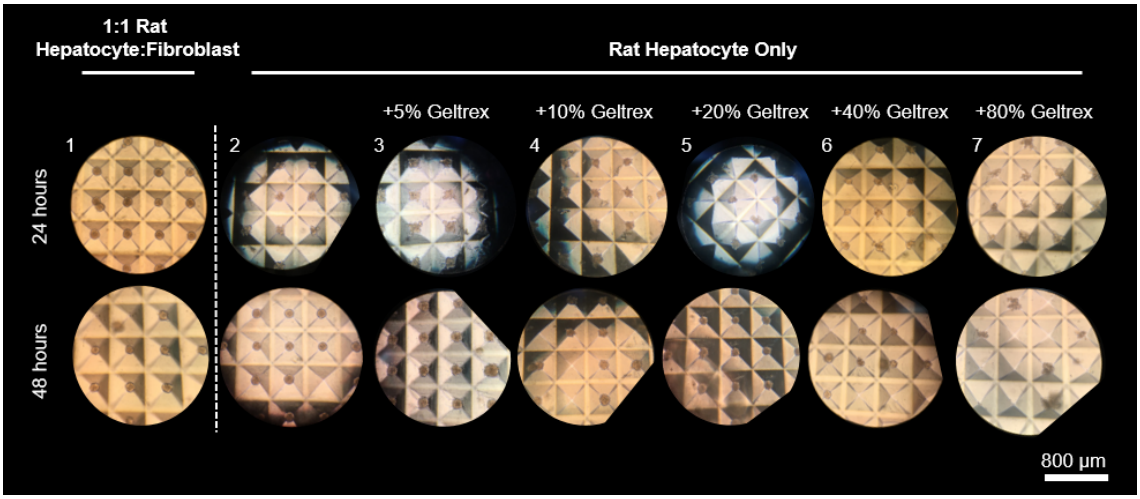

Figure 3-4: **Geltrex® does not accelerate aggregation of primary hepatocytes.** Primary rat hepatocytes were cultured in microwell molds with media supplemented with 5-80% Geltrex®. Brightfield images were captured at 24 and 48 hours post-seeding. Primary rat hepatocytes were co-seeded at a 1:1 ratio with normal human dermal fibroblasts as control. Unpublished data.

differences within 1 day post-seeding (data not shown). Lastly, we supplemented the cell seeding solution with Geltrex®, which is a basement membrane matrix mix that has been previously shown to promote spheroid aggregation [66], and is compatible with seeding in ultra-low attachment surfaces that are similar to the passivated microwells we use to prepare spheroids. We tested the addition of Geltrex® as a possible accelerant of spheroid aggregation in an attempt to de-couple the kinetics of compaction from the composition of the spheroid microstructure. As a representative model, we cultured primary rat hepatocytes (instead of primary human hepatocytes) with neonatal human dermal fibroblasts at a 1:1 ratio in microwell molds and observed full compaction within 24 hours (**Figure 3-4**, Column 1), which is consistent with our prior experience that primary rat hepatocytes achieve spheroid compaction more quickly than primary human hepatocytes, which can take upward of 5 days [16]. When we cultured primary rat hepatocytes alone in microwell molds, we did not observe spheroid compaction at the 24 hour timepoint, but did observe it at the 48 hour timepoint (**Figure 3-4**, Column 2). To query the impact of doping Geltrex® into the compaction media on hepatocyte aggregation, we supplemented the media with 5 to 80% Geltrex® at the time of seeding. Even at the highest concentration of Geltrex® supplementation, we did not observe accelerated kinetics of compaction (**Figure 3-4**, Column 3-7). Of note, typical Geltrex® supplementation is usually $<5\%$ v/v%, and in this experiment

we tested supplementation in regimes that compromised the presence of relevant nutrients in the growth media to test the full range of basement membrane matrix supplementation.

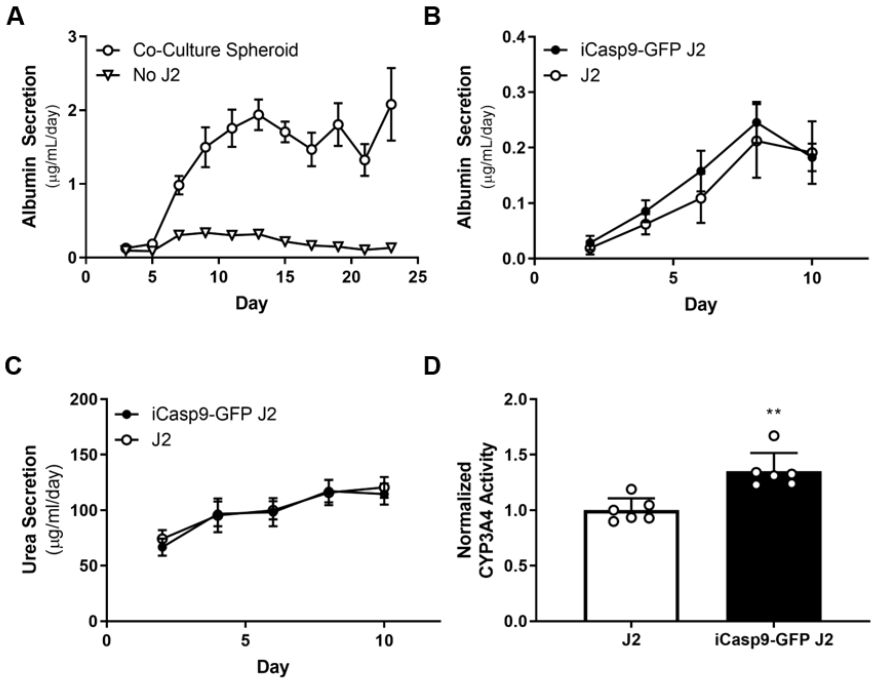

Figure 3-5: **iCasp9-GFP J2s support primary human hepatocyte in 3D ensemble format.** (A) 3D cultures consisting of pure hepatocytes or hepatocytes and fibroblasts were assayed for albumin secretion rate (n=9). J2s and iCasp9-GFP J2s were co-cultured with hepatocytes in spheroid-laden hydrogels and assay for albumin secretion rate (B, n=6), nitrogen metabolism (C, n=6), and basal CYP3A4 expression (D, n=6, **$p<0.001$). Adapted from [41].

For all subsequent studies, spheroids were prepared with 1:4 primary human hepatocyte:fibroblast seeding concentration, and we consistently achieved overnight compaction across multiple experiments. Resulting spheroids were encapsulated in a 10 mg/mL fibrin hydrogel (crosslinked with 1.25 U/ml thrombin). Fibroblast co-culture, which provided supportive cell-cell interactions and increased aggregation stability, significantly improved the rate of primary human hepatocyte albumin secretion from the ensembles (**Figure 3-5**A). Spheroid-laden hydrogels containing either J2s or iCasp9-GFP J2s both exhibited enhanced synthetic (albumin production; **Figure 3-5**B), metabolic (nitrogen metabolism; **Figure 3-5**C), and detoxification (CYP3A4 activity; **Figure 3-5**D) functions of hepatocytes.

3.2.2 CAMEO Enables On-Demand Removal of Fibroblasts from Embedded 3D Co-Cultures

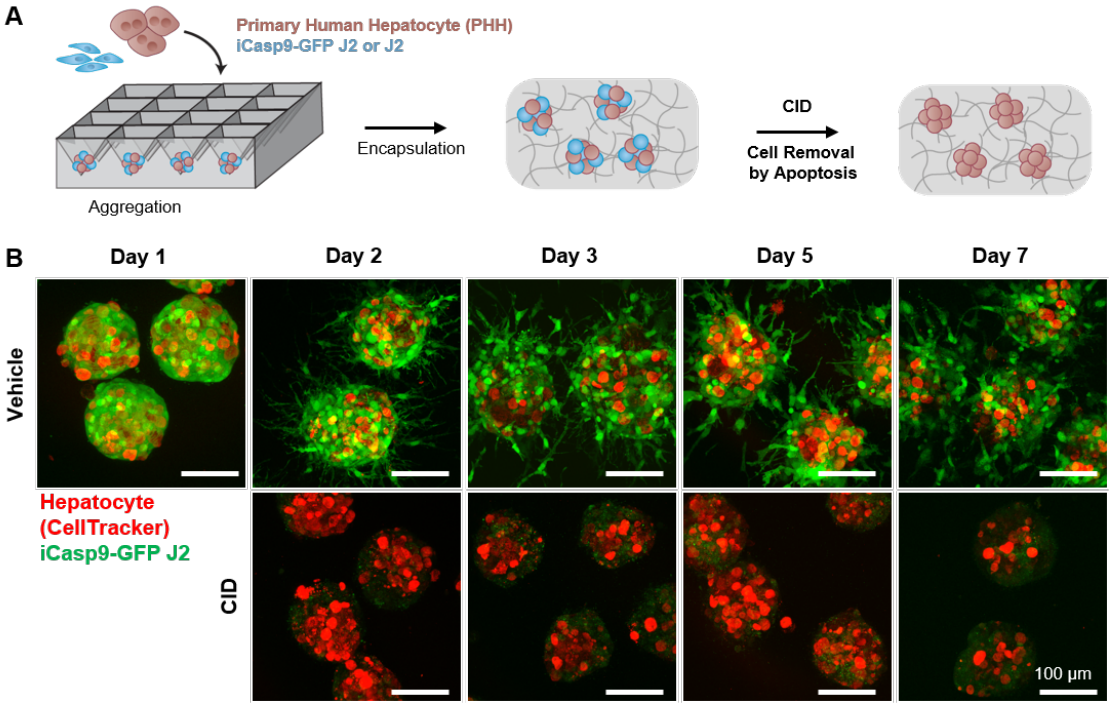

Figure 3-6: **iCasp9-GFP J2s were robustly removed from spheroid co-cultures after exposure to CID.** (A) Hepatocytes were aggregated with fibroblasts in microwell molds and treated with CID to remove fibroblasts via apoptosis. (B) Spheroid-laden hydrogels were treated with vehicle or CID on day 1 and imaged on day 1 through day 7 to assess the robustness of fibroblast elimination (scale bar = 100 μm). Adapted from [41].

We assessed the specificity of CAMEO in 3D by culturing hydrogel-encapsulated, multicellular spheroids (in which iCasp9-bearing fibroblasts are placed in close proximity to hepatocytes) and treated the ensembles with CID in an attempt to specifically eliminate iCasp9-GFP fibroblasts (**Figure 3-6**A). In these spheroid-laden hydrogel cultures, CID was able to access iCasp9-GFP J2s, leading to their robust and specific deletion throughout the hydrogel, without any apparent toxicity to co-cultured hepatocytes (**Figure 3-6**B). These results suggest that CAMEO can be employed by dosing embedded co-cultures with CID to trigger the removal of inducible apoptosis gene-bearin cells in 3d multicellular ensembles.

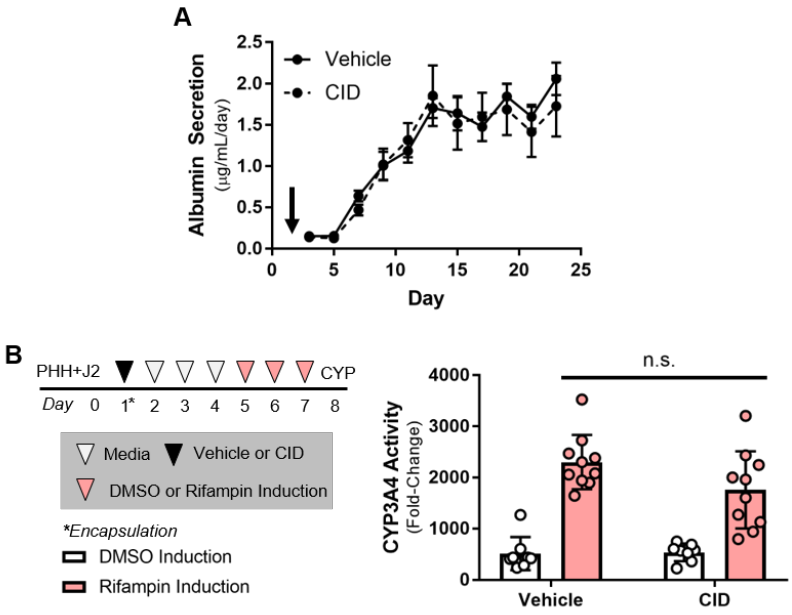

Figure 3-7: **Fibroblasts are not required to maintain hepatocyte function in 3D spheroid-laden cultures.** (A) Spheroid-laden hydrogels were dosed with CID on day 1 after co-culture initiation and albumin secretion rate was assayed for 3 weeks of culture (n=9). Fibroblast-depleted (CID) and fibroblast-intact (vehicle) cultures were treated with rifampin for 72 hours and assayed for induction of CYP3A4 activity (n=8-10). Adapted from [41].

.

3.2.3 Fibroblasts are Dispensable for Maintenance of Hepatocyte Function in 3D Spheroid-Laden Cultures

To probe the dependence of hepatocyte phenotypic stability on fibroblast co-culture in 3D, we deleted fibroblasts from spheroid-laden hydrogel cultures using CAMEO after 1 day of hepatocyte-fibroblast co-culture (**Figure 3-6**A). While 2D MPCC cultures were found to be dependent on fibroblast interactions for the extent of our experiment (1.5 weeks, **Figure 2-13**), fibroblast-depleted 3D cultures exhibited stable phenotype, as detected by albumin secretion rate, for up to 3 weeks (**Figure 3-7**A). Furthermore, fibroblast-depleted and fibroblast-intact cultures underwent similar induction of CYP3A4 activity in response to rifampin treatment (**Figure 3-7**B). Notably, when CID-triggered iCasp9-GFP J2 deletion was delayed until later time points (after 3 or 7 days of hepatocyte-fibroblast co-culture), hepatocyte function was negatively impacted, suggesting that primary hepatocytes cultured with J2s and embedded in fibrin are sensitive to deletion kinetics (**Figure 3-8**). Taken

together, these findings, enabled by CAMEO, demonstrate that there is a window of opportunity for fibroblast deletion in this particular tissue engineered context.

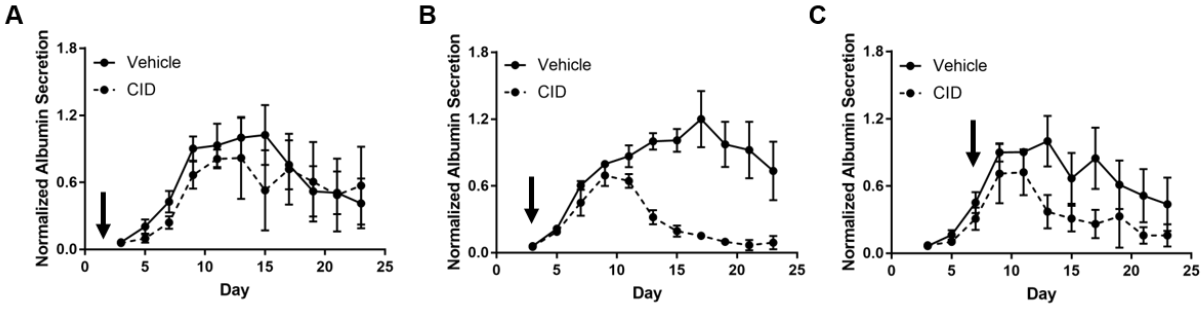

Figure 3-8: **Late removal of fibroblasts from 3D hepatic ensembles led to decreased liver-specific function.** Spheroid-laden hydrogels were treated with CID at day 1 (A), 3 (B), or 7 (C) after initiating co-culture and assayed for albumin secretion rate (n=9, normalized to day 15, arrows indicate dose day). Adapted from [41].

3.2.4 Effects of Fibroblast Removal at Later Stages of Co-Culture

As discussed above, later deletion (i.e. 3 or 7 days after initiation of hepatocyte-fibroblast co-culture) of fibroblasts from 3D hepatic ensembles had negative effects on hepatocyte function (**Figure 3-8**). It is possible that irregular apoptotic activity was linked to a pathophysiological process, which has been previously described in fetal and adult liver to be implicated in phenotypic dysfunction, tumorigenesis, and fibrosis/cirrhosis [293]. Poor hepatocyte function at later stages may also be due to a "bystander injury" effect caused by apoptosis of target cells. In anti-cancer therapy, the phenomenon refers to an unexpectedly large tumor-killing effect in the context of herpes simplex virus thymidine kinase (HSV-TK) inducible suicide gene therapy. In this approach, dosing ganciclovir (product which undergoes phosphorylation-based activation in TK-expressing cells) killed not only TK-expressing cells, but also neighboring non-TK-expressing cells. Multiple groups have converged upon a mechanism that invovles the expression of gap junction channels (involving connexin 32 and connexin 43), which enabled the cell-to-cell transfer of toxic ganciclovir metabolites [178, 285, 171].

We performed a literature-based analysis to assess the likelihood of gap channel-based

transfer of apoptotic intermediates or dimerized iCasp9 unimers between iCasp9-expressing and wild-type cells. Kim et al. demosntrated in a 2D co-culture of primary rat hepatocytes and 3T3 J2 murine fibroblasts that primary rat hepatocytes express connexin 32 and connexin 26, and murine fibroblasts expression connexin 43 at homotypic interfaces [132]. IN their study, heterotypic gap junctions were not detected, through the presence of fibrbolasts supported the expression homotypic hepatocyte gap junction proteins and hepatic function. In our 3D spheroid-laden hydrogels, which consist of primary *human* hepatocytes and murine fibroblasts, the expression of gap junction proteins that can form direct intecellular communication channels has yet to be evaluated. Relatedly, Karademir et al. elucidated the residues that are responsible for docking incompatibiltiy between connexin 36 (expressed by primary rat hepatocytes as per Kim et al. [132]) and connexin 43 (expressed by murine fibroblasts, as per Kim et al. [132]). Their study showed that rational substitution of multiple amino acid residues at the docking interface was necessary to enable stable binding [124]. Taken together, we do not expect to observe an iCasp9-specific bystander effect due to gap junction communication and transfer of apoptotic intermediates such as dimerized iCasp9 unimers. In a future study, we could directly evaluate the extent of any heterotypic gap junction communication and its relevance to a possible iCasp9-specific bystander effect by modulating gap junction function with a small molecule inhibitor such as 18β-glycyrrhetinic acid (which has been shown to be compatible with similar hepatocyte-fibroblast co-cultures) [132], or by manually introducing apoptotic intermediates, apoptotic bodies, or fluorescent dye (e.g. Lucifer Yellow for dye coupling studies) via microinjection. Notably, others have also concluded that the bystander effect is likely to be less relevant for suicide gene therapies driven by iCasp9 [299].

3.2.5 Presentation of Cues in 2D and 3D Microenvironments

A key finding in this work is that removal of stromal cells at early timepoints does not affect hepatocyte spheroid function (**Figure 3-8**). Of note, this finding is not reproduced in a similar 2D model (**Figure 2-13**), suggested that differences in the cell microenvironment across 2D and 3D contexts, such as presentation of cell-cell and cell-matrix interactions, may shed light on the underlying mechanism. Such interactions have been studied at length both within and beyond our group, though efforts have not yet pointed at a single or set of factors

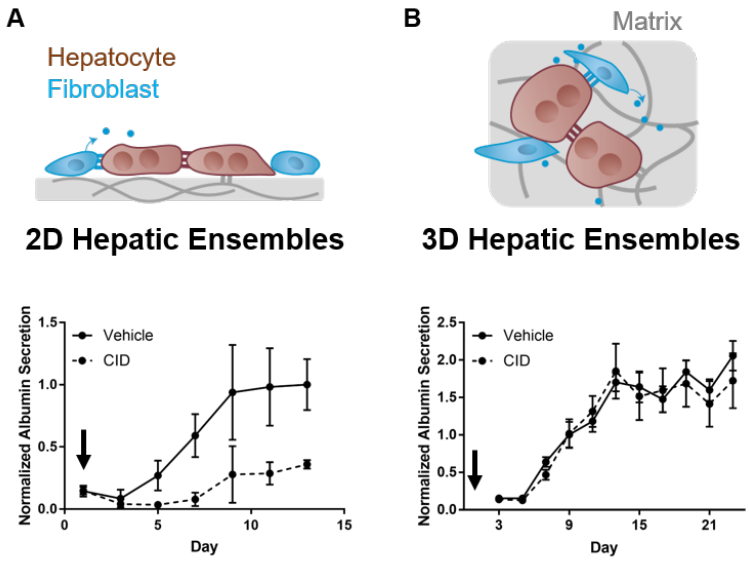

Figure 3-9: **Differential presentation of cues across culture formats may drive co-culture effects.** 2D hepatic ensembles (A) and 3D hepatic ensembles (B) consist of drastically different cell-cell and cell-material presentation, which may give rise to differences in effects on hepatocyte phenotype after fibroblast removal. Albumin plots of response to CID-triggered removal of fibroblasts are borrowed from **Figure 2-13**A and **Figure 3-8**A. Adapted from [41].

that can presented in a synthetic, acellular format to rescue primary human hepatocyte function [131, 86, 101, 130, 233, 234]. Studies of hepatocyte-only cultures have identified multiple factors which comprise the microenvironment that stabilize hepatocyte phenotypic stability [164, 158]. The niche is further modified in the presence of supportive fibroblasts, and includes juxtacine cadherin-based interaction (i.e. E-cadherin between hepatocytes [164]; T-cadherin between hepatocytes and fibroblasts [50]), paracrine interactions [116], and cell-matrix interactions [212].

Taken together, our findings with 2D and 3D hepatocyte-fibroblast ensembles using CAMEO motivated us to focus on differences in cell-cell interactions in the first 24 hours of co-culture. Below, we list the major differences in presentation of cues within the microenvironment, which may be responsible for the differential impact of fibroblast removal from our hepatic ensembles:

- juxtacrine interactions
- paracrine signaling

- autocrine signaling
- cell-matrix adhesion
- retention of biologically active cues in the matrix (e.g. sequestered paracrine factors, apoptotic debris)
- changes in nutrient concentration and oxygen tension
- *mechanical stress, due to physiological shear - which is more pertinent to microphysiological systems such as organ-on-chip platforms, and will not be discussed further in this body of work*

Most of the described interactions can occur between cells of the same identity (i.e. homotypic hepatocyte-hepatocyte interactions) or distinct identities (i.e. heterotypic hepatocyte-fibroblast interactions). As discussed above, it is well appreciated through these works that hepatocyte-fibroblast interactions are complex and multifactorial, and that the presentation of a single component from the hepatocyte-fibroblast interactome is not likely to be sufficient for rescuing and stabilizing hepatocyte phenotype. In the following experiments, we instead take the approach of preserving the entire interactome, and systematically removing particular types of interactions from the categories above. We selected elements of the interactome that were reasonably supported by literature, and also had available reagents and methods to enable precise manipulation.

3.2.6 Retention of Fibroblast-Derived Cues Does Not Drive Phenotypic Stability of Hepatocytes

After initial rescue with stromal support, it has been shown that presentation of certain supportive cues can enhance hepatocyte phenotypic stability [116, 129]. In our 3D spheroid-laden fibrin hydrogel cultures, apoptotic debris and fibroblast-derived paracrine factors and matrix are trapped in the hydrogel after CID-triggered deletion of fibroblasts 3-10, which may constitute a persisting supportive milieu for the hepatocytes. In 3D cell-laden hydrogels treated with CID, resultant apoptotic bodies are retained in the hydrogel matrix for the duration of a 3-week culture in vitro. To visualize, we encapsulated iCasp9-GFP fibroblasts in fibrin hydrogels and dosed with 50 nM CID or vehicle control. After fixation, we

stained samples for DNA (Hoechst) and apoptotic DNA nicks (TUNEL) and found higher amounts of TUNEL$^+$ DAPI$^+$ colocalization in CID-treated cultures (82% in CID-treated vs 0% in vehicle-treated, (**Figure 3-10**)). In contrast, residual apoptotic bodies in 2D cultures began to to detach from the tissue culture plastic surface within 30 minutes post-dose and were not readily detectable after downstream fixation and processing for brightfield and immunofluorescence imaging (data not shown). To test the hypothesis that retained apoptotic debris plays a major role in hepatocyte phenotypic stability, we focused on modifying the presence of fibroblast-derived components in lng-term culture after CID dosing by either dosing CID before fibrin encapsulation, or by encapsulating aggregating a biomaterial with reduced capacity to sequester proteins.

First, we dosed co-cultures with CID prior to encapsulation in fibrin hydrogels (instead of after encapsulation) and removed apoptotic debris and conditioned supernatant by differential centrifugation (**Figure 3-11**A). Since protocols for collection of apoptotic bodies require centrifugation speeds upwards of 1-2,000xg [50, 4], we were confident that we achieved sufficient depletion of the apoptotic body fraction, as well as other components of the conditioned supernatant, which have even smaller mass and would thus require even greater centrifugation speeds to pellet. After removing apoptotic bodies and conditioned supernatant, we encapsulated fibroblast-depeleted spheroids in fibrin hydrogel with fresh medium. We did not observe any significant differences in albumin secretion between the CID pre-encapsulation condition (i.e. hepatocyte-fibroblast spheroids dosed with CID prior to encapsulation), and the CID post-encapsulation conditions (i.e. hepatocyte-fibroblast spheroids dosed after encapsulation), suggesting that apoptotic debris and other retained fibroblast-derived factors were not the main drivers of hepatocyte phenotypic stability (**Figure 3-11**B).

Additionally, we reduced the retention of fibroblast-secreted proteins by encapsulating hepatic spheroids (containing primary human hepatocytes and iCasp9-GFP fibroblasts) in alginate, which, compared to fibrin, is less adhesive to cells and has a greatly reduced intrinsic binding capacity for paracrine factors, due to the lack of a promiscuous protein-binding domain (**Figure 3-11**A) [76, 174]. Spheroid-laden alginate beads were dosed with CID and cultured for a 2 week period. We assessed the secretion of human albumin as a proxy for hepatic function over two weeks, and observed no significant differences between untreated and CID-treated cultures (**Figure 3-11**C). Taken together, these results suggest that the maintenance of functional hepatocytes in 3D after elimination of fibroblasts is

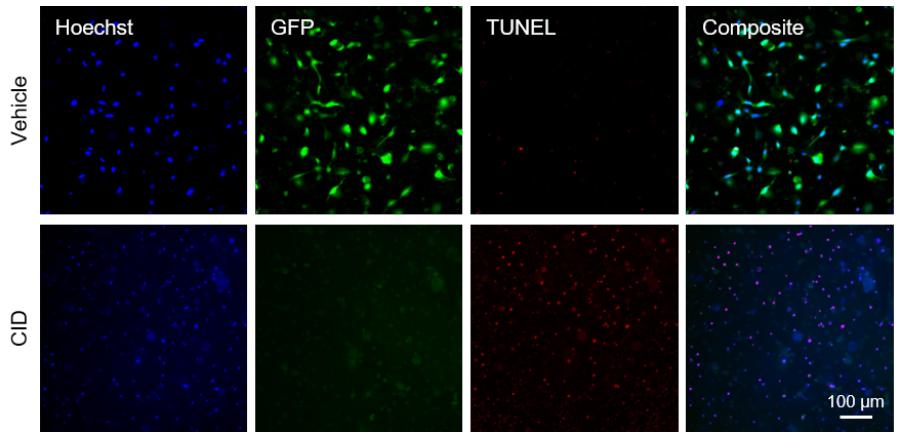

Figure 3-10: **Apoptotic debris is retained in fibrin hydrogels after CID treatment.** Representative images of colocalization of TUNEL and DNA stain in vehicle (0% colocalization) and CID-treated (82%) iCasp9-GFP J2 fibroblasts that were pre-encapsulated in a fibrin hydrogel (scale bar = 100 μ). Adapted from [41].

unlikely to be driven by the retention of either apoptotic bodies or of matrix-bound factors.

3.2.7 Early Provision of Cell-Cell and Cell-Matrix Interactions Drive Hepatocyte Phenotypic Stability in 3D

Given that the retention of sequestered paracrine factors and apoptotic bodies were not found to be critical cues for driving hepatocyte phenotypic stability in 3D, we then focused on specific cell-cell and cell-matrix adhesive factors that could be at play. Previous studies in monocultures formats suggest that E-cadherin-mediated cell-cell interactions and integrin β1-mediated cell-matrix interactions significantly contribute to hepatocyte phenotypic stability [164, 158]. In our 3D co-culture, we hypothesized that homotypic cell-cell interactions (such as E-cadherin engagement) and cell-matrix integrations (which require β1 integrin) were promoted by the inclusion of fibroblasts via compaction and deposition of matrix components (**Figure 3-12**A). To perturb these interactions, we incubated function-blocking monoclonal antibodies against human β1 integrin or human E-cadherin either with primary human hepatocytes before compaction (i.e. before co-culturing with fibroblasts), or after compaction and before encapsulation (**Figure 3-12**B). We specifically selected monoclonal antibodies with verified function-blocking activity (and not function-activating or neutralizing activity) based on several literature references and manufacturer specification documentation [164, 158, 212]. We found that transient, pre-compaction functional block-

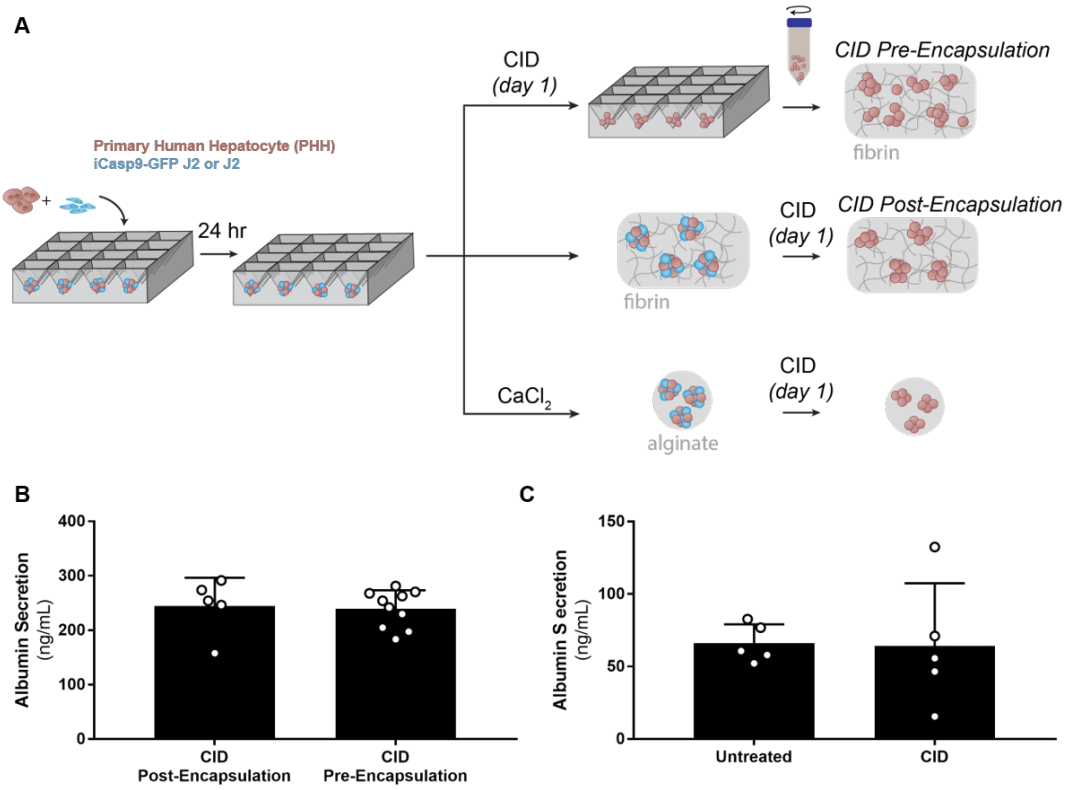

Figure 3-11: **Retention of apoptotic debris and other fibroblast-secreted proteins do not drive maintenance of hepatocyte phenotypic stability in 3D.** (A) Hepatocytes were aggregated with fibroblasts in microwell molds. Resulting spheroids were treated with CID prior to harvest from the microwell molds (followed by subsequent removal of apoptotic debris and conditioned supernatant via centrifugation, $60xg$, 6 minutes, 3 rounds; "Pre-Encapsulation"), encapsulated in fibrin and then treated with CID ("Post-Encapsulation"), or resuspended in 2 w/v% alginate and crosslinked in a warmed 2 w/v% calcium chloride bath. All cultures were dosed with CID on day 1. Collected supernatant was assayed for albumin secretion rate at day 3 for pre- and post-CID dosed spheroids encapsulated in fibrin hydrogels (B) and day 13 for alginate-encapsulated spheroids (C) (n=5-10, n.s. between groups). Adapted from [41].

ade of β1 integrin or E-cadherin significantly reduced albumin secretion at later time points, which we measured as a proxy for hepatocyte function (**Figure 3-12**C). When we blocked β1 integrin or E-cadherin post-compaction, hepatocyte function was slightly reduced but largely preserved, as compared to pre-compaction inhibition (**Figure 3-12**C). Taken together, these results suggest that adhesion via E-cadherin and β1 integrin were crucial for promoting longer-term hepatocyte phenotypic stability in a 3D hydrogel-laden co-culture,

and that even fleeting fibroblast co-culture is sufficient to establish these stabilizing effects early in culture (i.e. the first 24 hours after co-seeding in microwell molds). Importantly, it has been shown that cadherin and integrin-based interactions dramatically influence cellular behavior and interactions in a 3D niche [7], which may explain why stromal cell removal from 3D hepatic cultures (**Figure 3-7**) was more readily compensated for than in a similar 2D platform (**Figure 2-13**).

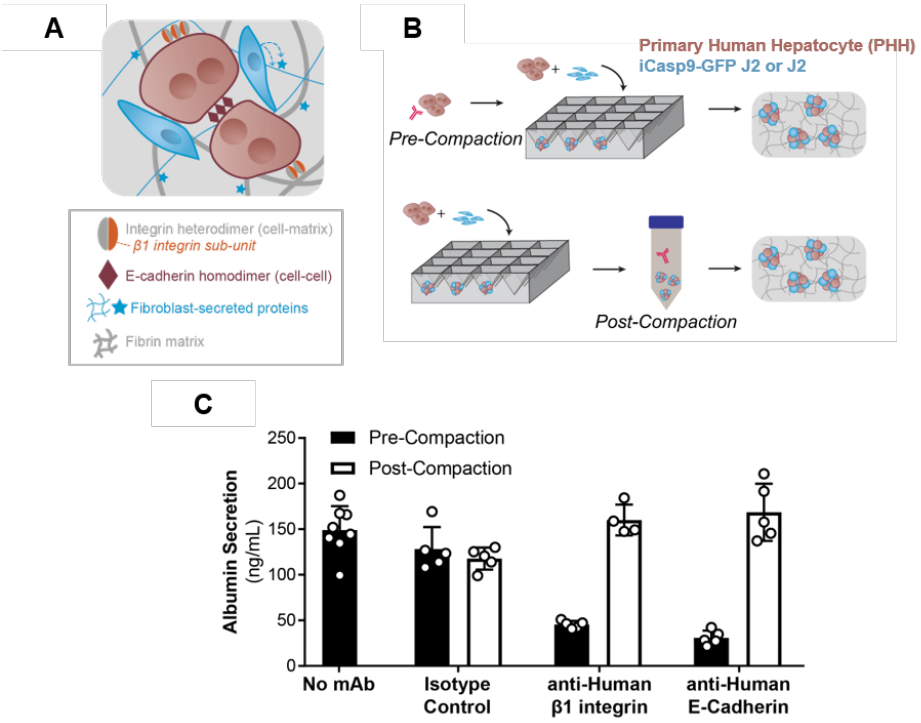

Figure 3-12: **Early provision of β1 integrin-mediated cell-matrix interactions and E-cadherin-mediated cell-cell interactions was required for hepatocyte phenotypic stability in 3D.** (A) Hepatocyte (brown) and fibroblast (blue) co-culture and encapsulation in fibrin (grey) hydrogels enabled the formation of integrin-mediated (dimer including orange β1 integrin subunit) cell-matrix interactions and E-cadherin-mediated (brown diamonds) cell-cell interactions. Fibroblasts modified the ECM by depositing matrix (blue). Secreted soluble factors (blue stars) can be bound to the matrix and act as a reservoir of paracrine factors. (B) Hepatocytes were incubated with function-blocking monoclonal antibodies against β1 integrin, E-cadherin or an isotype control before aggregation ("Pre-Compaction") or after compaction ("Post-Compaction"). After brief incubation (10 μg/ml, 20 minutes at 37°C) with the antibody, excess reagent was removed by centrifugation washes. (C) Resulting spheroids were encapsulated in fibrin hydrogels. Supernatant was analyzed for secreted human albumin on day 3 (n=5-8). Adapted from [41].

3.3 Conclusion

In this work, we leverage the CAMEO system discussed in Chapter 3, which consists of an inducible apoptosis switch that can be non-invasively triggered via the addition of a small molecule compound into the culture media. Specifically, we engineered a mouse fibroblast line, known to support primary hepatocytes of multiple species, to constitutively express a caspase-9-driven apoptotic switch. We cultured iCasp9-GFP fibroblasts with primary human hepatocytes and activated apoptosis, leading to subsequent removal of fibroblasts at different time points post co-culture initiation to query the temporal dependence of primary human hepatocytes on stromal support in 2D . We found, using our MPCC system, that primary human hepatocytes are dependent on fibroblast co-culture support, which corroborates previous findings with a similar co-culture system built and tested by Hui et al [116].

Unlike existing technologies from our lab and others that can manipulate cell-cell interactions only in 2D cultures, an inducible apoptosis switch-bearing cell population can be triggered in both 2D and 3D in vitro formats (as well as in vivo settings). In this Chapter, we build upon these prior findings and extend the use case of CAMEO for 3D multicellular ensembles. Similarly, we focus on the temporal role of fibroblasts in the maintenance of phenotypic stability of our 3D liver models. In this body of work, our 3D hepatic ensembles consist of hepatocyte-fibroblast spheroids that are encapsulated in a fibrin hydrogel and cultured in a static in vitro format that is amenable to medium-throughput experiments and analyses (i.e. in a 96-well plate). Here, we first demonstrate that CAMEO is compatible with 3D cultures, in the sense that iCasp9-bearing cells that are cultured in close proximity with non-iCasp9-bearing cells within a porous hydrogel microenvironment are still able to be apoptosed post-co-culture initiation. Interestingly, we observed that early removal of fibroblasts did not negatively impact the maintenance of primary human hepatocyte phenotype and function, and further discovered that crucial interactions in the first 24 hours of co-culture include both homotypic cell-cell (i.e. E-Cadherin engagement between primary human hepatocytes) and cell-matrix (i.e. $\beta 1$ integrin) interactions.

Our work with CAMEO for tissue engineering and cell therapy applications are a new contribution to the field. Previously, inducible caspase-9 has been deployed as a safety measure for engineered cell therapies (e.g. adoptive T cell therapy, engineered cell therapy, mesenchymal cell therapy) across a range of applications (e.g. regeneration, anti-cancer)

[60, 81, 258]. Recently, inducible apoptosis gene-engineered stromal cells were used to probe the contribution of cancer-associated fibroblasts to metastatic potential in vivo [235].

We envision that the CAMEO method will also impact the field of organoid biology (i.e. tissue cultures consisting of hiPSC, hESC, and other epithelial cells), in which stromal feeder layers are conventionally used to promote stem cell renewal and maintenance [49]. Feeder layers commonly consist of xenogeneic stromal cells (e.g. murine embryonic fibroblasts, murine 3T3 fibroblasts), which pose a significant translational challenge, thereby motivating the development of feeder-free and animal product-free strategies. Concerns with feeder layer cultures include overgrowth (i.e. limiting scale-up of tissue engineering by depleting nutrients and space), contamination of the target cell culture, and zoonosis [165, 49]. Transfer of zoonotic pathogens and immunogenic components can also happen through the use of conditioned medium; Martin et al. demonstrated that mammalian sialic acid Neu5Gc from conditioned medium elicited an antibody response in humans, thereby limiting clinical use [173]. In the case of hESCs and hPSCs, acellular support strategies for cell culture consisting of defined growth factor cocktails and functionalized culture surfaces have been elucidated [165, 62]. For most epithelial cells, the exact chemical and physical factors to create a perfect synthetic feeder substitute remain to be defined. Feeder cell support is thought to act through (a) growth factors, (b) detoxification of culture medium (e.g. removal of pro-apoptotic signals), (c) synthesis and provision of ECM proteins and/or (d) physical contact (e.g. mechanotransductive interactions, engagement of juxtacrine pathways). CAMEO may be useful as an additional degree of engineered control for dissecting these complex intercellular phenomena, which have been historically difficult to deconvolute.

3.4 Methods

3.4.1 Cell Culture

Primary cryopreserved human hepatocytes (Lot ZGF, 33-year-old, Caucasian, male; BioreclamationIVT) were maintained in high-glucose Dulbecco's modified Eagle's medium (DMEM) with 4.5 g/L glucose (CellGro) containing 10% (v/v) fetal bovine serum (FBS) (Gibco), 1% (v/v) ITS supplement (insulin, transferrin, sodium selenite; BD Biosciences), glucagon (70 ng/mL), dexamethasone (0.04 µg/mL), 0.015 M HEPES, and 1% (v/v) penicillin-

streptomycin (Invitrogen). In some experiments, we used freshly isolated primary rat hepatocytes, which were isolated from 2 to 3 month old adult female Lewis rats, as previously described [231]. 3T3-J2 murine fibroblasts were a kind gift provided by Howard Green (Harvard Medical School) and were cultured in DMEM with 4.5 g/L glucose, 10% bovine serum, and 1% (v/v) penicillin-streptomycin. Normal human dermal fibroblasts (Lonza) were cultured in DMEM with 4.5 g/L glucose, 10% fetal bovine serum, and 1% penicillin-streptomycin.

3.4.2 Hepatic Spheroid Culture and Encapsulation

Hepatic spheroids were cultured as described previously [257, 256, 41]. In brief, cryopreserved human hepatocytes were thawed and immediately plated with fibroblasts in AggreWells (400 μm pyramidal microwells) and incubated overnight at a 1:4 hepatocyte:fibroblast ratio. Where indicated, some optimization experiments involved the use of primary rat hepatocytes and neonatal human dermal fibroblasts, and were co-seeded in media supplemented with 5-80% Geltrex®. Hepatic spheroids (about 150 hepatocytes per spheroid, 100 µm diameter) were imaged and analyzed to quantify the extent of spheroid compaction. Individual spheroids were isolated manually using Fiji [228], and greyscale erosion was applied to threshold for hepatocytes (7 μm). Resulting morphologies were traced and measured for circularity. Resulting spheroids were embedded in fibrin (10 mg/mL bovine fibrinogen, 1.25 U/mL human thrombin; Sigma-Aldrich) using 96 microwell plates as molds. Spheroid-laden hydrogels were cultured in hepatocyte media supplemented with 10 μg/ml aprotinin, a serine protease inhibitor, to prevent hydrogel degradation. Alternatively, spheroids were cultured in alginate beads and hepatocyte media. Alginate beads were formed using sterilized 2% w/v alginate (Sigma-Aldrich) and 2% w/v calcium chloride (Sigma Aldrich), both dissolved in HEPES-buffered saline (20 mM HEPES, 150 mM NaCl in ddH2O). Spheroids were resuspended in alginate and added dropwise into a pre-warmed, stirred calcium chloride bath, then washed and collected using a 40 μm cell strainer before culturing in hepatocyte media.

3.4.3 CID Treatment

spheroid-laden hydrogels were dosed with 50 nM CID (1:10,000 dilution; B/B homodimerizer, AP20187; rapalog; Takara/ClonTech) for all co-culture experiments. Spheroids were

dosed with CID after encapsulation in fibrin hydrogels, except where noted in the text. In the case of pre-encapsulation CID treatment, spheroids were treated with 50 nM CID prior to harvest from microwell molds. The contents of the microwell molds (including hepatocytes, fibroblast-derived apoptotic debris, and conditioned media) were collected, diluted at least 5-fold, and centrifuged at $60xg$ for 6 minutes for 3 washes total in order to isolate hepatocytes via differential centrifugation. Pelleted hepatocytes were then encapsulated in fibrin hydrogels and cultured in hepatocyte media.

3.4.4 Functional Antibody Blockade

Primary human hepatocytes or compacted hepatocyte-fibroblast spheroids (immediately after harvest from microwell molds) were incubated with 10 μg/mL functional blocking monoclonal antibody (mouse anti-human β1 integrin, clone P5D2; mouse anti-human E-cadherin, clone 67A4; EMD Millipore) or an isotype control (Santa Cruz Biotechnology) for 20 minutes at 37 °C in hepatocyte media. Excess antibody was removed by centrifugation at $60xg$ for 6 minutes for 3 washes total. Pelleted hepatocytes were then encapsulated in fibrin hydrogels and cultured in hepatocyte media.

3.4.5 Biochemical Assays

Spent supernatant was collected from cultures every other day and stored at -20°C. Human albumin was quantified using an enzyme-linked immunosorbent assay using a sheep anti-rat albumin antibody (ELISA) (Bethyl Laboratories) and 3,3',5,5'-tetramethylbenzidine (TMB, Thermo Fisher). Urea concentration was measured using a colorimetric (diacetylmonoxime) assay with acid and heat (Stanbio Labs). CYP3A4 activity was assessed with the luminogenic P450-GloTM CYP450 assay kit (Promega) for nonlytic assays using cultured cells. Cultures were pre-treated with 25 µM rifampin or 1:1000 DMSO vehicle control prepared in hepatocyte maintenance media for 72 hours (daily replenishment) where indicated.

3.4.6 Immunofluorescence Imaging

For immunostaining of cellular constructs, tissues were fixed in 4% paraformaldehyde. For identification of primary human hepatocytes, tissues were incubated with primary antibody against human arginase-1 (rabbit, 1:400; Sigma-Aldrich) followed by Alexa Fluor®

546-conjugated rabbit anti-human secondary antibody (1:1000; Life Technologies). Alternatively, hepatocytes were visualized by pre-labeling with 1 µM CellTracker Deep Red (Thermo Fisher) for 20 minutes at 37°C. Nuclei were stained with Hoechst (1:2000).

3.4.7 Imaging

Fiji was used to uniformly adjust brightness/ contrast, pseudocolor, and merge images. Spheroid-laden hydrogels were imaged on a Zeiss 710 confocal microscope using a water immersion 40X objective or the Leica SP8 spectral confocal microscope using the 10X air or 25X water immersion objective. Live imaging was captured using a Nikon Spinning-disk Confocal Microscope with TIRF module.

3.4.8 Quantitation

iCasp9-GFP J2s were encapsulated as single cells in a fibrin hydrogel. Cultures were dosed with vehicle or CID and cultured for 3 weeks. Cultures were fixed with 4% paraformaldehyde, stained with Hoechst (1:2000) and imaged with a Nikon Ti-E inverted epifluorescent microscope. Number of cells (by counting nuclei) was quantified for 3 representative 20x field of views per sample.

3.4.9 Statistical Analysis

All data are expressed as mean ± standard deviation and/or visualized as dot plots (n = 3-10 as indicated). Statistical significance ($\alpha = 0.05$) was determined using the appropriate statistical test (unpaired 2-tailed t-test, 1-way ANOVA, 2-way ANOVA), and followed by multiple comparisons testing (Tukey's post hoc test) (GraphPad).

3.5 Acknowledgements

Dr. Arnav Chhabra was my thought partner and experimental teammate for all of this work. **Dr. Tiffany Vo**, **Dr. Quinton Smith**, **Trevor Nash**, **Keval Vyas**, **Dr. Jen Bays**, and **Dr. Linqing Li** provided insightful advice which was readily incorporated in this project - I am especially grateful to Jen and Linqing for entertaining my very rushed request for advice and discussion when I was pushing to finish my paper revision before the

COVID-19 pandemic shutdown.

Jeffrey Wyckoff and **Eliza Vasile** of the Imaging core of the Koch Institute Swanson Biotechnology Center were essential for capturing live videos and high-resolution stills of our 3D microlivers.

The late **Howard Green** of Harvard Medical School provided the 3T3-J2 fibroblast cell line as a kind gift. Wilson Wong of Boston University was crucial to initial discussions surrounding the feasibility of this work, and provided much helpful guidance and discussion.

This work was supported in part by the NIH (R01 EB008396, R01 EB000262, UG3 EB017103), Koch Institute Support (core) Grant P30-CA14051 from the National Cancer Institute, the National Science Foundation Cellular Metamaterials Engineering Research Center, and the Boston University Biological Design Center.

Chapter 4

TRANSLATE: Engineered Hepatic Ensembles as Cell Therapies

4.1 Introduction

In the preceding Chapters of this thesis, we discussed the development of tools that enable the study of underlying cell-cell interactions in hepatic ensembles comprised of primary human hepatocytes and murine fibroblasts. While these advances constitute significant progress for cell culture models of the human liver, the true relevance of clinical translation cannot be fully realized until these findings are properly adapted for in vivo implantation in both small and large animal models of health and disease, which is the first step toward translation to human patients with liver disease. Notably, our hepatic ensembles also act as fundamental building blocks for satellite cell therapies, and therefore this work is directly relevant to the development and optimization of the satellite cell therapy concept.

Our satellite cell therapies rely on defined tissue microarchitecture, which is not readily reproduced at scale. Specifically, we have previously found that tissues containing primary human hepatocytes, endothelial cells, and stromal cells in a geometrically-defined architecture have significantly increased capacity to respond to in vivo cues than their un-patterned counterparts [256, 257, 40]. Stevens et al. implanted multiple hepatic grafts of approximately 6 mm diameter and 2 mm thickness, which is a graft geometry that is compatible with oxygen exchange and nutrient demand [256]. However, these engineered tissues were not able to slow or reverse the progression of liver failure due to hereditary tyrosinemia

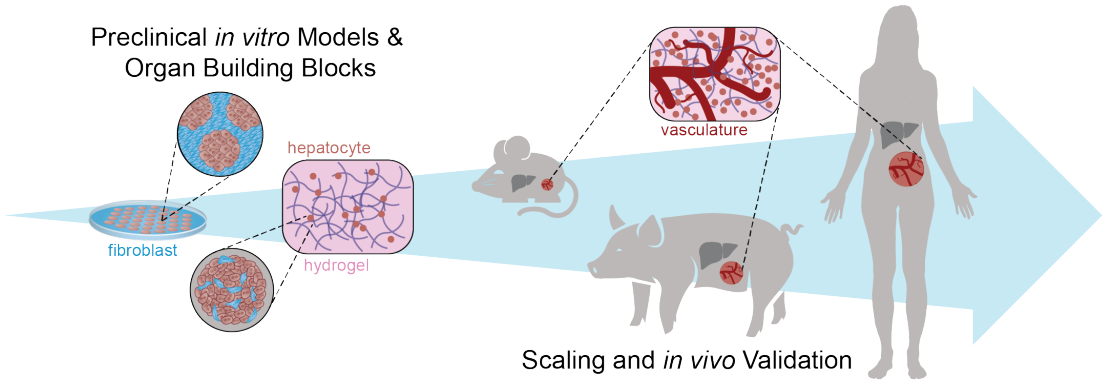

Figure 4-1: **Pathway of cell therapies for solid organ replacement or augmentation.** Preclinical 2D and 3D in vitro models enable the study of tissue-specific biology, and may also be re-purposed as building blocks for artificial tissues. The evolution of a solid cell therapy product may be subjected to additional requirements and constraints as the product is scaled and evaluated for safety in the clinic. Unpublished.

type I, likely because the grafts did not support enough cells to offset disease phenotype and sequelae. Each animal in this study had approximately 600k primary human hepatocytes, which constitutes only 0.4% of the hepatocyte mass in an average mouse liver. As per the Introduction to this thesis document, clinical studies on hepatocyte transplantation approximate that 0.5-5% of the total hepatocyte mass is required to correct inborn errors of metabolism, and closer to 10% of the total hepatocyte mass is needed to address acute liver failure [77, 202]. To approach these numbers, it is important to pursue both cell sourcing challenges (i.e. obtaining and expanding primary and stem-derived hepatocytes) and biomanufacturing challenges. In this Chapter, we will focus primarily on challenges related to biomanufacturing, and will continue to use primary human hepatocytes as our workhorse.

We will describe substantial progress we have made toward addressing challenges related to implementing our hepatic cell therapies as an example of a satellite cell therapy for serious organ injury and disease of human patients, including:

- Assessing the importance of an intact fibroblast population pre- and post-implantation
- Incorporating vasculature to meet nutrient and oxygen demands of scaled-up tissues
- Assessing optimal graft configuration to optimize in vivo performance (i.e. persistence of hepatic function, formation of perfusable vasculature)

- Validating compatibility with manufacturing methods that fabricate cell-dense tissue constructs
- Assessing of ability to surgically remove a hepatic graft to accomplish phenotype reversal

In this Chapter, we also define realistic constraints and considerations for small animal model testing and comment on challenges related to xenogeneic and allogeneic cell therapies.

4.2 Results & Discussion

4.2.1 Motivation for Engineered Vasculature in Hepatic Cell Therapies

In all instances of scaling cell therapies for solid organ disease, graft design must support and maintain vessel-like structures that enable an influx of nutrients and oxygen as well as the removal of waste products. In early clinical efforts, hepatocyte transplantation was shown to be highly inefficient, leading on average to engraftment of only 0.1-0.3% of the host liver mass following the infusion of 3-5% of the total recipient liver cells [77]. In cases of orthotopic injection, hepatocytes are subjected to an inhospitable disease-like environment, in which disease-associated cues could readily affect the viability and performance of engrafted donor cells. With satellite cell therapies, we decouple an organ-specific graft from the orthotopic location, and enable integration and functional persistence in a heterotopic (otherwise referred to as "satellite") location. Specifically, satellite cell therapies consist of cells housed in an engineered scaffold, and embedded cells have the benefit of existing in a defined microenvironment that enables high viability and performance, with the caveat that integration with the host is critical in order to provide bioactive function to the host. For the liver, as discussed in the Introduction, the placement of hepatic cell therapies is also readily compatible with such satellite anatomic locations. Aside from seminal work by Bucher et al. that revealed that regenerative stimuli resulting from liver injury is sufficiently captured in the systemic circulation as secreted, soluble cues, heterotopic transplantation (e.g. in the spleen, lymph node, subcutaneous space, mesenteric fat pad) has been demonstrated to provide a supportive microenvironment for hydrogel-encapsulated cell therapies

[213, 32, 266, 141, 256, 40].

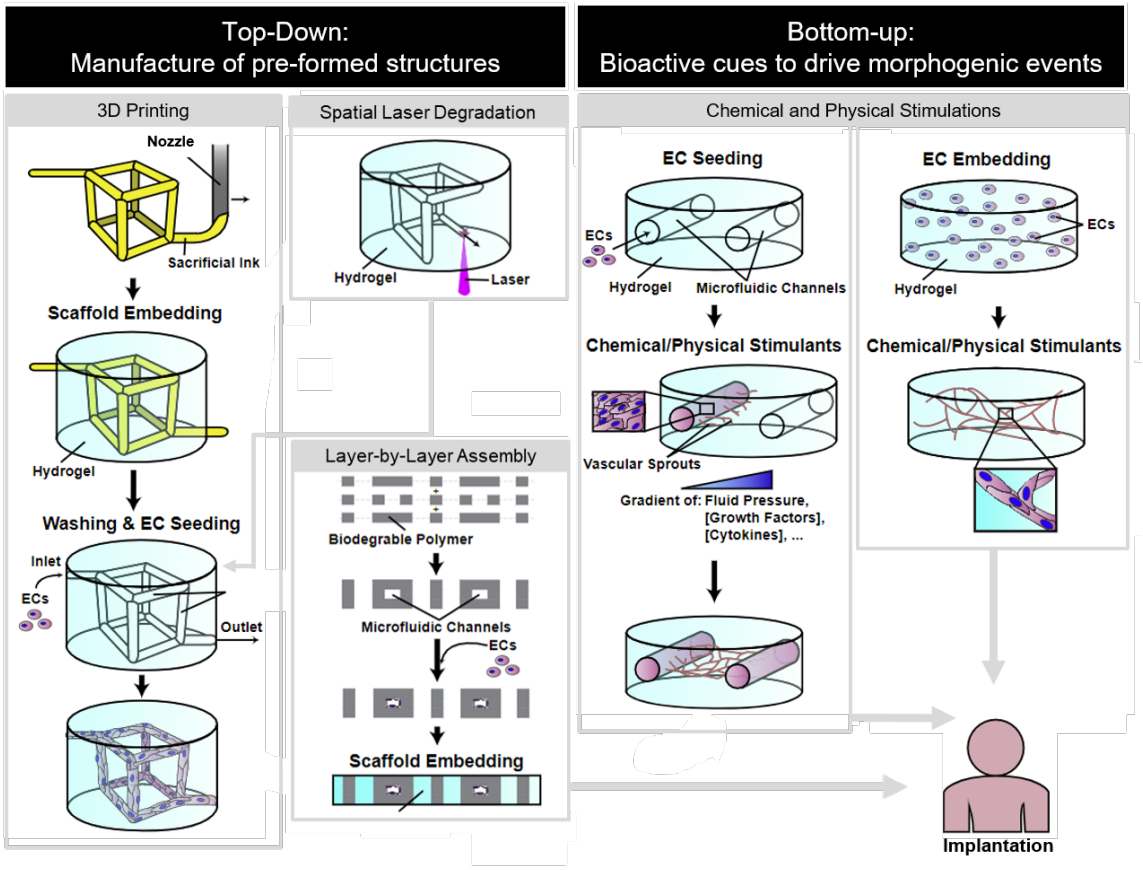

Figure 4-2: **Fabrication approaches for engineered microvessels.** Microvessels can be fabricated using either top-down (left) or bottom-up (right) approaches. Top-down approaches generally involve rational fabrication of pre-designed structures through 3D printing, spatial laser degradation, or layer-by-layer assembly. Resulting lumen structures can be lined with endothelial cells. Bottom-up approaches often leverage bioactive cues including chemical and physical stimulants that induce angiogenic sprouting or vasculogenesis self-assembly of endothelial cells to give rise to a network of interconnected microvasculature. Adapted from [245].

In such implantable satellite grafts, scaling of the graft is contingent on including or providing vasculature. Song et al. previously reviewed recent technologies related to fabrication approaches for engineered microvessels, and categorized the strategies as top-down manufacturing of pre-formed structures using 3D printing, spatial laser degradation, and layer-by-layer assembly, and bottom-up presentation of bioactive cues to endothelial cells in order to stimulate de novo vessels via vasculogenesis, or to coax angiogenic sprouting of new buds and vessels from existing vessel-like structures. It is likely that cell therapies for solid organs will make use of both of these approaches. Currently, it remains a challenge to:

1. integrate vessel structures across different length scales,

2. perform surgical anastamosis of inlet and outlet vessels to enable immediate integration with the host, and

3. prevent clotting and collapse of vessels in an engineered graft upon implantation and integration with the host.

Lastly, a challenge of vascular engineering includes the maintenance of an interconnected network in the presence of parenchymal cells. In our work, we have often observed that co-culture of two specialized cell populations (e.g. primary human hepatocytes and endothelial cells) will compromise the involved cell populations for myriad reasons, including increased metabolic demand and the introduction of new ingredients from disparate culture media recipes. In this vein, we performed optimization to balance the performance of both cell populations, and found that a 50:50 mixture of hepatocyte and endothelial cell media was ideal for co-culture, compared to other ratios or recipes in which growth factors and supplements were adjusted to compensate for other variables (data not shown).

4.2.2 CAMEO Reveals that Fibroblasts are Integration of Non-Vascularized Satellite Grafts

In pilot studies, we prepared satellite grafts consisting of only hepatocyte-fibroblast spheroids, as described in the Chapters 2 and 3, and relied on the fibrin gel housing and its natural vasculogenic potential to recruit host vasculature and drive integration with the host [189]. Specifically, we transduced primary human hepatocytes with AAV8 vectors carrying a CMV-driven firefly luciferase cassette in order to enable a noninvasive live animal imaging readout. Firefly luciferase-expressing hepatocytes were then prepared as spheroid-laden hydrogel grafts, treated with CID pre-implantation to remove the fibroblast population, and immediately implanted into the parametrial fat pad of nude mice (**Figure 4-3**A). As a readout of graft viability, we assessed the CMV-driven promoter activity in human hepatocytes contained in the implanted satellite graft at an early time point (3 days) after implantation using IVIS. We observed a 4.8-fold increase in luciferase activity in vehicle-treated (i.e. fibroblast-intact) satellite grafts compared to CID-treated (i.e. fibroblast-depleted) grafts, which suggests that the presence of fibroblasts in the graft could be a major driver of graft

integration and persistence in animals (**Figure 4-3**B). Additionally, hepatocyte viability of implanted grafts did not improve over a 2-week period post-implantation (data not shown). Furthermore, we show that the satellite grafts persist in the location of surgical placement by visualizing the luciferase activity pattern of representative mice (**Figure 4-3**C).

We have previously shown that inclusion of fibroblasts in the microstructure of the cellular compartment significantly improved integration and persistence of hepatic satellite grafts, compared to grafts with either no or fewer fibroblasts [257]. However, in the work by Stevens et. al. and Chen et al., it was not clear if the fibroblast population was only essential for initial stabilization of the hepatocytes [257, 40]. In this work, we used CAMEO to demonstrate that the continued presence of fibroblasts in hepatic satellite grafts is necessary for promoting graft viability and integration. It is otherwise generally well accepted that the inclusion of fibroblasts for hepatocyte function and endothelial morphogenesis is a robust method for enhancing performance, and circumventing the use of additional growth factors and cytokines [130, 131, 49, 84, 53, 12, 138, 259, 123, 18].

4.2.3 Development of Hepatic VasculoChip as a Satellite Graft

A primary reason for graft loss after pre-implant fibroblast removal in spheroid-only grafts could be due to the fact that satellite grafts are dependent on fibroblast-derived cues in the absence of an endothelial population. It has been shown across a large body of work that the inclusion of endothelial cells greatly enhances the potential for vasculogenesis and angiogenesis [245, 53, 12, 138, 259, 123]. Biomanufacturing methods can now reliably create structures at the same length scale as vessels that comprise native capillary beds (i.e. between 1-10 μm print resolution with common 3D-printing techniques at build speeds, volumes, and conditions compatible with biologically active inks and matrices; reviewed more in depth in [280, 193]).

However, the formation of a complex and intricate capillary bed-like network, which is critical for supporting the metabolic demand and overall health of tissues and organs, is not currently possible. In this work, we leveraged a microfluidic vasculogenesis model consisting of needle-molded channels that were seeded to create endothelialized lumens, and surrounded with a fibrin hydrogel containing randomly seeded endothelial cells and fibroblasts, as previously described in [246]. This device, termed the VasculoChip, was cultured

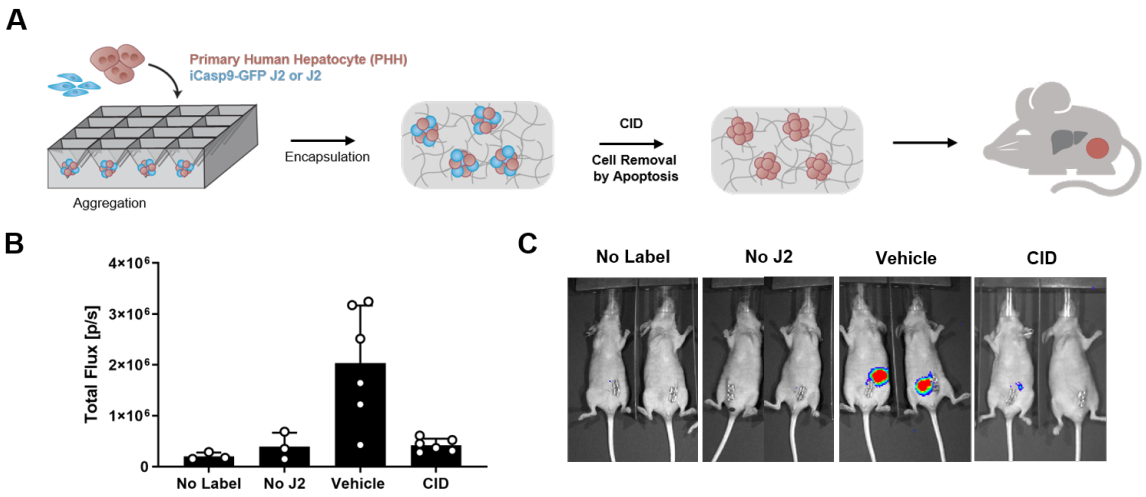

Figure 4-3: **Pre-implantation removal of fibroblasts from spheroid-only grafts results in early graft loss.** (A) Primary human hepatocytes were modified with AAV2/8 to constitutively express firefly luciferase to enable non-invasive assessment of viability in live animals. Modified hepatocytes were co-seeded with fibroblasts in microwell molds to form spheroids, encapsulated in fibrin hydrogels, and treated with CID prior to implantation into the fat pad of nude mice. (B) On day 3 post-implant, graft viability was assessed via IVIS (n=3-6 mice per experimental group; total flux of bioluminescence, p/s). (C) Representative images of 2 mice per cohort (red = highest signal, purple = lowest signal). Unpublished.

under flow and formed perfusable, endothelial-lined networks which were connected to 2 needle-molded channels (device dimensions: 1 mm length, 1 mm width, 800 μm thickness). We adapted the VasculoChip to co-culture with hepatocyte-fibroblast spheroids (hereby referred to as Hepatic VasculoChip). We assessed performance of the Hepatic VasculoChip as well as iterations of the device without endothelialized lumens or bulk endothelial cells, and observed that hepatocyte performance was enhanced over time in the Hepatic VasculoChip configuration (**Figure 4-4**A). We further demonstrated that the device could be scaled-up (device dimensions: 6 mm diameter with 2 mm thickness) as an implantable satellite graft that is compatible with manual manipulation with microsurgical tools and anchoring with 5-0 sutures, and that the scaled-up device could host 4 lumenized endothelial channels and the formation of a perfusable, capillary bed network (**Figure 4-4**B). We performed immunofluorescent imaging of Hepatic VasculoChip devices and detected intact hepatocyte-fibroblast spheroids and interconnected vascular morphology (**Figure 4-4**C).

The Hepatic VasculoChip is reliant on the initial inclusion of a fibroblast population

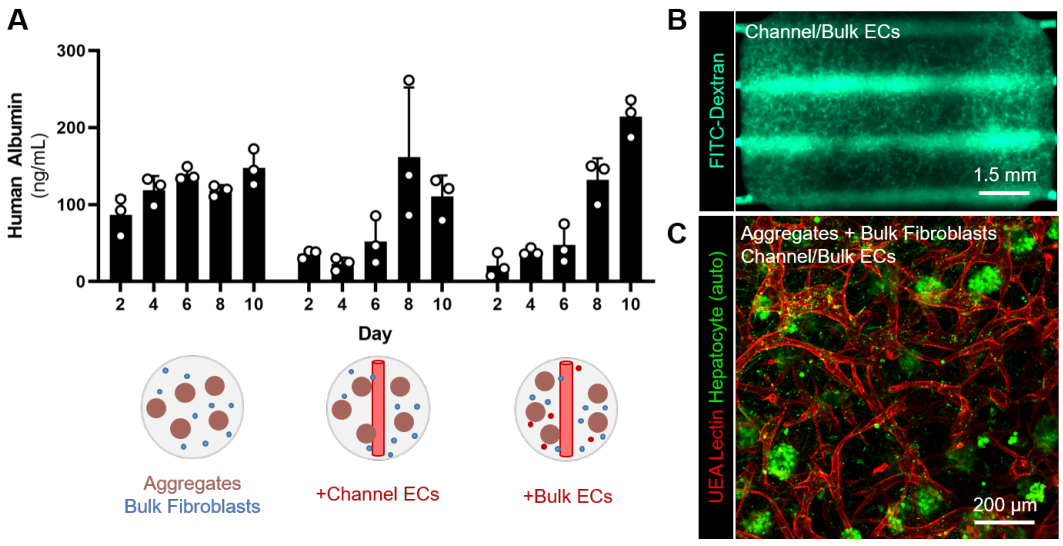

Figure 4-4: **Hepatic VasculoChip: Hepatic spheroids are compatible with microfluidic VasculoChip device in vitro.** (A) Hepatic spheroids were seeded in microfluidic VasculoChip devices either with fibroblasts in the bulk (left), with fibroblasts in the bulk surrounding an endothelialized lumen (middle), or with fibroblasts and endothelial cells in the bulk surrounding an endothelialized lumen (right; i.e. VasculoChip with hepatic spheroids). Devices were cultured in vitro on a rocker and supernatant was analyzed for albumin secretion. (B) Devices consisted of 4-channel configuration, and formed microvessels that were connected to the needle-molded lumenized vessels, as visualized by perfusion with lysine-fixable FITC-dextran. (C) Hepatic spheroids (autofluorescence signal) and endothelial cell channels (UEA lectin staining) were visualized in the Hepatic VasculoChip device at day 10 (scale bar = 200 μm). Unpublished.

not only to stabilize hepatocyte-fibroblast spheroids, but also to drive vascular morphogenesis. Using CAMEO, we queried the importance of fibroblasts past an early stage of co-culture. All fibroblasts in the following experiments were growth-arrested iCasp9-GFP NHDFs, including the fibroblast compartment of the hepatocyte-fibroblast spheroids and the fibroblasts seeded in the bulk of the hydrogel to drive neovascularization. We seeded 2-channel Hepatic VasculoChip devices and removed the entire fibroblast population on day 5 of in vitro culture (**Figure 4-5**A). Devices were fixed at day 7 immediately after perfusion of lysine-fixable FITC dextran through the inlet and outlet channels, and visualized using confocal fluorescence microscopy. In both vehicle-treated (i.e. fibroblast-intact) and CID-treated (i.e. fibroblast-removed) devices, we detected hepatocytes using a hepatocyte-specific marker (arginase-1), suggesting that hepatocytes were viable and maintained phenotype. We also observed that hepatocytes appeared to be constrained to their spheroid-like

structures, which is consistent with our prior observation of little to no migration of primary human hepatocytes post-seeding or encapsulation. Additionally, we also observe UEA lectin staining of endothelial networks, which were able to transport and retain dextran without significant leakage (**Figure 4-5**B). Lastly, we also performed functional analysis of hepatocyte function, and detected a significant improvement in secreted albumin levels and urea production levels in Hepatic VasculoChip devices treated with CID to remove the iCasp9-bearing cell population, compared to devices with intact fibroblasts (**Figure 4-5**C). Taken together, here we demonstrate that the Hepatic VasculoChip supports functional neovascularization and hepatocyte phenotypic stability across multiple axes, even following the removal of the entire fibroblast population via CAMEO.

Toward in vivo applications, we then proceeded to construct scaled-up 4-channel Hepatic VasculoChip devices and assess hepatic performance over a 10 day period in vitro after CID-driven deletion of fibroblasts at day 3 (with a repeat dose at day 4 to ensure maximum ablation of the iCasp-bearing fibroblast population) (**Figure 4-6**A). We assessed levels of secreted human albumin every other day and observed an increase in albumin secretion in CID-dosed devices compared to vehicle-treated and non-treated devices after administration of CID. Differences between groups were increasingly pronounced through day 8, and reached statistical significance compared to fibroblast-intact groups by the endpoint of 10 days of in vitro culture (**Figure 4-6**B). By eye, we observed that vasculature began to form around day 5 to 7 post-seeding, and that some devices had structurally-collapsed vessels by day 8 and 10 post-seeding (data not shown). These results suggest that the deletion of fibroblasts from 4-Channel Hepatic VasculoChip devices enhances the function of vascularized engineered hepatic tissues in vitro through 10 days of culture, though there may be a trade-off with the maintenance of integrity of engineered vasculature at longer culture time frames. In next steps, we proceeded to assess and optimize a timeline for implantation of satellite grafts comprised of 4-Channel Hepatic VasculoChip devices.

To assess the role of pre-formed, perfusable vasculature in the integration and persistence of satellite grafts, we prepared 4-Channel Hepatic VasculoChip devices with iCasp9-bearing NHDF, primary human hepatocytes, and HUVECs, and dosed devices at day 3 and 4 post-seeding with CID to remove fibroblasts. Devices were implanted at 3 different time points after the initial CID dose, including (1) two days later for a total of 5 days of in vitro culture, (2) 4 days later for a total of 7 days of in vitro culture, and (3) 7 days later for a total of

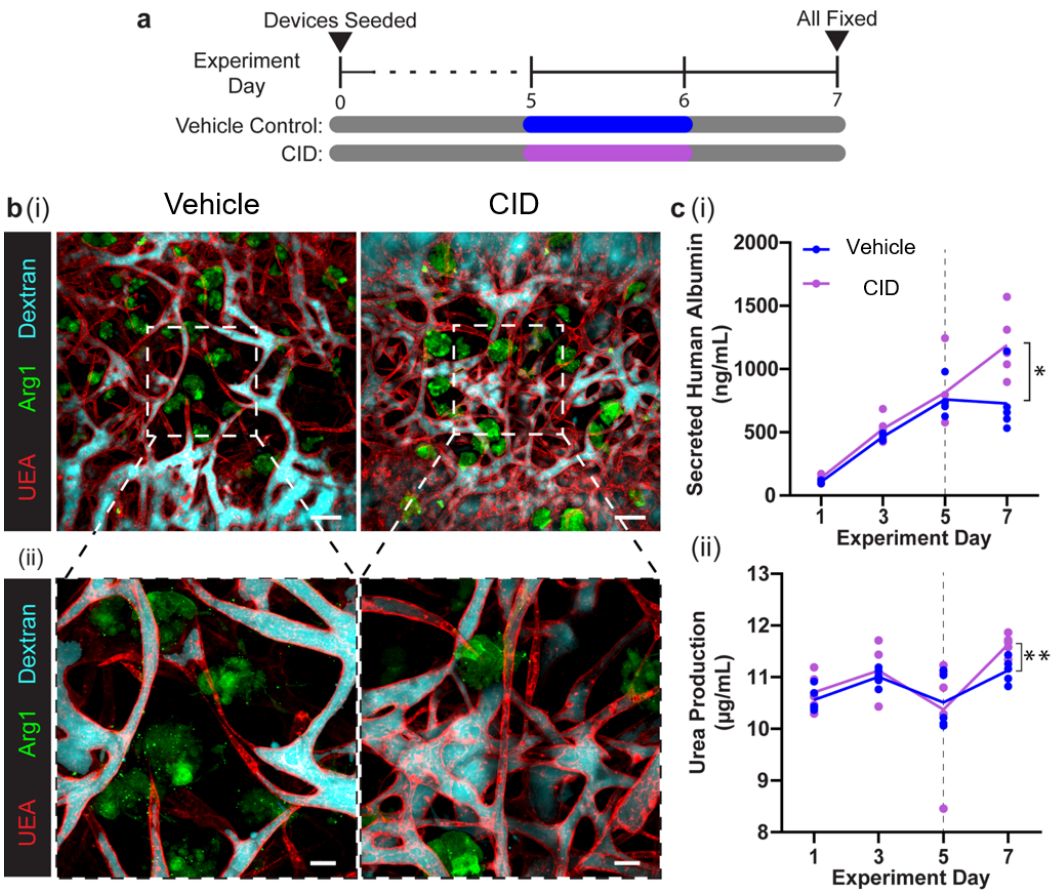

Figure 4-5: **Deletion of fibroblasts from 2-Channel Hepatic VasculoChip enhances the function of vascularized engineered hepatic tissues in vitro.** (A) Two-channel Hepatic VasculoChip devices were seeded with hepatic aggregates and endothelial cells, treated with vehicle or CID at day 5 to remove fibroblasts, and fixed on day 7. (B) Representative max projections of dextran-perfused (cyan) vehicle- and CID-treated devices stained for UEA human-specific lectin (red) and human arginase-1 (green) (scale bar = 150 (i) or 50 (ii) μm). (C) Spent supernatant was analyzed for secreted human albumin (i) and urea production (dotted vertical line indicates dose day; n=4-5, *p<0.05, **p<0.01). Adapted from [246].

10 days of in vitro culture (**Figure 4-7**A). Hepatic VasculoChips were surgically implanted into the fat pad of nude mice, and blood was collected over a 2 week time period to assess graft performance. Blood was centrifuged, and the resulting plasma fraction was assayed for human-specific albumin secretion using an ELISA assay that does not have cross-reactivity with rodent albumin. We expected to detect human albumin in the blood of animals in which the graft was integrated (i.e. viable, vascularized, and anastomosed to the host circulation) and the hepatocytes were phenotypically stable (i.e. able to perform liver-specific function

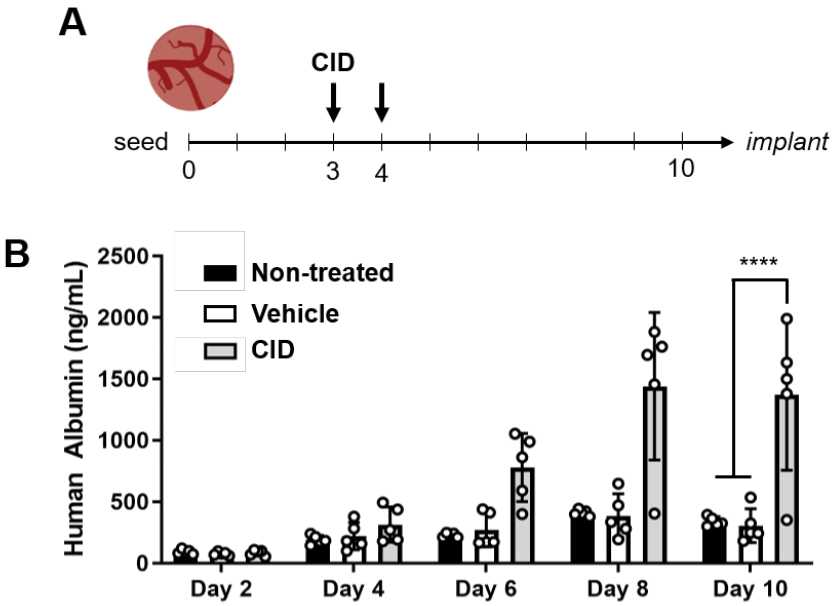

Figure 4-6: **Deletion of fibroblasts from 4-Channel Hepatic VasculoChip enhances the function of vascularized engineered hepatic tissues in vitro.** (A) Four-channel Hepatic VasculoChip devices were seeded with hepatic aggregates and endothelial cells, and were either untreated or treated with vehicle or CID at day 3 and day 4 to remove fibroblasts, and cultured until day 10 in vitro. (B) Spent supernatant was analyzed for secreted human albumin (n=5, $*p<0.0001$). Unpublished.

such as production of secreted proteins and metabolites).

In mice implanted with grafts that were cultured for a total of 5 days in vitro, we found either low or no detectable levels of albumin in the blood plasma (**Figure 4-7**A). In mice receiving grafts that were cultured for a total of 7 days in vitro, we found high initial values of human albumin (ranging from 400-800 ng/mL), which rapidly dropped by day 5 post-implantation in both non-treated and CID-treated grafts (**Figure 4-7**B). Initial albumin levels at day 2 were modestly higher in CID-treated graft-bearing mice, though grafts with intact fibroblasts had modestly higher levels of human albumin after 1 week post-implantation. Lastly, mice receiving grafts that were cultured for a total of 10 days in vitro overall had lower albumin levels compared to the initial human albumin values of grafts that were implanted after 7 days of in vitro culture (**Figure 4-7**C). Similarly, human-specific albumin secretion was modestly higher in CID-treated graft-bearing mice at early time points, and rapidly dropped to low and undetectable levels by 1 week post-implantation. We surmise that initial graft performance in vivo was related to the formation

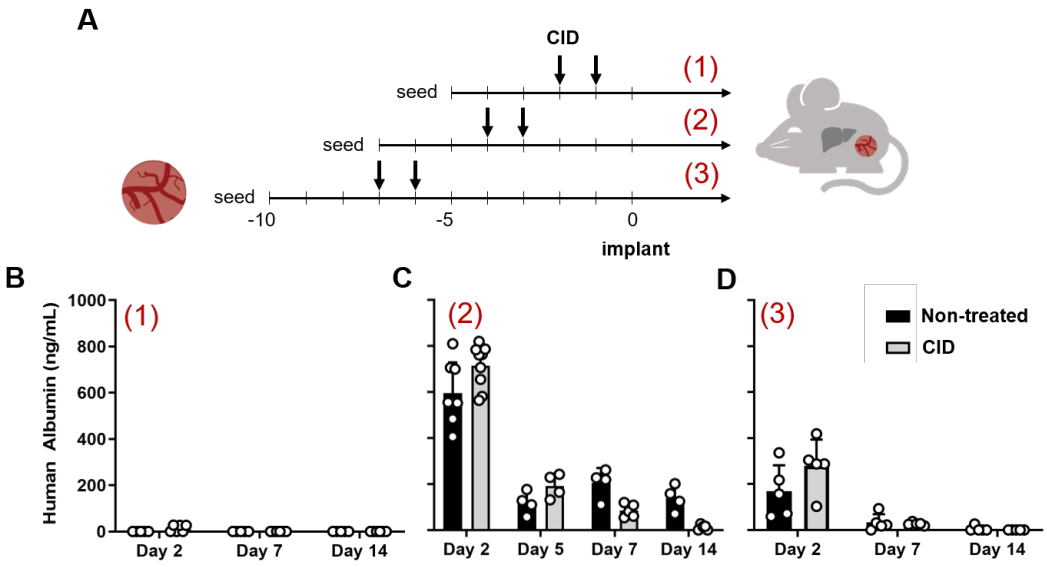

Figure 4-7: **Graft performance in vivo depends on in vitro culture period after fibroblast deletion from 4-Channel Hepatic VasculoChip.** (A) Hepatic VasculoChips were seeded and cultured in vitro for 3 days before triggering CID-driven removal of fibroblasts. Devices were then cultured in vitro for an additional two (1), four (2), or seven (3) days prior to implantation into the fat pad of nude mice. (B-D) Human albumin was quantified in the plasma fraction of collected blood samples over a 2 week period (n=4-8). Unpublished.

and maintenance of vessels in the Hepatic VasculoChip. It is possible that grafts implanted after 5 days of in vitro pre-culture had not formed fully perfusable vasculature, though we previously observed the semblance of intact vasculature in devices prior to 8 days of in vitro culture. Across our experimental cohorts, we observed ideal performance of hepatic grafts when devicess were pre-cultured for 7 days in vitro. We also note that vasculature appeared to have partially collapsed by day 8 or 10 of in vitro culture, and saw accordingly low albumin secretion levels in grafts implanted after 10 days of in vitro culture. In this condition, the low but detectable (80-300 ng/mL) values of human albumin may be due to the recovery of collapsed vessels, or the effect of a partial intact population of vessels. Taken together, these findings suggest that hepatic satellite grafts are sensitive to the in vitro pre-conditioning period leading up to graft implantation.

We further hypothesized that the removal of fibroblasts prior to implantation was a driver of graft loss and lack of maintenance, as per our earlier findings that fibroblasts were required for graft viability in a simpler graft (i.e. hepatocyte-fibroblast spheroids only; **Figure 4-3**.

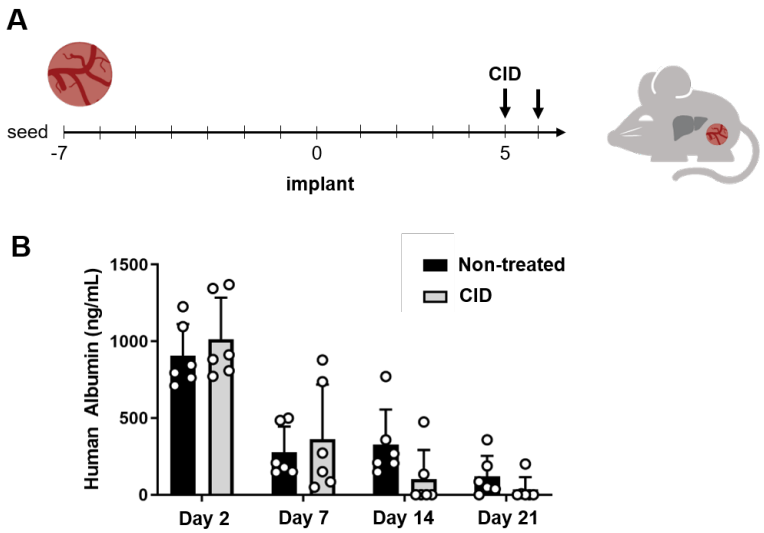

Figure 4-8: **In vivo deletion of fibroblasts from implanted 4-Channel Hepatic VasculoChip did not improve graft persistence.** (A) 4-Channel Hepatic VasculoChip devices (with intact fibroblasts) were implanted in the fat pad of nude mice. CID was administered intraperitoneally at day 5 and 6 post-implantation. (B) Human albumin was quantified in collected blood samples for 3 weeks (n=6). Unpublished.

Thus, we assessed the deletion of fibroblasts from Hepatic VasculoChips after implantation to the fat pad of nude mice. Based our assessment of ideal implantation time frame (**Figure 4-7**), we prepared Hepatic VasculoChips using a 7-day in vitro pre-culture timeline, implanted all devices with fibroblasts intact, and then injected a solution of CID (prepared as per the manufacturer's suggestions for in vivo dose administration) intraperitoneally on days 5 and 6 after implantation to trigger apoptosis in vivo. In related studies with iCasp9-bearing cell-laden grafts, we confirmed that intraperitoneal administration of CID led to ablation of iCasp9-bearing cells even in an in vivo setting (data not shown). Additionally, we did not observe any acute toxicity effects to the animals after CID administration. We collected blood from animals and prepared the plasma fraction for downstream analysis of human-specific proteins over a period of 3 weeks post-implantation. We found that human albumin secretion into the blood reproduced the trend and levels of human albumin secreted by satellite grafts that were treated with CID pre-implantation on a different dosing schedule (**Figure 4-7**C, in vitro dose of CID on day 3 and 4 with implantation on day 7; **Figure 4-8**, in vivo dose of CID on day 5 post-implantation, with devices cultured similarly for 7 days in vitro). These findings suggest that the presence of fibroblasts during the early

post-implantation phase did not improve the integration and maintenance of the satellite graft, which is in contrast with our findings in vitro (**Figure 4-4, 4-5, 4-6**).

4.2.4 Implantation Considerations: Host Immune System

There are several reasons that may contribute to why the satellite grafts did not persist long-term in the animals, including rejection by the animal host immune system and non-ideal graft geometry. Below, we will discuss considerations for each of these categories in the context of our results and relevant literature detailing related hepatocyte-fibroblast grafts. Similarly, prior work in our lab utilized nude mice as the workhorse for implantation studies. Chen et al. implanted hepatic satellites contained in non-degradable, poly(ethylene glycol)-RGDS hydrogel scaffolds into the fat pad of nude mice [40], and observed persistence for up to 3 months. Similarly, Stevens et al. implanted hepatic satellites in natural material-based matrices into the fat pad of nude mice for up to 4 weeks [257]. Furthermore, Stevens et al. demonstrated that hepatic satellites in natural material-based matrices were also able to persist and functionally expand in the fat pad of immunodeficient mice with hereditary tyrosinemia type I [256].

In our studies, we implanted satellite grafts into the fat pad of nude mice, which lack a thymus, and thus are unable to produce T cells that assist with recognition of and attack against a foreign graft. We expected that these satellite grafts would demonstrate similar time frames of persistence in vivo, but did not observe this trend in our studies. It is possible that the fibrin hydrogel (which can be quickly degraded in vivo) did not provide sufficient protection against the host immune attack, as we would have expected a non-degradable poly(ethylene glycol) hydrogel to do as per studies by Chen et al. [40]. In fact, Chen et al. demonstrated that the poly(ethylene glycol) hydrogel was able to protect from graft loss in the intraperitoneal space in mice with fully competent immune systems. This is corroborated by a body of work that notes a relationship between hydrogel porosity and the invasion of cells and vessels: porosity can be readily controlled through a materials science approach, including but not limited to the choice of monomer building block size, co-polymerization with a degradable or sacrificial material, and tuning degradation kinetics with enzyme-sensitive or hydrolytically-degradable linkers [44, 195] . We also built satellite grafts with different human hepatocyte donors compared to studies by Chen et al. and Stevens et al.,

which may interact differently with the murine immune system. Furthermore, Chen et al. demonstrated that a direct transplanation of hepatocytes into an immunocompetent Swiss-Webster mouse model led to loss of cell function by day 4 post-implantation as measured by IVIS, which is similar to the timeline of our graft loss withint he first week post-implantation.

More recently, NSG (NOD *scid* gamma) mice have become the gold standard for humanized mouse studies, and have demonstrated broad utility through demonstration of human cancer xenografts in mice [119, 236]. In addition to T cell deficiency like nude mice, NSG mice are also B and NK cell-deficient. In next steps of this work, we assessed the utility of NSG mice for human satellite grafts and hypothesized that we would observe improved graft persistence due to a further deficiencies of the host immune system compared to that of nude mice.

4.2.5 Implantation Considerations: Graft Configuration

Besides animal immune system interactions with our human cell-containing satellite grafts, another driver of graft loss could be sub-optimal satellite graft composition and microarchitecture. Stevens et al. previously demonstrated that graft architecture was a major driver in the ability of the graft to respond to in vivo injury-associated cues, and many have previously found that microarchitecture greatly impacts both hepatocyte viability and phenotype as well as endothelial cell angiogenesis and vasculogenesis [256, 245, 20]. In this work, we primarily focused on a recent device featured in a publication by Song et al., in which needle-molded channels form a lumen that can be endothelialized, and co-seeding with fibroblasts and endothelial cells in the surrounding hydrogel was conducive to the formation of perfusable, functional neovasculature [246]. While we found that these devices supported both hepatocyte phenotype and function as well as formation of functional vasculature in vitro, we consistently observed that these satellite grafts were not able to persist in vivo. We optimized the manufacture of these satellite grafts to identify the ideal pre-implantation culture period as well as pre- and post-implantation removal of fibroblasts via CAMEO, but did not observe improvement of graft persistence that recapitulated trends from prior studies by Stevens et al. and Chen et al. [257, 256, 40]. We also observed that grafts were red to the eye upon explant (data not shown), suggesting that red blood cells were able to infiltrate the graft, and then likely clotted or were captured in the vessels after collapse or

occlusion. This observation suggests that the formed engineered vasculature may be difficult to maintain after implantation. In the future, surgical anastamosis of the graft inlet and outlet vessels may be necessary ensure flow-based maintenance of the graft.

Pivoting from an approach in which we combine the top-down manufacture of needle-molded channels as well as the bottom-up assembly of a capillary bed, we focused on using templated endothelial cords, which were previously described by Stevens et al. and Baranski et al. [256, 11]. We performed process optimization of the cords fabrication process (which consists of an 8-hour protocol with high sensitivity to the user) to increase reproducibility and reduce failure points leading to inconsistency of engineered cords structure (data not shown). The cords geometry was previously shown to act as a template for formation of neovascular architecture after implantation [11]. We also assessed the utility of tri-cell spheroids containing primary human hepatocytes, fibroblasts, and endothelial cells (data not shown) but leave the further optimization and assessment of this configuration for future work.

4.2.6 Satellite Graft Geometry Impacts in vivo Persistence

Given the considerations regarding immune background and graft geometry discussed in the preceding two subsections, we designed an experiment to test the impact of satellite graft geometry in NSG mice (lacking an injury stimulus). We tested 3 graft configurations head-to-head: hepatocyte-fibroblast spheroids, hepatocyte-fibroblast spheroids with random endothelial cells, and hepatocyte-fibroblast spheroids with templated endothelial cords (**Figure 4-9**A). All satellite grafts contained roughly 250-300k hepatocytes and 600k endothelial cells per animal and were implanted to the fat pad in the peritoneal space. We collected blood samples twice-weekly until 35 days post-implant, and then collected blood samples weekly for downstream human albumin level analysis. We found that spheroid-only grafts and spheroid with random endothelial cell grafts outperformed grafts containing spheroids and templated endothelial cells (**Figure 4-9**B), which was in contrast with findings from Stevens et al. in the context of mice with liver injury [256].

In some mice, we surgically retrieved the satellite graft at day 35 post-implantation in order to assess the impact on measurable phenotype (i.e. we hypothesize that human albumin is entirely produced by the engineered satellite graft). In one representative mouse,

human albumin levels were undetectable after removal of the graft (**Figure 4-9**C). In comparison, a representative mouse with an unperturbed, intact graft continued to secrete measurable levels of human albumin into the circulation. Importantly, this also suggests that the parenchymal compartment of our satellite grafts do not migrate out of the satellite graft housing, which is an important element of safety for the clinical translation of satellites as cell therapies. In immediate future work, we will construct satellite grafts with iCasp9-bearing fibroblasts to assess the role of fibroblasts in implant integration and persistence. We propose experiments in which all or a partial population of fibroblasts in the graft contain the iCasp9 gene.

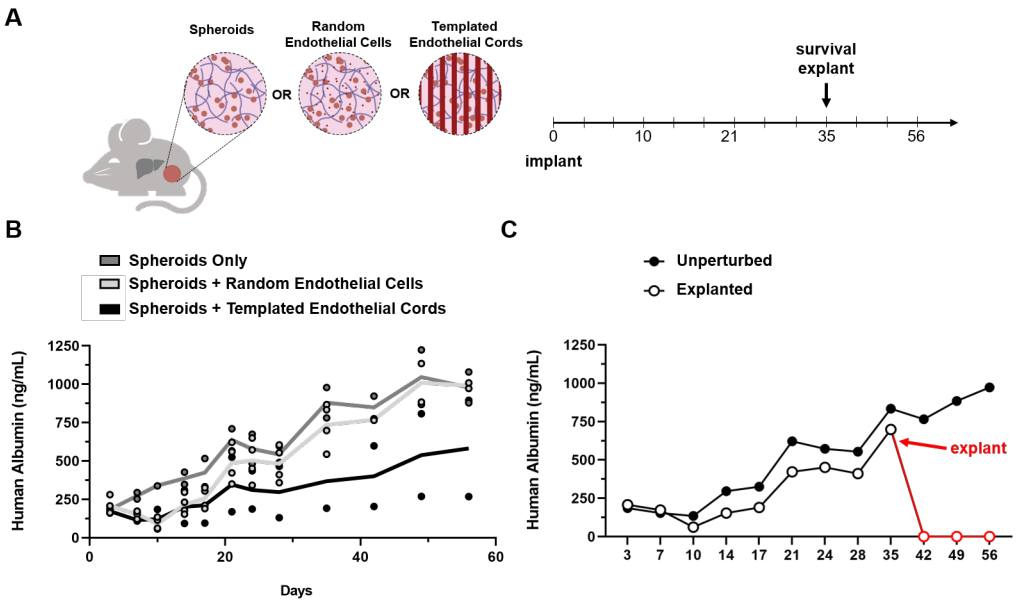

Figure 4-9: **Graft microarchitecture and cellular composition impacts in vivo persistence and performance, and can be reversed by survival explant.** (A) Hepatic spheroid-only (left), hepatic spheroid and random endothelial cell (middle) or hepatic spheroid and templated endothelial cell (right) grafts were implanted in the fat pad of NSG mice. In some mice, grafts were retrieved during a survival surgery performed on day 35 post-implantation. (B) Human albumin was quantified in blood plasma for 56 days (n=2-4). (C) In a representative mouse with a graft containing hepatic spheroids and random endothelial cells, surgical removal of the graft on day 35 (red arrow) led to an immediate drop to undetectable levels of human albumin (red symbols, red line) (n=1). Unpublished.

4.2.7 Hepatic Spheroids as Building Blocks for Cell-Dense Constructs

Lastly, we assessed our ability to use hepatic spheroids as organ building blocks for highly cell-dense constructs. We aimed to show that hepatic spheroids could be compatible with denser constructs because this would enable an increase in the cell dose of our satellite cell therapy while staying within geometric constraints.

Thus far, we have shown that hepatic spheroids can be readily encapsulated in both synthetic and naturally-derived biopolymers, and can be cultured under both static and dynamic conditions in the presence of a vascular compartment [257, 256, 40, 246]. In these formats, we compose our satellite grafts using a density of roughly 10^6 cells/mL. Moving toward higher cell densities, we piloted our hepatic spheroids with a recently developed biomanufacturing protocol for forming highly dense cellular constructs (10^8 cells/mL) known as Sacrificial Writing into Functional Tissue (SWIFT) [239]. Importantly, SWIFT printing is an attractive scaling technique for our hepatic satellite grafts because it both increases the overall cell density and is compatible with building block units with defined microstructure and microarchitecture. SWIFT-printed tissues are formed by harvesting and compacting spheroids and then directly extruding a sacrificial vessel network into the spheroid slurry. Using a temperature-based trigger, the resultant slurry is then polymerized and the printed fugitive ink is simultaneously cleared, resulting in a perfusable lumen that can be endothelialized and cultured under flow (**Figure 4-10**A). For these experiments, we used freshly isolated primary rat hepatocytes because each donor can provide up to 200 M hepatocytes, and we frequently required between 50-100 M hepatocytes for each experiment. Primary rat hepatocytes are less resource restricted and have been commonly used in our lab and across the field to perform pilot experiments, such as in this set of studies in which we explore compatibility with scaling. In the future, we envision that adaptation to use of primary human hepatocytes would not pose a significant biological risk, and that we can perform the bulk of the manufacturing risk mitigation using primary rat hepatocytes.

SWIFT-printed hepatic tissues retained the lumen structure formed by the sacrificial lumen print for several days of in vitro culture (**Figure 4-10**B). Additionally, after day 10 of in vitro culture, tissues contained arginase-1^+ hepatocytes and phalloidin$^+$ hepatocytes and fibroblasts, suggesting that tissues were viable and phenotypically stable (**Figure 4-10**B).

Lastly, we performed in vitro culture under flow via pump perfusion of two SWIFT-printed constructs; SWIFT-printed tissues secreted rat albumin continually over a period of 10 days in vitro, suggesting that tissues remained functional over an extended culture period. These pilots lay the groundwork for building cell-dense tissue constructs with biomanufacturing methods such as but not limited to SWIFT printing.

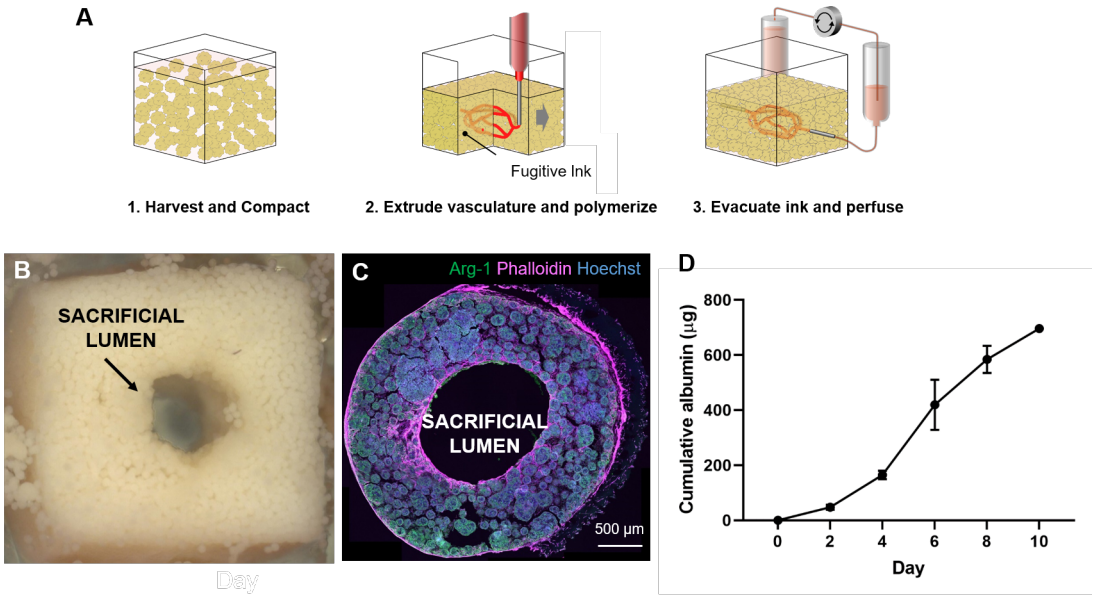

Figure 4-10: **Hepatic spheroids are compatible with cell-dense embedded printing.** (A) Sacrificial writing into functional tissue (SWIFT) printing allows for direct printing of bio-compatible, fugitive ink into a dense slurry of spheroids. In brief, spheroids are harvested and compacted in a desired mold (1), and then a printer extrudes fugitive ink to prescribe the geometry of vascular channels (2), which are then sacrificed and act as perfusable channels for dynamic in vitro culture (3). (B) Representative image of SWIFT-printed channel on day 0, immediately after gelation (arrow indicates sacrificial lumen). (C) Representative image of sacrificial lumen after 10 days of in vitro culture of a tissue containing primary rat hepatocytes (arginase-1, green) and fibroblast (F-actin, phalloidin, magenta) spheroids (nuclei counterstained with Hoechst; scale bar = 500 μm). (D) Spent supernatant was collected from in vitro culture over 10 days, and secreted rat albumin was quantified (n=2 tissues). Panel A adapted from [239]. Panels B-D are unpublished.

4.3 Conclusions

In this Chapter, we have described a workflow for optimizing tissues containing hepatic spheroids with engineered vasculature with the end-goal of implantation into animal models

for preclinical testing. First, we show that inclusion of fibroblasts and endothelial cells represent crucial cell compartments of a satellite graft, and have implications for in vivo integration, function, and persistence. We also demonstrate that CAMEO is compatible with the Hepatic VasculoChip, and that fibroblast deletion improves hepatic phenotype in vitro. We show that graft integration and performance is sensitive to the pre-conditioning period in vitro. Importantly, we discuss important considerations for the choice of immunodeficient mouse model, and share preliminary work that compares the performance of different graft microarchitecture and cellular composition in NSG mice (which are more immunodeficient than the nude mice we used previously). Lastly, we demonstrate an important aspect of safety for satellite grafts by showing phenotype reversal upon a survival explant of the satellite graft. Further considerations for designing and testing satellite graft therapies in both healthy and diseased mouse models are described in the following Chapter.

4.4 Methods

4.4.1 Cell Culture

Human umbilical vein endothelial cells (HUVEC; pooled from 4 donors; Lonza) were cultured in Endothelial Growth Medium-2 (EGM-2, Lonza) and used before passage 7 for all experiments. Normal human dermal fibroblasts (NHDF; single donor; Lonza) were cultured in high-glucose Dulbecco's modified Eagle's medium (DMEM) with 4.5 g/L glucose (CellGro) containing 10% (v/v) fetal bovine serum (FBS) (Gibco) and 1% (v/v) penicillin-streptomycin (Invitrogen). Primary cryopreserved human hepatocytes (Lot ZGF, 33-year-old, Caucasian, male; BioreclamationIVT) were maintained in high-glucose Dulbecco's modified Eagle's medium (DMEM) with 4.5 g/L glucose (CellGro) containing 10% (v/v) fetal bovine serum (FBS) (Gibco), 1% (v/v) ITS supplement (insulin, transferrin, sodium selenite; BD Biosciences), glucagon (70 ng/mL), dexamethasone (0.04 µg/mL), 0.015 M HEPES, and 1% (v/v) penicillin-streptomycin (Invitrogen). In some experiments, we used freshly isolated primary rat hepatocytes, which were isolated from 2 to 3 month old adult female Lewis rats, as previously described [231]. Multicellular cultures containing both hepatocytes and HUVECs were maintained with a 50:50 mixture of hepatocyte media and EGM-2 media.

4.4.2 Lentiviral Transduction

iCasp9-GFP NHDFs were generated by lentivirally transducing NHDFs using a 3rd generation lentiviral system with an iCasp9-IRES-GFP plasmid, as previously described elsewhere (gift from David Spencer, Addgene; #15567 pMSCV-F-del Casp9.IRES.GFP; cloned in-house to a lentivirus plasmid backbone with an SFFV promoter) [258, 246, 41]. Briefly, individual plasmids were co-transfected into HEK-293T cells with pVSVG, pRSV-REV, and pMDLg/pRRE using the calcium phosphate transfection method. Supernatants containing the assembled viruses were collected after 48 hours and precipitated using PEG-IT (SBI). The concentrated viral pellet was resuspended in PBS and stored at -80°C. NHDFs and HUVECs were transduced in growth media overnight with the appropriate lentiviral titers that had been optimized for minimal changes in cell morphology and proliferation. The cells were then washed in PBS the next day and fed with fresh growth media for expansion. For iCasp9-GFP NHDFs, a GFP^{hi} population (top 30%) was selected via flow-assisted cytometry (FACSMelody, BD Biosciences).

4.4.3 Hepatic Spheroid Culture

Hepatic spheroids were cultured as described previously [257, 256, 41]. In brief, cryopreserved human hepatocytes were thawed and immediately plated with NHDFs or iCasp9-GFP NHDFs in AggreWells (400 μm pyramidal microwells) and incubated overnight at a 1:1 or 1:2 hepatocyte:fibroblast ratio.

4.4.4 Hepatic VasculoChip Seeding

"VasculoChip" microfluidic devices were prepared as described previously [246]. Molds for two- and four-channel VasculoChip devices were constructed using stereolithography (Proto Labs). Polydimethylsiloxane (PDMS) was cured at a standard mixing ratio (10:1 base:activator) overnight at 60°C in the mold, and individual devices were cut and plasma-bonded to glass slides. To enhance ECM bonding to the PDMS walls, the surface within the tissue chamber of the devices was functionalized with 0.01% poly-L-lysine and 1% glutaraldehyde following plasma-activation and washed overnight in distilled water. On the day of seeding, devices were soaked in 70% ethanol and dried for sterilization. Acupuncture needles (300 μm diameter) (Hwato) were blocked with 0.1% (w/v) bovine serum albumin

(BSA) (Sigma) in phosphate buffer saline (PBS) for 45 minutes and inserted through the two needle guides. Devices with needles were further sterilized via UV exposure for at least 15 minutes. On the day of device seeding, NHDFs or iCasp9-GFP NHDFs were growth-arrested with 10 µg/mL mitomycin in FGM-2 for 2.5 hours and thoroughly washed 5 times with FBM. We note that mitomycin C-arrested and untreated NHDFs performed similarly in their ability to support vascular morphogenesis, and we used growth-arrested cells for all studies in this work. Both HUVECs and NHDFs were lifted from culture plates using TrypLE Express (Gibco), centrifuged at 200xg for 5 minutes, and resuspended to a concentration of 20 million cells/mL in EGM-2. A solution of HUVECs (3 million cells/mL), NHDFs or iCasp9-GFP NHDFs (0, 1 million, 3 million, or 6 million cells/mL), fibrinogen (2.5 mg/mL), thrombin (1 U/mL) in EGM-2 was prepared for the bulk hydrogel region of each device. For devices with hepatocytes, a solution of HUVECs (3 million cells/mL), iCasp9-GFP NHDFs (total of 6 million cells/mL), hepatic aggregates (0.36 million aggregates/mL with about 150 hepatocytes per aggregate), fibrinogen (2.5 mg/mL), thrombin (1 U/mL) was made in a 1:1 media mixture of EGM-2 and hepatocyte maintenance media. After the addition of thrombin, the solution was quickly injected into the tissue chamber, and the devices were repeatedly rotated while the solution polymerized. Appropriate media was added to each well of the device, and the devices were placed in the incubator (37 °C, 5% carbon dioxide). After 15 minutes, the needles were carefully removed from the devices to create 300 μm hollow channels between the wells. Each channel of the device was seeded with additional HUVECs at 2 million cells/mL for at least 5 minutes on each side (top and bottom) in the incubator. Each device received 200 μµL of appropriate media daily and was cultured on the rocker inside the incubator.

4.4.5 Hepatic Graft Encapsulation and Endothelial Cord Fabrication

Tissue graft molds were fabricated by preparing polydimethylsiloxane washer-shaped gaskets (inner diameter, 5/8"; outer diameter, 1"). Washer-shaped gaskets were autoclaved for sterilization and then placed in sterile 60 mm Petri dishes using sterile tweezers. Endothelial cords were prepared as described previously [256, 11, 39]. To created templated endothelial cords, HUVECs were suspended at a density of 10 million HUVEC/mL in liquid rat tail col-

lagen I (2.5 mg/mL) (BD Biosciences) and centrifuged into polydimethylsiloxane channels. Collagen was polymerized at 37 °C and constructs were incubated in EBM-2 basal medium for 4 hours to allow for cord formation. Endothelial cord arrays were then released from the molds and embedded atop a layer of fibrin (10 mg/mL bovine fibrinogen, 1.25 U/mL human thrombin; Sigma-Aldrich) within the washer-shaped gasket. Subsequently, a layer of fibrin containing hepatic aggregates was polymerized on top of the endothelial cords, thus encasing the cords in a sandwich of "blank" fibrin gel and hepatic aggregates. For spheroid-only grafts, a bottom layer of fibrin was first polymerized in the washer-shaped gasket, and then a layer of fibrin containing hepatic aggregates was polymerized atop. For spheroid grafts containing random endothelial cells, a bottom layer of fibrin was first polymerized in the washer-shaped gasket, and then a layer of fibrin containing hepatic aggregates and single-cell HUVECs (600k per graft) was polymerized atop. Grafts were polymerized for 40 minutes atv37°C and then hydrated with a 1:1 mixture of EGM-2 and hepatocyte maintenance media. Media was replaced with CO2-independent medium such as DMEM:Nutrient Mixture F-12 (Gibco) or media supplemented with 25 mM HEPES before transferring to the animal facility for implantation.

4.4.6 Animal Implantation

All surgical procedures were conducted according to protocols approved by the Massachusetts Institute of Technology Institutional Animal Care and Use Committee. All mice were handled aseptically and kept in separate containment areas or imaged in equipment specifically designated for immunodeficient mice to avoid opportunistic infection with *C. bovis*. Four- to 8-week old female CAnN.Cg-*Foxn1*^{nu}/Crl (BALB/c Nude; Charles River Laboratories, #194, Homozygous) or NOD.Cg-*Prkdc*^{scid} *Il2rg*^{tm1Wjl}/SzJ (NSG; The Jackson Laboratory, #005557) mice were anesthetized using isoflurane and injected subcutaneously with buprenorphine SR-LAB (slow-release buprenorphine; ZooPharm, 1.0 mg/kg, once preoperatively for 72 hours of post-operative analgesia) prior to surgery. An abdominal laparotomy was performed on each animal using sterile surgical technique, and hepatic tissue constructs were sutured to the mesenteric or parametrial fat pad in the intraperitoneal space using 5-0 multi-filament silk sutures (Ethicon) (1 tissue per animal, 250-500k hepatocytes per animal). Tissue grafts were prepared using a sterile 6 mm biopsy punch immediately

prior to implantation. The incisions were closed aseptically using 5-0 multi-filament silk sutures in a continuous suture pattern for the muscle layer, and the skin was held in place with sterile wound clips.

4.4.7 In vivo CID Administration

For in vivo administration, CID (B/B homodimerizer, AP20187; rapalog; Takara/ClonTech) was prepared as per the following formulation: 4% ethanol, 10% poly(ethylene glycol)-400, and 1.75% Tween-20 in Milli-Q distilled water. The solution was prepared fresh and sterile-filtered prior to intraperitoneal injection (200 μL per animal).

4.4.8 Live Bioluminescence Imaging

To enable non-invasive imaging of functional hepatocytes, primary human hepatocytes were transduced in suspension culture immediately upon thawing with an adeno-associated virus expressing firefly luciferase under a CMV promoter (AAV2/8.CMV.Luciferase2.SVPA, MOI = $10e^7$ gc/hepatocyte; Gene Transfer Vector Core, The Schepens Eye Research Institute) before compaction in AggreWells with fibroblasts. For viral transduction, concentrated virus was spiked into hepatocyte maintenance medium during incubation in AggreWells overnight; subsequently, hepatocytes were harvested and re-plated with murine fibroblasts as described above. Resultant aggregates were incorporated into grafts and implanted into mice. Immediately before bioluminescence imaging, mice were injected intraperitoneally with 100 μL of D-luciferin (48 mg/mL, Gold Bio) and imaged using the IVIS Spectrum (Xenogen) system and Living Image software (Caliper Life Sciences).

4.4.9 Blood Collection and Euthanasia

Blood samples were collected during the experiment via saphenous vein bleeds or at the terminal point via cardiac puncture or retro-orbital bleed. Samples were collected using lithium-heparin tubes (Microvette® 200 Capillary Blood Collection Tube Conical Bottom, Skirted Lithium Heparin Additive; Sarstedt) and centrifuged to produce the plasma fraction, which was then frozen until analysis. At sacrifice (day 10 to 56 post-implantation), grafts were explanted and fixed with 4% paraformaldehyde.

4.4.10 SWIFT Printing

Embedded, cell-dense prints were prepared as described previously [239]. As the sacrificial ink, 15% (w/w) gelatin stock solution in phosphate buffered saline without calcium or magnesium was prepared at 85°C for 12 hours while stirring. The resulting solution was adjusted to pH 7.5 using a 2 N NaOH, mixed with 2% (v/v) red food coloring to enable visualization during printing, and then sterile-filtered and stored at 4°C until use. For hepatic tissue fabrication, hepatic spheroids were compacted via centrifugation at $60x$g, then resuspended in 10 mg/mL bovine fibrinogen and 1.25 U/mL human thrombin and centrifuged again at $60x$g at 4°C create a spheroid-dense slurry. The slurry was prepared either in a perfusion chamber mold [239] or a gelatin-molded disk for in vitro culture, and centrifuged at $60x$g at 4°C for compaction. A vascular network was printed by extruding gelatin sacrificial ink in a straight line through the spheroid-dense slurry matrix, and then the entire tissue was transferred to a 37°C, 5% Co2 incubator for 45 minutes to complete gelation of the spheroid-dense slurry matrix and melt the sacrificial gelatin ink. Tissues were perfused for up to 10 days and media was collected from the collection chamber every other day. At the end of the experiment, tissues were fixed in 4% formaldehyde, soaked in sucrose solution for cryoprotection, and prepared for cryosectioning (40-60 μm slices) in Optimal Cutting Temperature (OCT) on a Superfrost Plus slide (VWR Inc.).

4.4.11 Immunofluorescence Imaging

In some samples, lysine-fixable FITC-conjugated 500 kDa dextran solution (1.5 mg/mL) was added to the devices before imaging to visualize vessel lumens. Tissue sections were blocked and incubated with primary antibodies against arginase-1 (rabbit, 1:400; Sigma-Aldrich) or with Alexa Fluor^{TM} 568-conugated F-actin (Phalloidin; 1:200; Life Technologies), and followed with species-appropriate secondary antibodies conjugated to fluorophores if necessary. HUVECs were stained with UEA lectin (1:500) for 1 hour at room temperature, followed by secondary goat anti-rabbit Alexa Fluor^{TM} 568 (1:1000) overnight at 4°C.

4.4.12 Biochemical Assays

Blood plasma was thawed and human albumin was quantified using an enzyme-linked immunosorbent assay using the sheep anti-rat albumin antibody (ELISA) (Bethyl Laborato-

ries) and 3,3',5,5'-tetramethylbenzidine (TMB, Thermo Fisher).

4.4.13 Imaging

Images were captured on a Zeiss Confocal microscope, or with the Leica SP8 confocal microscope (Leica, Wetzlar, Germany) using either a Leica 10x/0.30NA W U-V-I WD-3.60 Water or 25x/0.96NA W VISIR WD-2.50 Water objective, and Leica LAS X imaging software.

4.4.14 Statistical Analysis

All data are expressed as mean ± standard deviation and/or visualized as dot plots (n =2-8 as indicated). Statistical significance ($\alpha = 0.05$) was determined using the appropriate statistical test (unpaired 2-tailed t-test, 1-way ANOVA, 2-way ANOVA), and followed by multiple comparisons testing (Tukey's post hoc test) GraphPad).

4.5 Acknowledgements

I am thankful to **Dr. Tiffany Vo**, **Trevor R. Nash**, and **Keval N. Vyas** for training me in techniques related to the preparation and implantation of hepatic tissue grafts into small animal models. I am especially indebted to Tiffany and Trevor for carrying out our initial in vivo pilots while I was still completing training with the Division of Comparative Medicine. I am incredibly grateful to **Dr. Hyun-Ho Greco Song**: the other "half" of our surgical dream team; some of the work in this Chapter has been reproduced from his recent publication [246] and review [245]; **Prof. Christopher Chen** and **Prof. Jennifer Lewis** (for their mentorship and providing a boundless source of inspiration both scientifically and personally); **Now-Prof. Mark Skylar Scott** and **Dr. Sebastien Uzel** (for mayonnaise, patties, and all that is good with scientific food puns – even if not all of our bosses enjoyed it); and **Dr. Luba Perry** (for providing crucial input on vascular graft read-outs and patiently making our first set of templated endothelial cords - and then teaching us how to make our own!). Lastly, I am indebted to **Dr. Arnav Chhabra** and **Keval N. Vyas**, who were and continue to be amazing scientific partners in this work.

I would also like to thank **Hilda "Scooter" Holcombe** (Associate Director of the Division of Comparative Medicine) and **Virginia Spanoudaki** (Scientific Director of the Preclinical

Imaging & Testing Facility of the Koch Institute Swanson Biotechnology Center), who provided essential support and advice for working with immunodeficient mice and performing live animal imaging of our tissue grafts.

This work was supported in part by the NIH (R01 EB008396, R01 EB000262, UG3 EB017103), Koch Institute Support (core) Grant P30-CA14051 from the National Cancer Institute, the National Science Foundation Cellular Metamaterials Engineering Research Center, and the Boston University Biological Design Center.

Chapter 5

FUTURE PERSPECTIVES

5.1 Introduction

In the preceding chapters of this thesis, we mainly focus on describing applications of the CAMEO technology to the development of satellite cell therapies for the liver, which we frame in the context of tissue engineering and regenerative medicine. In this Chapter, we will (1) describe additional use cases of CAMEO for engineering organogenesis and (2) outline potential projects that fall outside of these spaces. We substantiate some of these ideas with preliminary data in the body of this Chapter.

5.2 CAMEO for Engineered Organogenesis

5.2.1 Multiplex Demonstration of CAMEO

In next steps, we aim to leverage CAMEO to more closely examine the contribution of stromal cells to the phenotypic stability of hepatocytes in a variety of multicellular, tissue engineered platforms for the study of human liver biology and development of implantable grafts. From a clinical perspective, the inclusion of stroma in a co-culture can be limiting, due to the additional complexity, as well as the potential to serve as a significant nutrient sink and transport barrier. Aside from enabling removal for practical and translational purposes, we envision that inducible apoptosis genes can also be deployed in other compartments of multicellular tissue ensembles in order to study interactions and their impact on phenotype

and function. We expect CAMEO to be readily incorporated into a variety of cell types because most cell populations are genetically tractable as per lentiviral modification protocols. Thus, we envision vast utility in the investigation of multicellular microenvironments and dissection of requirements for phenotypic stability, network formation, in vivo host integration, and more. Importantly, eventual clinical application of multicellular engineered livers may require incorporation of additional non-parenchymal cell types such as Kupffer cells, stellate cells, liver sinusoidal endothelial cells, and cholangiocytes to include an immune component, build a perfusable vascular network, and grow a biliary tree, respectively.

5.2.2 CAMEO in the Clinic

CAMEO offers a preclinical tool that will enable the precise, systematic removal of cells from complex multicellular ensembles with temporal control. Furthermore, we envision that orthogonal inducible apoptosis genes could be designed to enable a multiplexed evolution of the CAMEO platform, and that various triggers could include other synthetic small molecules or natural derivatives as well as light-, electric field-, magnetic field-inducible gene circuits [303, 142, 278, 301]. The choice of trigger could relate to the location of the cell therapy, i.e. a light-inducible trigger would likely need to be implanted subcutaneously.

The administration of CID has been previously demonstrated to be safe and efficacious in both humans and animals and there exist established regulatory frameworks in development that may enable cell therapies to include xenogeneic components [60, 81, 258, 229]. Additionally, other supportive stromal cells of human origin have been shown to enhance the phenotypic stability of hepatocytes [256], and can be used as a substitute for 3T3-J2 murine fibroblasts if necessary. Lastly, interestingly, we envision that CAMEO-driven generation of apoptotic debris may actually be a useful immunomodulatory strategy for inducing therapeutic immune tolerance to xenogeneic or allogeneic cell therapies [214, 261]. Taken together, we posit that CAMEO is useful not only for dissecting the role of various cell populations in implant integration and persistence in the host, but also enables new approaches in a clinical setting.

5.2.3 Synthetic Biology to Control Paracrine Cues for Organogenesis and Expansion

In this thesis, we mainly focus on the removal of cells via apoptosis as a way to control cell-cell interactions in a spatiotemporal fashion. Besides the ablation of a cell population, we can also employ a similar synthetic biology-driven framework to control other biological cues that drive relevant cell behaviors and states, such as cell expansion and vascular morphogenesis. In this section, we will more fully describe a research plan for employing tools from synthetic biology and genetic engineering in order to control specific paracrine factors toward this end.

Firstly, a major challenge of hepatic cell-based therapies is rooted in cell sourcing. While hepatocytes have a native capacity to undergo multiple rounds of replication in vivo in response to a regenerative stimulus, this ability is lost ex vivo. The limited source of hepatocytes is a major bottleneck for the translation of hepatic cell-based therapies, and there is much interest in identifying molecules that drive expansion as well as enhance hepatic function. In work by Shan et al., a high-throughput screen was used to identify small molecules that induce proliferation and/or enhancement of hepatocyte function [234]. Of note, the hepatocyte screening platform consisted of both hepatocytes and fibroblasts, which leaves the possibility that the identified factors acted indirectly on hepatocytes via action on fibroblasts.

Additionally, we could curate a list of known mitogens that are involved in regeneration in vivo. In a development context, it is known that the Hippo-Yap and Wnt/β-catenin pathways play a prominent role in regulating liver mass [302, 112, 275]. Relatedly, effectors of these pathways appear to drive hepatocyte expansion and vascular elaboration upon injury [252, 30]. Specifically, in seminal work done by Ding et al., it was shown that liver sinusoidal endothelial cells drive liver regeneration through the secretion of angiocrine factors Wnt2 and HGF [61]. To build on preliminary advances [275, 190] in testing these and additional factors in vitro, we propose to do functional testing of cell-cell signaling factors and physiological cues (i.e. shear stress [163]) that regulate hepatocyte expansion and proliferative angiogenesis. We can employ synthetic biology tools, as we did with CAMEO, to engineer the inducible or constitutive knockdown or over-expression of these factors to significantly impair or enhance tissue function and expansion, respectively. We will generate cell lines with desired engineered expression and then use them to form our satellite implants. In

some cases, we will engineer support cells such as fibroblasts to express inductive signals instead. We envision that these experiments will lay the groundwork for identifying factors that contribute to synthetic tissue expansion, which can be employed for in vitro as well as in situ expansion.

5.3 CAMEO Beyond Tissue Engineering

In this section, we will describe additional use cases for CAMEO that are beyond immediate applications in tissue engineering and regenerative medicine.

5.3.1 Gene Manipulation in Multicellular Cultures

CAMEO has applications in drug discovery and personalized medicine. In a set of experiments related to a previous publication by Mancio-Silva et al., we demonstrate that CAMEO can enable the genetic manipulation of hepatocyte-fibroblast co-cultures [168]. In this work, we dosed 2D MPCCs (consisting of primary human hepatocytes and 3T3-J2 murine fibroblasts) with an siRNA targeting CYP3A4, which is a liver-specific drug metabolism enzyme. MPCCs were sequentially seeded with primary hepatocytes on day 0 and fibroblasts on day 1 (**Figure 5-1**A). Hepatocyte islands were transduced with CYP3A4 siRNA on day 0 post-seeding, resulting in a 94.9% knockdown compared to untreated controls (**Figure 5-1**A). Alternatively, MPCCs were cultured for one week before siRNA treatment in order to stabilize hepatocyte phenotype and function prior to gene manipulation. At day 7, MPCCs with intact fibroblasts had a markedly reduced knockdown efficiency of CYP3A4 activity (approximately 17.9%) (**Figure 5-1**B). We hypothesized that the fibroblasts were acting as a barrier and/or a sink for the CYP3A4 siRNA. To test this hypothesis, we employed CAMEO to remove the seeded fibroblast cells prior to administering CYP3A4 siRNA treatment. In CID-pre-treated cultures, the knockdown efficiency at day 7 was restored to 93.2%, which is similar to the efficiency on day 0 prior to fibroblast seeding (**Figure 5-1**B). These results demonstrate a proof-of-concept application for CAMEO that harmonizes with applications in drug development and personalized medicine.

Beyond use cases in 2D platforms, CAMEO could also enable cell-specific access in 3D hepatic ensembles in in vitro and in vivo settings. For example, we envision that clearance of fibroblasts or other disposable cell types would enable genetic manipulation of cell types that

require matrix embedding or co-culture to undergo differentiation and/or acquire phenotypic stability.

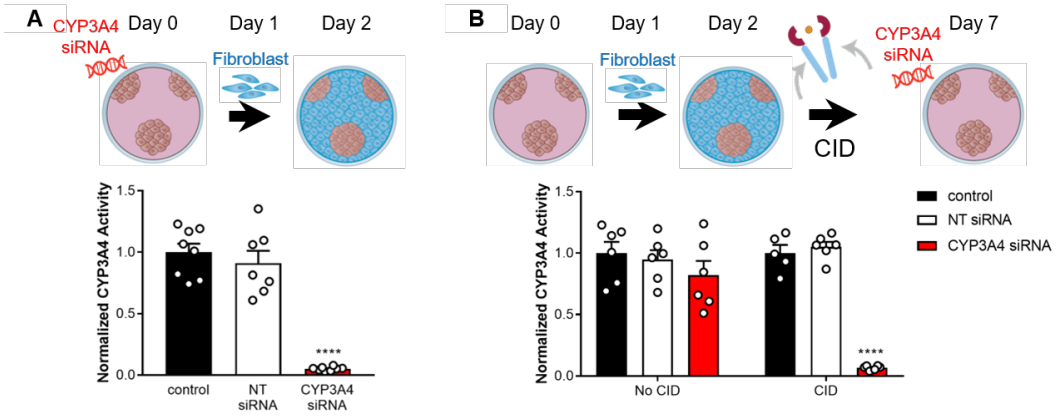

Figure 5-1: **Removal of fibroblasts expands capabilities of MPCCs as a testbed for therapeutic candidates** (A) MPCCs were seeded sequentially with primary human hepatocytes on day 0 and 3T3-J2 murine fibroblasts on day 1. Hepatocytes were dosed with CYP3A4 siRNA on day 0, prior to fibroblast co-culture. MPCCs assayed for CYP3A4 activity. (B) Hepatocytes were co-cultured with fibroblasts for 7 days in the MPCC format and dosed with CID to remove fibroblasts before treatment with CYP3A4 siRNA. MPCCs were assayed for CYP3A4 activity. (n=6-8, ****$p<0.0001$ vs. control). Unpublished.

5.4 Assessment of Satellite Cell Therapies in Disease Models

In this thesis, we have focused on the testing of satellite cell therapies in healthy mouse models that lack injury stimulus. As a first step, optimization of satellite graft geometry and performance is most quickly screened in these mouse models, though immediate next steps must involve mouse models that sustain acute or chronic liver-specific injury stimuli. Here, we discuss realistic constraints and considerations for testing satellite cell therapies in small animal models. We also comment on considerations for developing allogeneic or xenogeneic cell therapies, in which the use of immunosuppressed or immunodeficient animal models is necessary for testing immune-mismatched tissue construct performance.

We adapted our list of considerations from Rahman et al. [216] and describe each

component as follows:

- **Reversibility of disease phenotype:** the disease model must consist of an injury process that is reversible, in a measurable fashion (e.g. by biochemical serum biomarkers that are compatible with clinical trial endpoints; neurological; histopathological; mortality)
- **Physiological fidelity to human pathology:** the disease model should recapitulate specific symptoms and/or timeline of progression that has been described in the clinical literature
- **Surgical implantation window:** the disease model must be compatible with implantation of a satellite cell therapy, i.e. IAUCUC-approved compatibility to ensure humane treatment of animals that experience a laparotomy procedure, and the satellite cell therapy is not affected by administration of any compounds used to induce disease and injury
- **Titration of disease severity:** an animal model that is based on dosed compounds or surgical intervention should be able to be titrated between sub-lethal and lethal injury levels in a reproducible fashion by the operator (with regard to resulting pathology on a predictable timeline)
- **Reduction of Hazardous Materials:** the disease model should not utilize toxins or chemicals that pose a risk to the staff that carry out the experiment
- **Compatibility with immunosuppression or immunocompromised background:** the disease model is available on an immunodeficient background; in cases where inflammation is a major driver of disease pathology, it will be important to consider further development of the model prior to experimentation; furthermore, drug-drug interactions or side effects from the administration of immunosuppressive drugs should also be considered
- **Precedence:** a history of usage across multiple research groups, with proven reproducibility
- **Refractory to existing treatments:** a disease model that is not well addressed by existing approaches that are easily accessible to the target patient population, e.g.

gene therapy for hemophilia or sofosbuvir for viral hepatitis C

The aforementioned features contribute to an overall difficulty in identifying adequate mouse models that allow for the study of clinically relevant disease treatment and resolution, especially in the setting of allogeneic and xenogeneic cell therapies. Animal models to consider include disease resulting from viral or parasitic insult (e.g. hepatitis viruses, schistosomiasis), autoimmune origin, toxin action (e.g. alcohol, carbon tetrachloride, thioacetamide, acetaminophen, dimethyl or dietyl nitrosamine, concanavalin A, ethanol, D-galactosamine and/or lipopolysaccharide), imbalanced diets (e.g. DDC, methionine-deficient, choline-deficient, high fat, fructose), surgical intervention (e.g. common bile duct ligation, 70-100% hepatectomy, devascularization by portacaval shunt and hepatic artery clamping), genetic background (e.g. TBF-β1 over-expression, ornithine transcarbamylase deficiency, Bcl-xL knockout, Abcb4 knockout, PDGF overexpression, NTx-PD-1 knockout, FNRG: hereditary tyrosinema type I, alpha-1 antitrypsin deficiency, hereditary hemochromatosis, carbamoyl phosphate synthetase 1 deficiency, hemophilias, TK-NOG), biologics (e.g. anti-CD95 antibody) and combinations of the above [216, 162]. Multiple models could be used to capture various aspects of human clinical progression. In the future, new models could be developed that address a larger overlap of the ideal criteria listed above. Currently, the use of the FNRG and TK-NOG model are most prominent for immune-mismatched cell therapies.

5.5 Acknowledgements

Dr. Liliana Mancio-Silva was my scientific partner in the gene manipulation work. I also credit my various mentors across industry from internships at Clarion (life science consulting firm), RA Capital Management (multi-stage biotech investment company), Flagship Pioneering (life science venture capital firm and incubator), and Novartis Institute of Biomedical Research (the innovation engine of the big pharma giant, Novartis) with growing my interest across the healthcare and biotech spaces, which has helped me contextualize my scientific contributions and curiosities in a new light.

Bibliography

[1] Lauren M. Aleksunes, Michael Goedken, and José E. Manautou. Up-regulation of NAD(P)H quinone oxidoreductase 1 during human liver injury. *World Journal of Gastroenterology : WJG*, 12(12):1937, March 2006. Publisher: Baishideng Publishing Group Inc.

[2] Fawzi Aoudjit and Kristiina Vuori. Integrin Signaling in Cancer Cell Survival and Chemoresistance. *Chemotherapy Research and Practice*, 2012, 2012.

[3] Sumeet K. Asrani, Harshad Devarbhavi, John Eaton, and Patrick S. Kamath. Burden of liver diseases in the world. *Journal of Hepatology*, 70(1):151–171, 2019.

[4] Georgia K. Atkin-Smith, Stephanie Paone, Damien J. Zanker, Mubing Duan, Than K. Phan, Weisan Chen, Mark D. Hulett, and Ivan K. H. Poon. Isolation of cell type-specific apoptotic bodies by fluorescence-activated cell sorting. *Scientific Reports*, 7, January 2017.

[5] Marcus KH Auth, Ruth E Joplin, Masashi Okamoto, Yuichi Ishida, Paul McMaster, James M Neuberger, Roman A Blaheta, Thomas Voit, and Alastair J Strain. Morphogenesis of primary human biliary epithelial cells: Induction in high-density culture or by coculture with autologous human hepatocytes. *Hepatology*, 33(3):519–529, 2001.

[6] Hisaya Azuma, Nicole Paulk, Aarati Ranade, Craig Dorrell, Muhsen Al-Dhalimy, Ewa Ellis, Stephen Strom, Mark A Kay, Milton Finegold, and Markus Grompe. Robust expansion of human hepatocytes in fah-/-/rag2-/-/il2rg-/- mice. *Nature biotechnology*, 25(8):903–910, 2007.

[7] Brendon M. Baker and Christopher S. Chen. Deconstructing the third dimension – how 3D culture microenvironments alter cellular cues. *Journal of Cell Science*, 125(13):3015–3024, July 2012.

[8] Shyam Sundhar Bale, Sharon Geerts, Rohit Jindal, and Martin L Yarmush. Isolation and co-culture of rat parenchymal and non-parenchymal liver cells to evaluate cellular interactions and response. *Scientific reports*, 6:25329, 2016.

[9] T. Eric Ballard, Shuai Wang, Loretta M. Cox, Mark A. Moen, Stacy Krzyzewski, Okechukwu Ukairo, and R. Scott Obach. Application of a Micropatterned Cocultured Hepatocyte System To Predict Preclinical and Human-Specific Drug Metabolism. *Drug Metabolism and Disposition: The Biological Fate of Chemicals*, 44(2):172–179, February 2016.

[10] Pedro M Baptista, Mohummad M Siddiqui, Genevieve Lozier, Sergio R Rodriguez, Anthony Atala, and Shay Soker. The use of whole organ decellularization for the generation of a vascularized liver organoid. *Hepatology*, 53(2):604–617, 2011.

[11] Jan D. Baranski, Ritika R. Chaturvedi, Kelly R. Stevens, Jeroen Eyckmans, Brian Carvalho, Ricardo D. Solorzano, Michael T. Yang, Jordan S. Miller, Sangeeta N. Bhatia, and Christopher S. Chen. Geometric control of vascular networks to enhance engineered tissue integration and function. *Proceedings of the National Academy of Sciences*, 110(19):7586–7591, May 2013. Publisher: National Academy of Sciences Section: Physical Sciences.

[12] David M Barry, Yeon Koo, Pieter R Norden, Lyndsay A Wylie, Ke Xu, Chonlarat Wichaidit, D Berfin Azizoglu, Yi Zheng, Melanie H Cobb, George E Davis, et al. Rasip1-mediated rho gtpase signaling regulates blood vessel tubulogenesis via non-muscle myosin ii. *Circulation research*, 119(7):810–826, 2016.

[13] Bodo B Beck, Sandra Habbig, Katalin Dittrich, Dirk Stippel, Ingrid Kaul, Friederike Koerber, Heike Goebel, Eduardo C Salido, Markus Kemper, Jochen Meyburg, et al. Liver cell transplantation in severe infantile oxalosis—a potential bridging procedure to orthotopic liver transplantation? *Nephrology Dialysis Transplantation*, 27(7):2984–2989, 2012.

[14] David J Beebe, Jeffrey S Moore, Joseph M Bauer, Qing Yu, Robin H Liu, Chelladurai Devadoss, and Byung-Ho Jo. Functional hydrogel structures for autonomous flow control inside microfluidic channels. *Nature*, 404(6778):588–590, 2000.

[15] J Belghiti, D Sommacale, F Dondéro, F Zinzindohoué, A Sauvanet, and F Durand. Auxiliary liver transplantation for acute liver failure. *HPB*, 6(2):83–87, 2004.

[16] Catherine C Bell, Delilah FG Hendriks, Sabrina ML Moro, Ewa Ellis, Joanne Walsh, Anna Renblom, Lisa Fredriksson Puigvert, Anita CA Dankers, Frank Jacobs, Jan Snoeys, et al. Characterization of primary human hepatocyte spheroids as a model system for drug-induced liver injury, liver function and disease. *Scientific reports*, 6:25187, 2016.

[17] William Bernal and Julia Wendon. Acute liver failure. *New England Journal of Medicine*, 369(26):2525–2534, 2013.

[18] Sangeeta. N. Bhatia, U. J. Balis, Martin. L. Yarmush, and Mehmet Toner. Effect of cell–cell interactions in preservation of cellular phenotype: cocultivation of hepatocytes and nonparenchymal cells. *The FASEB Journal*, 13(14):1883–1900, November 1999.

[19] Sangeeta N Bhatia and Donald E Ingber. Microfluidic organs-on-chips. *Nature biotechnology*, 32(8):760–772, 2014.

[20] Sangeeta N. Bhatia, Gregory H. Underhill, Kenneth S. Zaret, and Ira J. Fox. Cell and Tissue Engineering for Liver Disease. *Science translational medicine*, 6(245):245sr2, July 2014.

[21] Eva Bianconi, Allison Piovesan, Federica Facchin, Alina Beraudi, Raffaella Casadei, Flavia Frabetti, Lorenza Vitale, Maria Chiara Pelleri, Simone Tassani, Francesco Piva,

et al. An estimation of the number of cells in the human body. *Annals of human biology*, 40(6):463–471, 2013.

[22] Bahri M. Bilir, Denis Guinette, Fritz Karrer, David A. Kumpe, Joe Krysl, Janet Stephens, Loris McGavran, Alina Ostrowska, and Janette Durham. Hepatocyte transplantation in acute liver failure. *Liver Transplantation*, 6:32–40, Feb 2000.

[23] Moses T Bility, Liguo Zhang, Michael L Washburn, T Anthony Curtis, Grigoriy I Kovalev, and Lishan Su. Generation of a humanized mouse model with both human immune system and liver cells to model hepatitis c virus infection and liver immunopathogenesis. *Nature protocols*, 7(9):1608–1617, 2012.

[24] Mina J. Bissell and Derek Radisky. Putting tumours in context. *Nature Reviews Cancer*, 1(1):46–54, October 2001.

[25] Cara K Black, Kareem M Termanini, Oswaldo Aguirre, Jason S Hawksworth, and Michael Sosin. Solid organ transplantation in the 21st century. *Annals of translational medicine*, 6(20), 2018.

[26] Challice L Bonifant, Hollie J Jackson, Renier J Brentjens, and Kevin J Curran. Toxicity and management in car t-cell therapy. *Molecular Therapy-Oncolytics*, 3:16011, 2016.

[27] Caroline Bonnans, Jonathan Chou, and Zena Werb. Remodelling the extracellular matrix in development and disease. *Nature Reviews. Molecular Cell Biology*, 15(12):786–801, December 2014.

[28] Jeffrey T Borenstein, H Terai, Kevin R King, EJ Weinberg, MR Kaazempur-Mofrad, and JP Vacanti. Microfabrication technology for vascularized tissue engineering. *Biomedical microdevices*, 4(3):167–175, 2002.

[29] Jean Botha, June Fabian, Harriet Etheredge, Francesca Conradie, and Caroline T Tiemessen. Hiv and solid organ transplantation: where are we now. *Current HIV/AIDS Reports*, 16(5):404–413, 2019.

[30] L Boulter, O Govaere, T G Bird, S Radulescu, P Ramachandran, A Pellicoro, R A Ridgway, S S Seo, B Spee, N van Rooijen, O J Sansom, J P Iredale, S Lowell, T Roskams, and S J Forbes. Macrophage-derived wnt opposes notch signaling to specify hepatic progenitor cell fate in chronic liver disease. *Nature Medicine*, 18(4):572–579, 2012.

[31] Helge Bruns, Ulrich Kneser, Stephanie Holzhüter, Beate Roth, Jantjeline Kluth, Peter M Kaufmann, Dietrich Kluth, and Henning C Fiegel. Injectable liver: a novel approach using fibrin gel as a matrix for culture and intrahepatic transplantation of hepatocytes. *Tissue engineering*, 11(11-12):1718–1726, 2005.

[32] N.L.R. Bucher, J.F. Scott, and J.C. Aub. Regeneration of the Liver in Parabiotic Rats. *Cancer Research*, 11(6):457–465, 1951.

[33] Ronald W Busuttil and John A Goss. Split liver transplantation. *Annals of surgery*, 229(3):313, 1999.

[34] Jun Cai, Yang Zhao, Yanxia Liu, Fei Ye, Zhihua Song, Han Qin, Sha Meng, Yuezhou Chen, Rudan Zhou, Xijun Song, et al. Directed differentiation of human embryonic stem cells into functional hepatic cells. *Hepatology*, 45(5):1229–1239, 2007.

[35] Eric S Carlisle, Muthumarthanda R Mariappan, Kevin D Nelson, Brett E Thomes, Richard B Timmons, Anca Constantinescu, Robert C Eberhart, and Paul E Bankey. Enhancing hepatocyte adhesion by pulsed plasma deposition and polyethylene glycol coupling. *Tissue engineering*, 6(1):45–52, 2000.

[36] Benoît Carpentier, Aude Gautier, and C Legallais. Artificial and bioartificial liver devices: present and future. *Gut*, 58(12):1690–1702, 2009.

[37] G Catapano, MC Di Lorenzo, C Della Volpe, L De Bartolo, and C Migliaresi. Polymeric membranes for hybrid liver support devices: the effect of membrane surface wettability on hepatocyte viability and functions. *Journal of Biomaterials Science, Polymer Edition*, 7(11):1017–1027, 1996.

[38] Alec E. Cerchiari, James C. Garbe, Noel Y. Jee, Michael E. Todhunter, Kyle E. Broaders, Donna M. Peehl, Tejal A. Desai, Mark A. LaBarge, Matthew Thomson, and Zev J. Gartner. A strategy for tissue self-organization that is robust to cellular heterogeneity and plasticity. *Proceedings of the National Academy of Sciences of the United States of America*, 112(7):2287–2292, February 2015.

[39] Ritika R. Chaturvedi, Kelly R. Stevens, Ricardo D. Solorzano, Robert E. Schwartz, Jeroen Eyckmans, Jan D. Baranski, Sarah Chase Stapleton, Sangeeta N. Bhatia, and Christopher S. Chen. Patterning Vascular Networks In Vivo for Tissue Engineering Applications. *Tissue Engineering. Part C, Methods*, 21(5):509–517, May 2015.

[40] A. A. Chen, D. K. Thomas, L. L. Ong, R. E. Schwartz, T. R. Golub, and S. N. Bhatia. Humanized mice with ectopic artificial liver tissues. *Proceedings of the National Academy of Sciences*, 108(29):11842–11847, July 2011.

[41] Amanda X Chen, Arnav Chhabra, Hyun-Ho Greco Song, Heather E Fleming, Christopher S Chen, and Sangeeta N Bhatia. Controlled apoptosis of stromal cells to engineer human microlivers. *Advanced Functional Materials*, page 1910442, 2020.

[42] Zhuo Cheng, Zhiying He, Yongchao Cai, Cheng Zhang, Gongbo Fu, Hengyu Li, Wen Sun, Changcheng Liu, Xiuliang Cui, Beifang Ning, et al. Conversion of hepatoma cells to hepatocyte-like cells by defined hepatocyte nuclear factors. *Cell research*, 29(2):124–135, 2019.

[43] Onpan Cheung and Arun J Sanyal. Abnormalities of lipid metabolism in nonalcoholic fatty liver disease. In *Seminars in liver disease*, volume 28, pages 351–359. © Thieme Medical Publishers, 2008.

[44] Yu-Chieh Chiu, Ming-Huei Cheng, Holger Engel, Shu-Wei Kaeo, Jeffery C Larson, Shreya Gupta, and Eric M Brey. The role of pore size on vascularization and tissue remodeling in peg hydrogels. *Biomaterials*, 32(26):6045–6051, 2011.

[45] Leila Choucha Snouber, Andrei Bunescu, Marie Naudot, Cécile Legallais, Céline Brochot, Marc Emmanuel Dumas, Bénédicte Elena-Herrmann, and Eric Leclerc. Metabolomics-on-a-chip of hepatotoxicity induced by anticancer drug flutamide and

its active metabolite hydroxyflutamide using hepg2/c3a microfluidic biochips. *Toxicological Sciences*, 132(1):8–20, 2013.

[46] Kian-Ngiap Chua, Wei-Seng Lim, Pengchi Zhang, Hongfang Lu, Jie Wen, Seeram Ramakrishna, Kam W Leong, and Hai-Quan Mao. Stable immobilization of rat hepatocyte spheroids on galactosylated nanofiber scaffold. *Biomaterials*, 26(15):2537–2547, 2005.

[47] Napoleon E Cieza, Marian Porubsky, and Tun Jie. Advances in immunosuppressive therapy. In *Technological Advances in Surgery, Trauma and Critical Care*, pages 545–559. Springer, 2015.

[48] Linda G Cima, Donald E Ingber, Joseph P Vacanti, and Robert Langer. Hepatocyte culture on biodegradable polymeric substrates. *Biotechnology and bioengineering*, 38(2):145–158, 1991.

[49] Raquel Costa-Almeida, Raquel Soares, and Pedro L. Granja. Fibroblasts as maestros orchestrating tissue regeneration. *Journal of Tissue Engineering and Regenerative Medicine*, 12(1):240–251, 2018.

[50] Rossella Crescitelli, Cecilia Lässer, Tamas G. Szabó, Agnes Kittel, Maria Eldh, Irma Dianzani, Edit I. Buzás, and Jan Lötvall. Distinct RNA profiles in subpopulations of extracellular vesicles: apoptotic bodies, microvesicles and exosomes. *Journal of Extracellular Vesicles*, 2, September 2013.

[51] Linda Custer and Claudy J-P Mullon. Oxygen delivery to and use by primary porcine hepatocytes in the hepatassist™ 2000 system for extracorporeal treatment of patients in end-stage liver failure. In *Oxygen Transport to Tissue XX*, pages 261–271. Springer, 1998.

[52] Matthew D Davidson, David A Kukla, and Salman R Khetani. Microengineered cultures containing human hepatic stellate cells and hepatocytes for drug development. *Integrative Biology*, 9(8):662–677, 2017.

[53] George E Davis and Charles W Camarillo. An $\alpha 2\beta 1$ integrin-dependent pinocytic mechanism involving intracellular vacuole formation and coalescence regulates capillary lumen and tube formation in three-dimensional collagen matrix. *Experimental cell research*, 224(1):39–51, 1996.

[54] George E Davis, Katherine R Speichinger, Pieter R Norden, Dae Joong Kim, and Stephanie LK Bowers. Endothelial cell polarization during lumen formation, tubulogenesis, and vessel maturation in 3d extracellular matrices. In *Cell Polarity 1*, pages 205–220. Springer, 2015.

[55] Achilles A Demetriou, James F Whiting, David Feldman, Stanley M Levenson, N Roy Chowdhury, Albert D Moscioni, Michael Kram, et al. Replacement of liver function in rats by transplantation of microcarrier-attached hepatocytes. *Science*, 233(4769):1190–1192, 1986.

[56] Tobias Deuse, Xiaomeng Hu, Alessia Gravina, Dong Wang, Grigol Tediashvili, Chandrav De, William O Thayer, Angela Wahl, J Victor Garcia, Hermann Reichenspurner,

et al. Hypoimmunogenic derivatives of induced pluripotent stem cells evade immune rejection in fully immunocompetent allogeneic recipients. *Nature biotechnology*, 37(3):252–258, 2019.

[57] Aaron D DeWard, Junji Komori, and Eric Lagasse. Ectopic transplantation sites for cell-based therapy. *Current opinion in organ transplantation*, 19(2):169, 2014.

[58] Anil Dhawan, Ragai R Mitry, Robin D Hughes, Sharon Lehec, Claire Terry, Sanjay Bansal, Rupen Arya, Jim J Wade, Anita Verma, Nigel D Heaton, et al. Hepatocyte transplantation for inherited factor vii deficiency. *Transplantation*, 78(12):1812–1814, 2004.

[59] Anil Dhawan, Juliana Puppi, Robin D Hughes, and Ragai R Mitry. Human hepatocyte transplantation: current experience and future challenges. *Nature reviews Gastroenterology & hepatology*, 7(5):288, 2010.

[60] Antonio Di Stasi, Siok-Keen Tey, Gianpietro Dotti, Yuriko Fujita, Alana Kennedy-Nasser, Caridad Martinez, Karin Straathof, Enli Liu, April G. Durett, Bambi Grilley, Hao Liu, Conrad R. Cruz, Barbara Savoldo, Adrian P. Gee, John Schindler, Robert A. Krance, Helen E. Heslop, David M. Spencer, Cliona M. Rooney, and Malcolm K. Brenner. Inducible Apoptosis as a Safety Switch for Adoptive Cell Therapy. *http://dx.doi.org/10.1056/NEJMoa1106152*, November 2011.

[61] Bi-Sen Ding, Daniel J Nolan, Jason M BUtler, Daylon James, Alexander O Babazadeh, Zev Rosenwaks, Vivek Mittal, Hiedki Kobayashi, Koji Shido, David Lyden, Thomas N Sato, Sina Y Rabbany, and Shahin Rafii. Inductive angiocrine signals from sinusoidal endothelium are required for liver regeneration. *Nature*, 468:310–315, 2010.

[62] Dennis E. Discher, David J. Mooney, and Peter W. Zandstra. Growth factors, matrices, and forces combine and control stem cells. *Science (New York, N.Y.)*, 324(5935):1673–1677, June 2009.

[63] G. Donati, B. Stagni, F. Piscaglia, N. Venturoli, A. M. Morselli-Labate, L. Rasciti, and L. Bolondi. Increased prevalence of fatty liver in arterial hypertensive patients with normal liver enzymes: role of insulin resistance. *Gut*, 53(7):1020–1023, July 2004.

[64] Yu Du, Gauri Khandekar, Jessica Llewellyn, William Polacheck, Christopher S Chen, and Rebecca G Wells. A bile duct-on-a-chip with organ-level functions. *Hepatology*, 71(4):1350–1363, 2020.

[65] Yuanyuan Du, Jinlin Wang, Jun Jia, Nan Song, Chengang Xiang, Jun Xu, Zhiyuan Hou, Xiaohua Su, Bei Liu, Tao Jiang, et al. Human hepatocytes with drug metabolic function induced from fibroblasts by lineage reprogramming. *Cell stem cell*, 14(3):394–403, 2014.

[66] Clémence Dubois, Robin Dufour, Pierre Daumar, Corinne Aubel, Claire Szczepaniak, Christelle Blavignac, Emmanuelle Mounetou, Frédérique Penault-Llorca, and Mahchid Bamdad. Development and cytotoxic response of two proliferative mda-mb-231 and non-proliferative sum1315 three-dimensional cell culture models of triple-negative basal-like breast cancer cell lines. *Oncotarget*, 8(56):95316, 2017.

[67] James C. Y. Dunn, Ronald G. Tompkins, and Martin L. Yarmush. Long-Term in Vitro Function of Adult Hepatocytes in a Collagen Sandwich Configuration. *Biotechnology Progress*, 7(3):237–245, 1991.

[68] Collin D Edington, Wen Li Kelly Chen, Emily Geishecker, Timothy Kassis, Luis R Soenksen, Brij M Bhushan, Duncan Freake, Jared Kirschner, Christian Maass, Nikolaos Tsamandouras, et al. Interconnected microphysiological systems for quantitative biology and pharmacology studies. *Scientific reports*, 8(1):1–18, 2018.

[69] Antony J Ellis, Robin D Hughes, Julia A Wendon, Joseph Dunne, Peter G Langley, James H Kelly, Gardar T Gislason, Norman L Sussman, and Roger Williams. Pilot-controlled trial of the extracorporeal liver assist device in acute liver failure. *Hepatology*, 24(6):1446–1451, 1996.

[70] Chris Estes, Homie Razavi, Rohit Loomba, Zobair Younossi, and Arun J Sanyal. Modeling the epidemic of nonalcoholic fatty liver disease demonstrates an exponential increase in burden of disease. *Hepatology*, 67(1):123–133, 2018.

[71] Jinyong Fan, Yi Shang, Yingjin Yuan, and Jun Yang. Preparation and characterization of chitosan/galactosylated hyaluronic acid scaffolds for primary hepatocytes culture. *Journal of Materials Science: Materials in Medicine*, 21(1):319–327, 2010.

[72] Sheung-Tat Fan, Chung-Mau Lo, Chi-Leung Liu, Boon-Hun Yong, John Ka-Fat Chan, and Irene Oi-Lin Ng. Safety of donors in live donor liver transplantation using right lobe grafts. *Archives of surgery*, 135(3):336–340, 2000.

[73] Geoffrey C Farrell, Derrick Van Rooyen, Lay Gan, and Shivrakumar Chitturi. Nash is an inflammatory disorder: pathogenic, prognostic and therapeutic implications. *Gut and liver*, 6(2):149, 2012.

[74] S Feng, NP Goodrich, JL Bragg-Gresham, DM Dykstra, JD Punch, MA DebRoy, Stuart M Greenstein, and RM Merion. Characteristics associated with liver graft failure: the concept of a donor risk index. *American Journal of Transplantation*, 6(4):783–790, 2006.

[75] Henning C Fiegel, Joerg Havers, Ulrich Kneser, Molly K Smith, Tim Moeller, Dietrich Kluth, David J Mooney, Xavier Rogiers, and Peter M Kaufmann. Influence of flow conditions and matrix coatings on growth and differentiation of three-dimensionally cultured rat hepatocytes. *Tissue engineering*, 10(1-2):165–174, 2004.

[76] Claudia Fischbach, Hyun Joon Kong, Susan X. Hsiong, Marta B. Evangelista, Will Yuen, and David J. Mooney. Cancer cell angiogenic capability is regulated by 3D culture and integrin engagement. *Proceedings of the National Academy of Sciences*, 106(2):399–404, January 2009. Publisher: National Academy of Sciences Section: Biological Sciences.

[77] Robert A Fisher and Stephen C Strom. Human hepatocyte transplantation: worldwide results. *Transplantation*, 82(4):441–449, 2006.

[78] Stuart J Forbes and Philip N Newsome. Liver regeneration—mechanisms and models to clinical application. *Nature reviews Gastroenterology & hepatology*, 13(8):473, 2016.

[79] Peter A Galie, Duc-Huy T Nguyen, Colin K Choi, Daniel M Cohen, Paul A Janmey, and Christopher S Chen. Fluid shear stress threshold regulates angiogenic sprouting. *Proceedings of the National Academy of Sciences*, 111(22):7968–7973, 2014.

[80] Yuan Gao, Zhijun Cao, Xi Yang, Mohamed A. Abdelmegeed, Jinchun Sun, Si Chen, Richard D. Beger, Kelly Davis, William F. Salminen, Byoung-Joon Song, Donna L. Mendrick, and Li-Rong Yu. Proteomic analysis of acetaminophen-induced hepatotoxicity and identification of heme oxygenase 1 as a potential plasma biomarker of liver injury. *Proteomics. Clinical Applications*, 11(1-2), 2017.

[81] Tessa Gargett and Michael P. Brown. The inducible caspase-9 suicide gene system as a "safety switch" to limit on-target, off-tumor toxicities of chimeric antigen receptor T cells. *Frontiers in Pharmacology*, 5, October 2014.

[82] Rolf Gebhardt. Metabolic zonation of the liver: regulation and implications for liver function. *Pharmacology & therapeutics*, 53(3):275–354, 1992.

[83] R. Glicklis, L. Shapiro, R. Agbaria, J. C. Merchuk, and S. Cohen. Hepatocyte behavior within three-dimensional porous alginate scaffolds. *Biotechnology and Bioengineering*, 67(3):344–353, February 2000.

[84] Patricio Godoy, Nicola J. Hewitt, Ute Albrecht, Melvin E. Andersen, Nariman Ansari, Sudin Bhattacharya, Johannes Georg Bode, Jennifer Bolleyn, Christoph Borner, Jan Böttger, Albert Braeuning, Robert A. Budinsky, Britta Burkhardt, Neil R. Cameron, Giovanni Camussi, Chong-Su Cho, Yun-Jaie Choi, J. Craig Rowlands, Uta Dahmen, Georg Damm, Olaf Dirsch, María Teresa Donato, Jian Dong, Steven Dooley, Dirk Drasdo, Rowena Eakins, Karine Sá Ferreira, Valentina Fonsato, Joanna Fraczek, Rolf Gebhardt, Andrew Gibson, Matthias Glanemann, Chris E. P. Goldring, María José Gómez-Lechón, Geny M. M. Groothuis, Lena Gustavsson, Christelle Guyot, David Hallifax, Seddik Hammad, Adam Hayward, Dieter Häussinger, Claus Hellerbrand, Philip Hewitt, Stefan Hoehme, Hermann-Georg Holzhütter, J. Brian Houston, Jens Hrach, Kiyomi Ito, Hartmut Jaeschke, Verena Keitel, Jens M. Kelm, B. Kevin Park, Claus Kordes, Gerd A. Kullak-Ublick, Edward L. LeCluyse, Peng Lu, Jennifer Luebke-Wheeler, Anna Lutz, Daniel J. Maltman, Madlen Matz-Soja, Patrick McMullen, Irmgard Merfort, Simon Messner, Christoph Meyer, Jessica Mwinyi, Dean J. Naisbitt, Andreas K. Nussler, Peter Olinga, Francesco Pampaloni, Jingbo Pi, Linda Pluta, Stefan A. Przyborski, Anup Ramachandran, Vera Rogiers, Cliff Rowe, Celine Schelcher, Kathrin Schmich, Michael Schwarz, Bijay Singh, Ernst H. K. Stelzer, Bruno Stieger, Regina Stöber, Yuichi Sugiyama, Ciro Tetta, Wolfgang E. Thasler, Tamara Vanhaecke, Mathieu Vinken, Thomas S. Weiss, Agata Widera, Courtney G. Woods, Jinghai James Xu, Kathy M. Yarborough, and Jan G. Hengstler. Recent advances in 2D and 3D in vitro systems using primary hepatocytes, alternative hepatocyte sources and non-parenchymal liver cells and their use in investigating mechanisms of hepatotoxicity, cell signaling and ADME. *Archives of Toxicology*, 87(8):1315–1530, August 2013.

[85] Germán G Gornalusse, Roli K Hirata, Sarah E Funk, Laura Riolobos, Vanda S Lopes, Gabriel Manske, Donna Prunkard, Aric G Colunga, Laïla-Aïcha Hanafi, Dennis O Clegg, et al. Hla-e-expressing pluripotent stem cells escape allogeneic responses and lysis by nk cells. *Nature biotechnology*, 35(8):765, 2017.

[86] Francine Goulet, Claire Normand, and Odette Morin. Cellular interactions promote tissue-specific function, biomatrix deposition and junctional communication of primary cultured hepatocytes. *Hepatology*, 8(5):1010–1018, 1988.

[87] Valerie Gouon-Evans, Lise Boussemart, Paul Gadue, Dirk Nierhoff, Christoph I Koehler, Atsushi Kubo, David A Shafritz, and Gordon Keller. Bmp-4 is required for hepatic specification of mouse embryonic stem cell–derived definitive endoderm. *Nature biotechnology*, 24(11):1402–1411, 2006.

[88] Laura Gramantieri, Pasquale Chieco, Catia Giovannini, Michela Lacchini, Davide Treré, Gian Luca Grazi, Annamaria Venturi, and Luigi Bolondi. GADD45-alpha expression in cirrhosis and hepatocellular carcinoma: relationship with DNA repair and proliferation. *Human Pathology*, 36(11):1154–1162, November 2005.

[89] Linda G. Griffith and Melody A. Swartz. Capturing complex 3D tissue physiology in vitro. *Nature Reviews Molecular Cell Biology*, 7(3):211–224, March 2006.

[90] Linda G Griffith, BEN Wu, Michael J Cima, MARK J Powers, BEVERLY Chaignaud, and Joseph P Vacanti. In vitro organogenesis of liver tissue. *Annals of the New York Academy of Sciences*, 831:382–397, 1997.

[91] Marko Gröger, Knut Rennert, Benjamin Giszas, Elisabeth Weiß, Julia Dinger, Harald Funke, Michael Kiehntopf, Frank T Peters, Amelie Lupp, Michael Bauer, et al. Monocyte-induced recovery of inflammation-associated hepatocellular dysfunction in a biochip-based human liver model. *Scientific reports*, 6(1):1–16, 2016.

[92] Markus Grompe and Stephen Strom. Mice with human livers. *Gastroenterology*, 145(6):1209–1214, 2013.

[93] Mariann Grossman, Daniel J Rader, David WM Muller, Daniel M Kolansky, Karen Kozarsky, Bernard J Clark, Evan A Stein, Paul J Lupien, H Bryan Brewer, Steven E Raper, et al. A pilot study of ex vivo gene therapy for homozygous familial hypercholesterolaemia. *Nature medicine*, 1(11):1148–1154, 1995.

[94] Christiane Guguen-Guillouzo, Bruno Clément, Georges Baffet, Carole Beaumont, Edith Morel-Chany, Denise Glaise, and André Guillouzo. Maintenance and reversibility of active albumin secretion by adult rat hepatocytes co-cultured with another liver epithelial cell type. *Experimental cell research*, 143(1):47–54, 1983.

[95] Christiane Guguen-Guillouzo and André Guillouzo. Modulation of functional activities in cultured rat hepatocytes. In V. A. Najjar, editor, *Enzyme Induction and Modulation*, Developments in molecular and cellular biochemistry, pages 35–56. Springer US, Boston, MA, 1983.

[96] Edgardo E Guibert, Alexander Y Petrenko, Cecilia L Balaban, Alexander Y Somov, Joaquín V Rodriguez, and Barry J Fuller. Organ preservation: current concepts and new strategies for the next decade. *Transfusion Medicine and Hemotherapy*, 38(2):125–142, 2011.

[97] André Guillouzo, Anne Corlu, Caroline Aninat, Denise Glaise, Fabrice Morel, and Christiane Guguen-Guillouzo. The human hepatoma heparg cells: a highly differentiated model for studies of liver metabolism and toxicity of xenobiotics. *Chemico-biological interactions*, 168(1):66–73, 2007.

[98] Sanjeev Gupta, Giridhar R Gorla, and Adil N Irani. Hepatocyte transplantation: emerging insights into mechanisms of liver repopulation and their relevance to potential therapies. *Journal of hepatology*, 30(1):162–170, 1999.

[99] Annie Tang Gutsche, Hungnan Lo, Joanne Zurlo, James Yager, and Kam W Leong. Engineering of a sugar-derivatized porous network for hepatocyte culture. *Biomaterials*, 17(3):387–393, 1996.

[100] Mariah S Hahn, Lakeshia J Taite, James J Moon, Maude C Rowland, Katie A Ruffino, and Jennifer L West. Photolithographic patterning of polyethylene glycol hydrogels. *Biomaterials*, 27(12):2519–2524, 2006.

[101] G. A. Hamilton, S. L. Jolley, D. Gilbert, D. J. Coon, S. Barros, and E. L. LeCluyse. Regulation of cell morphology and cytochrome P450 expression in human hepatocytes by extracellular matrix and cell-cell interactions. *Cell and Tissue Research*, 306(1):85–99, October 2001.

[102] Xiao Han, Mengning Wang, Songwei Duan, Paul J Franco, Jennifer Hyoje-Ryu Kenty, Preston Hedrick, Yulei Xia, Alana Allen, Leonardo MR Ferreira, Jack L Strominger, et al. Generation of hypoimmunogenic human pluripotent stem cells. *Proceedings of the National Academy of Sciences*, 116(21):10441–10446, 2019.

[103] Masami Hasegawa, Kenji Kawai, Tetsuya Mitsui, Kenji Taniguchi, Makoto Monnai, Masatoshi Wakui, Mamoru Ito, Makoto Suematsu, Gary Peltz, Masato Nakamura, et al. The reconstituted 'humanized liver'in tk-nog mice is mature and functional. *Biochemical and biophysical research communications*, 405(3):405–410, 2011.

[104] V Hasirci, Francois Berthiaume, SP Bondre, JD Gresser, DJ Trantolo, M Toner, and DL Wise. Expression of liver-specific functions by rat hepatocytes seeded in treated poly (lactic-co-glycolic) acid biodegradable foams. *Tissue engineering*, 7(4):385–394, 2001.

[105] Betul Hatipoglu. Islet cell transplantation and alternative therapies. *Endocrinology and metabolism clinics of North America*, 45(4):923–931, 2016.

[106] B He and A Mitchell. Laparoscopic donor nephrectomy for ectopic kidney. In *Transplantation proceedings*, volume 44, pages 3051–3054. Elsevier, 2012.

[107] Toshitaka Hoppo, Junji Komori, Rohan Manohar, Donna Beer Stolz, and Eric Lagasse. Rescue of lethal hepatic failure by hepatized lymph nodes in mice. *Gastroenterology*, 140(2):656–666, 2011.

[108] Simon P Horslen, Timothy C McCowan, Timothy C Goertzen, Phyllis I Warkentin, Hung Bo Cai, Stephen C Strom, and Ira J Fox. Isolated hepatocyte transplantation in an infant with a severe urea cycle disorder. *Pediatrics*, 111(6):1262–1267, 2003.

[109] ML Houchin and EM Topp. Chemical degradation of peptides and proteins in plga: a review of reactions and mechanisms. *Journal of pharmaceutical sciences*, 97(7):2395–2404, 2008.

[110] Huili Hu, Helmuth Gehart, Benedetta Artegiani, Carmen LÖpez-Iglesias, Florijn Dekkers, Onur Basak, Johan van Es, Susana M. Chuva de Sousa Lopes, Harry Begthel,

Jeroen Korving, Maaike van den Born, Chenhui Zou, Corrine Quirk, Luis Chiriboga, Charles M. Rice, Stephanie Ma, Anne Rios, Peter J. Peters, Ype P. de Jong, and Hans Clevers. Long-Term Expansion of Functional Mouse and Human Hepatocytes as 3D Organoids. *Cell*, 175(6):1591–1606.e19, November 2018.

[111] Pengyu Huang, Ludi Zhang, Yimeng Gao, Zhiying He, Dan Yao, Zhitao Wu, Jin Cen, Xiaotao Chen, Changcheng Liu, Yiping Hu, et al. Direct reprogramming of human fibroblasts to functional and expandable hepatocytes. *Cell stem cell*, 14(3):370–384, 2014.

[112] Meritxell Huch, Craig Dorrell, Sylvia F Boj, Johan H van Es, Vivian S W Li, Marc van de Wetering, Toshiro Sato, Karien Hamer, Nobuo Saski, Milton J Finegold, Annelise Haft, Robert G Vries, Markus Grompe, and Hans Clevers. In vitro expansion of single lgr5+ liver stem cells induced by wnt-driven regeneration. *Nature*, 494:247–250, 2013.

[113] Meritxell Huch, Helmuth Gehart, Ruben Van Boxtel, Karien Hamer, Francis Blokzijl, Monique MA Verstegen, Ewa Ellis, Martien Van Wenum, Sabine A Fuchs, Joep de Ligt, et al. Long-term culture of genome-stable bipotent stem cells from adult human liver. *Cell*, 160(1-2):299–312, 2015.

[114] Dongeun Huh, Geraldine A Hamilton, and Donald E Ingber. From 3d cell culture to organs-on-chips. *Trends in cell biology*, 21(12):745–754, 2011.

[115] Dongeun Huh, Yu-suke Torisawa, Geraldine A Hamilton, Hyun Jung Kim, and Donald E Ingber. Microengineered physiological biomimicry: organs-on-chips. *Lab on a Chip*, 12(12):2156–2164, 2012.

[116] E. E. Hui and S. N. Bhatia. Micromechanical control of cell-cell interactions. *Proceedings of the National Academy of Sciences*, 104(14):5722–5726, April 2007.

[117] Elliot E. Hui and Sangeeta N. Bhatia. Silicon Microchips for Manipulating Cell-cell Interaction. *JoVE (Journal of Visualized Experiments)*, 7(7):e268, August 2007.

[118] Yuichi Ishida, Sharon Smith, Lorraine Wallace, Takaharu Sadamoto, Masashi Okamoto, Marcus Auth, Mario Strazzabosco, Luca Fabris, Juan Medina, Jesús Prieto, et al. Ductular morphogenesis and functional polarization of normal human biliary epithelial cells in three-dimensional culture. *Journal of hepatology*, 35(1):2–9, 2001.

[119] Fumihiko Ishikawa, Masaki Yasukawa, Bonnie Lyons, SHuro Yoshida, Toshihiro Miyamoto, Takeshi Watanabe, Koichi Akashi, Leonard D Shultz, and Mine Harada. Development of functional human blood and immune systems in nod/scid/il2 receptor γ chain(null) mice. *Blood*, 106(5):1565–1573, 2005.

[120] Laura J Itle, Won-Gun Koh, and Michael V Pishko. Hepatocyte viability and protein expression within hydrogel microstructures. *Biotechnology progress*, 21(3):926–932, 2005.

[121] Kumar Jayant, Isabella Reccia, Francesco Virdis, and AM James Shapiro. The role of normothermic perfusion in liver transplantation (transit study): a systematic review of preliminary studies. *HPB Surgery*, 2018, 2018.

[122] Satoshi Kaihara, Jeffrey Borenstein, Rahul Koka, Sonal Lalan, Erin R Ochoa, Michael Ravens, Homer Pien, Brian Cunningham, and Joseph P Vacanti. Silicon micromachining to tissue engineer branched vascular channels for liver fabrication. *Tissue engineering*, 6(2):105–117, 2000.

[123] Makoto Kamei, W Brian Saunders, Kayla J Bayless, Louis Dye, George E Davis, and Brant M Weinstein. Endothelial tubes assemble from intracellular vacuoles in vivo. *Nature*, 442(7101):453–456, 2006.

[124] Levent B. Karademir, Hiroshi Aoyama, Benny Yue, Honghong Chen, and Donglin Bai. Engineered Cx26 variants established functional heterotypic Cx26/Cx43 and Cx26/Cx40 gap junction channels. *The Biochemical Journal*, 473(10):1391–1403, 2016.

[125] Erdal Karamuk, Jörg Mayer, Erich Wintermantel, and Toshihiro Akaike. Partially degradable film/fabric composites: Textile scaffolds for liver cell culture. *Artificial organs*, 23(9):881–884, 1999.

[126] S Kasai, M Sawa, K ONODERA, S HIRAI, et al. Cellulose microcarrier for high-density culture of hepatocytes. In *Transplantation proceedings*, volume 24, pages 2933–2934, 1992.

[127] Alon Kedem, Anat Perets, Iris Gamlieli-Bonshtein, Mona Dvir-Ginzberg, Solly Mizrahi, and Smadar Cohen. Vascular endothelial growth factor-releasing scaffolds enhance vascularization and engraftment of hepatocytes transplanted on liver lobes. *Tissue engineering*, 11(5-6):715–722, 2005.

[128] Salman R Khetani, Dustin R Berger, Kimberly R Ballinger, Matthew D Davidson, Christine Lin, and Brenton R Ware. Microengineered liver tissues for drug testing. *Journal of laboratory automation*, 20(3):216–250, 2015.

[129] Salman R Khetani and Sangeeta N Bhatia. Microscale culture of human liver cells for drug development. *Nature Biotechnology*, 26(1):120–126, January 2008.

[130] Salman R. Khetani, Alice A. Chen, Barbara Ranscht, and Sangeeta N. Bhatia. T-cadherin modulates hepatocyte functions in vitro. *The FASEB Journal*, 22(11):3768–3775, November 2008.

[131] Salman R. Khetani, Greg Szulgit, Jo A. Del Rio, Carrolee Barlow, and Sangeeta N. Bhatia. Exploring interactions between rat hepatocytes and nonparenchymal cells using gene expression profiling. *Hepatology*, 40(3):545–554, September 2004.

[132] Dongjoo Kim, Yoonjae Seo, and Soonjo Kwon. Role of gap junction communication in hepatocyte/fibroblast co-cultures: Implications for hepatic tissue engineering. *Biotechnology and Bioprocess Engineering*, 20(2):358–365, April 2015.

[133] Hyun Jung Kim, Dongeun Huh, Geraldine Hamilton, and Donald E Ingber. Human gut-on-a-chip inhabited by microbial flora that experiences intestinal peristalsis-like motions and flow. *Lab on a Chip*, 12(12):2165–2174, 2012.

[134] Mihye Kim, Ji Youn Lee, Caroline N Jones, Alexander Revzin, and Giyoong Tae. Heparin-based hydrogel as a matrix for encapsulation and cultivation of primary hepatocytes. *Biomaterials*, 31(13):3596–3603, 2010.

[135] Pilnam Kim, Keon Woo Kwon, Min Cheol Park, Sung Hoon Lee, Sun Min Kim, and Kahp Yang Suh. Soft lithography for microfluidics: a review. *Biochip Journal*, 2008.

[136] Stephen S Kim, Hirofumi Utsunomiya, John A Koski, Benjamin M Wu, Michael J Cima, Jane Sohn, Kanae Mukai, Linda G Griffith, and Joseph P Vacanti. Survival and function of hepatocytes on a novel three-dimensional synthetic biodegradable polymer scaffold with an intrinsic network of channels. *Annals of surgery*, 228(1):8, 1998.

[137] N Kobayashi, T Okitsu, M Maruyama, T Totsugawa, and Y Kosaka. Development of a cellulose-based microcarrier containing cellular adhesive peptides for a bioartificial liver. In *Transplantation proceedings*, volume 35, pages 443–444, 2003.

[138] Wonshill Koh, Rachel D Mahan, and George E Davis. Cdc42-and rac1-mediated endothelial lumen formation requires pak2, pak4 and par3, and pkc-dependent signaling. *Journal of cell science*, 121(7):989–1001, 2008.

[139] David B Kolesky, Kimberly A Homan, Mark A Skylar-Scott, and Jennifer A Lewis. Three-dimensional bioprinting of thick vascularized tissues. *Proceedings of the national academy of sciences*, 113(12):3179–3184, 2016.

[140] David B Kolesky, Ryan L Truby, A Sydney Gladman, Travis A Busbee, Kimberly A Homan, and Jennifer A Lewis. 3d bioprinting of vascularized, heterogeneous cell-laden tissue constructs. *Advanced materials*, 26(19):3124–3130, 2014.

[141] Junji Komori, Lindsey Boone, Aaron DeWard, Toshitaka Hoppo, and Eric Lagasse. The mouse lymph node as an ectopic transplantation site for multiple tissues. *Nature Biotechnology*, 30(10):976–983, October 2012. Number: 10 Publisher: Nature Publishing Group.

[142] Krzysztof Krawczyk, Shuai Xue, Peter Buchmann, Ghislaine Charpin-El-Hamri, Pratik Saxena, Marie-Didiée Hussherr, Jiawei Shao, Haifeng Ye, Mingqi Xie, and Martin Fussenegger. Electrogenetic cellular insulin release for real-time glycemic control in type 1 diabetic mice. *Science*, 368(6494):993–1001, 2020.

[143] Cecile M. Krejsa, Christopher C. Franklin, Collin C. White, Jeffrey A. Ledbetter, Gary L. Schieven, and Terrance J. Kavanagh. Rapid activation of glutamate cysteine ligase following oxidative stress. *The Journal of Biological Chemistry*, 285(21):16116–16124, May 2010.

[144] Gabriel A Kwong, Geoffrey Von Maltzahn, Gayathree Murugappan, Omar Abudayyeh, Steven Mo, Ioannis A Papayannopoulos, Deanna Y Sverdlov, Susan B Liu, Andrew D Warren, Yury Popov, et al. Mass-encoded synthetic biomarkers for multiplexed urinary monitoring of disease. *Nature biotechnology*, 31(1):63–70, 2013.

[145] Matthias Längin, Tanja Mayr, Bruno Reichart, Sebastian Michel, Stefan Buchholz, Sonja Guethoff, Alexey Dashkevich, Andrea Baehr, Stefanie Egerer, Andreas Bauer, et al. Consistent success in life-supporting porcine cardiac xenotransplantation. *Nature*, 564(7736):430–433, 2018.

[146] Robert Lanza, Robert Langer, Joseph P Vacanti, and Anthony Atala. *Principles of tissue engineering*. Academic press, 2020.

[147] Dr Laybutt, AM Preston, MC Akerfeldt, JG Kench, AK Busch, AV Biankin, and TJ Biden. Endoplasmic reticulum stress contributes to beta cell apoptosis in type 2 diabetes. *Diabetologia*, 50(4):752–63, 2007. Library Catalog: www.ncbi.nlm.nih.gov.

[148] Hanmin Lee, Robert A Cusick, Fiona Browne, Tae Ho Kim, Peter X Ma, Hirofumi Utsunomiya, Robert Langer, and Joseph P Vacanti. Local delivery of basic fibroblast growth factor increases both angiogenesis and engraftment of hepatocytes in tissue-engineered polymer devices1. *Transplantation*, 73(10):1589–1593, 2002.

[149] Jae Sung Lee, Sang Heon Kim, Young Jin Kim, Toshihiro Akaike, and Sung Chul Kim. Hepatocyte adhesion on a poly [n-p-vinylbenzyl-4-o-β-d-galactopyranosyl-d-glucoamide]-coated poly (l-lactic acid) surface. *Biomacromolecules*, 6(4):1906–1911, 2005.

[150] Kuen Yong Lee, Martin C Peters, Kenneth W Anderson, and David J Mooney. Controlled growth factor release from synthetic extracellular matrices. *Nature*, 408(6815):998–1000, 2000.

[151] Seung-A Lee, Edward Kang, Jongil Ju, Dong-Sik Kim, Sang-Hoon Lee, et al. Spheroid-based three-dimensional liver-on-a-chip to investigate hepatocyte–hepatic stellate cell interactions and flow effects. *Lab on a Chip*, 13(18):3529–3537, 2013.

[152] Cheri Y. Li, Kelly R. Stevens, Robert E. Schwartz, Brian S. Alejandro, Joanne H. Huang, and Sangeeta N. Bhatia. Micropatterned Cell–Cell Interactions Enable Functional Encapsulation of Primary Hepatocytes in Hydrogel Microtissues. *Tissue Engineering. Part A*, 20(15-16):2200–2212, August 2014.

[153] Cheri Y Li, David K Wood, Caroline M Hsu, and Sangeeta N Bhatia. Dna-templated assembly of droplet-derived peg microtissues. *Lab on a chip*, 11(17):2967–2975, 2011.

[154] Jieliang Li, Jilun Pan, Liguo Zhang, and Yaoting Yu. Culture of hepatocytes on fructose-modified chitosan scaffolds. *Biomaterials*, 24(13):2317–2322, 2003.

[155] Keguo Li, Yun Wang, Zhenchuan Miao, Dayong Xu, Yuefeng Tang, and Meifu Feng. Chitosan/gelatin composite microcarrier for hepatocyte culture. *Biotechnology letters*, 26(11):879–883, 2004.

[156] Chya-Yan Liaw, Shen Ji, and Murat Guvendiren. Engineering 3d hydrogels for personalized in vitro human tissue models. *Advanced healthcare materials*, 7(4):1701165, 2018.

[157] Christine Lin, Julianne Shi, Amanda Moore, and Salman R. Khetani. Prediction of Drug Clearance and Drug-Drug Interactions in Microscale Cultures of Human Hepatocytes. *Drug Metabolism and Disposition: The Biological Fate of Chemicals*, 44(1):127–136, January 2016.

[158] Ruei-Zeng Lin, Li-Fang Chou, Chi-Chen Michael Chien, and Hwan-You Chang. Dynamic analysis of hepatoma spheroid formation: roles of E-cadherin and β1-integrin. *Cell and Tissue Research*, 324:411–422, 2006.

[159] Ruei-Zhen Lin and Hwan-You Chang. Recent advances in three-dimensional multicellular spheroid culture for biomedical research. *Biotechnology Journal: Healthcare Nutrition Technology*, 3(9-10):1172–1184, 2008.

[160] Yi Lin and Zhongjie Sun. In Vivo Pancreatic beta-Cell–Specific Expression of Anti-aging Gene Klotho: A Novel Approach for Preserving beta-Cells in Type 2 Diabetes. *Diabetes*, 64(4):1444–1458, April 2015.

[161] Valerie A Liu and Sangeeta N Bhatia. Three-dimensional photopatterning of hydrogels containing living cells. *Biomedical microdevices*, 4(4):257–266, 2002.

[162] Yan Liu, Christoph Meyer, Chengfu Xu, Honglei Weng, Claus Hellerbrand, Peter ten Dijke, and Steven Dooley. Animal models of chronic liver diseases. *American Journal of Physiology-Gastrointestinal and Liver Physiology*, 304(5):G449–G468, 2013.

[163] Linda Lorenz, Jennifer Axnick, Tobias Buschmann, Carina Henning, Sofia Urner, Shentong Fang, Harri Nurmi, Nicole Eichhorst, Richard Holtmeier, Kalman Bodis, John-Hee Hwang, Karsten mussig, Daniel Eberhard, Jorg Sypmann, Oliver Kuss, Michael Roden, Kari Alitalo, Dieter Haussinger, and Eckhard Lammert. Mechanosensing by $\beta 1$ integrin induces angiocrine signals for liver growth and survival. *Nature*, 562:128–132, 2018.

[164] Jennifer L. Luebke-Wheeler, Geir Nedredal, Le Yee, Bruce P. Amiot, and Scott L. Nyberg. E-cadherin protects primary hepatocyte spheroids from cell death by a caspase-independent mechanism. *Cell Transplantation*, 18(12):1281–1287, 2009.

[165] Matthias P. Lutolf, Penney M. Gilbert, and Helen M. Blau. Designing materials to direct stem-cell fate. *Nature*, 462(7272):433–441, November 2009.

[166] Alistair J Makin. Acetaminophen-induced hepatotoxicity: predisposing factors and treatments. *Adv Intern Med*, 42:453–483, 1997.

[167] Michael Malinchoc, Patrick S Kamath, Fredric D Gordon, Craig J Peine, Jeffrey Rank, and Pieter CJ Ter Borg. A model to predict poor survival in patients undergoing transjugular intrahepatic portosystemic shunts. *Hepatology*, 31(4):864–871, 2000.

[168] Liliana Mancio-Silva, Heather E Fleming, Alex B Miller, Stuart Milstein, Abigail Liebow, Patrick Haslett, Laura Sepp-Lorenzino, and Sangeeta N Bhatia. Improving drug discovery by nucleic acid delivery in engineered human microlivers. *Cell Metabolism*, 29(3):727–735, 2019.

[169] Sandra March, Elliot E Hui, Gregory H Underhill, Salman Khetani, and Sangeeta N Bhatia. Microenvironmental regulation of the sinusoidal endothelial cell phenotype in vitro. *Hepatology*, 50(3):920–928, 2009.

[170] Sandra March, Vyas Ramanan, Kartik Trehan, Shengyong Ng, Ani Galstian, Nil Gural, Margaret A. Scull, Amir Shlomai, Maria Mota, Heather E. Fleming, Salman R. Khetani, Charles M. Rice, and Sangeeta N. Bhatia. Micropatterned coculture of primary human hepatocytes and supportive cells for the study of hepatotropic pathogens. *Nature protocols*, 10(12):2027–2053, December 2015.

[171] P. Marconi, M. Tamura, S. Moriuchi, D. M. Krisky, A. Niranjan, W. F. Goins, J. B. Cohen, and J. C. Glorioso. Connexin 43-enhanced suicide gene therapy using herpesviral vectors. *Molecular Therapy: The Journal of the American Society of Gene Therapy*, 1(1):71–81, January 2000.

[172] Virna Marin, Elisabetta Cribioli, Brian Philip, Sarah Tettamanti, Irene Pizzitola, Andrea Biondi, Ettore Biagi, and Martin Pule. Comparison of Different Suicide-Gene Strategies for the Safety Improvement of Genetically Manipulated T Cells, November 2012. Archive Location: 140 Huguenot Street, 3rd Floor New Rochelle, NY 10801 USA Library Catalog: www.liebertpub.com Publisher: Mary Ann Liebert, Inc. 140 Huguenot Street, 3rd Floor New Rochelle, NY 10801 USA.

[173] Maria J Martin, Alysson Muotri, Fred Gage, and Ajit Varki. Human embryonic stem cells express an immunogenic nonhuman sialic acid. *Nature Medicine*, 11(2):228–232, February 2005.

[174] Mikaël M. Martino, Priscilla S. Briquez, Adrian Ranga, Matthias P. Lutolf, and Jeffrey A. Hubbell. Heparin-binding domain of fibrin(ogen) binds growth factors and promotes tissue repair when incorporated within a synthetic matrix. *Proceedings of the National Academy of Sciences*, 110(12):4563–4568, March 2013. Publisher: National Academy of Sciences Section: Biological Sciences.

[175] Arthur J Matas, DE Sutherland, Michael W Steffes, S Michael Mauer, A Sowe, Richard L Simmons, and John S Najarian. Hepatocellular transplantation for metabolic deficiencies: decrease of plasms bilirubin in gunn rats. *Science*, 192(4242):892–894, 1976.

[176] J Mayer, E Karamuk, T Akaike, and E Wintermantel. Matrices for tissue engineering-scaffold structure for a bioartificial liver support system. *Journal of controlled release*, 64(1-3):81–90, 2000.

[177] Giuseppe Mazza, Krista Rombouts, Andrew Rennie Hall, Luca Urbani, Tu Vinh Luong, Walid Al-Akkad, Lisa Longato, David Brown, Panagiotis Maghsoudlou, Amar P Dhillon, et al. Decellularized human liver as a natural 3d-scaffold for liver bioengineering and transplantation. *Scientific reports*, 5(1):1–15, 2015.

[178] Marc Mesnil and Hiroshi Yamasaki. Bystander Effect in Herpes Simplex Virus-Thymidine Kinase/Ganciclovir Cancer Gene Therapy: Role of Gap-junctional Intercellular Communication1. *Cancer Research*, 60(15):3989–3999, August 2000. Publisher: American Association for Cancer Research Section: Review.

[179] HJ Metselaar, EJ Hesselink, S De Rave, FJW Ten Kate, JS Lameris, THN Groenland, CB Reuvers, W Weimar, OT Terpstra, and SW Schalm. Recovery of failing liver after auxiliary heterotopic transplantation. *The Lancet*, 335(8698):1156–1157, 1990.

[180] Jordan S Miller, Kelly R Stevens, Michael T Yang, Brendon M Baker, Duc-Huy T Nguyen, Daniel M Cohen, Esteban Toro, Alice A Chen, Peter A Galie, Xiang Yu, et al. Rapid casting of patterned vascular networks for perfusable engineered three-dimensional tissues. *Nature materials*, 11(9):768–774, 2012.

[181] Michio Mito and Mitsuo Kusano. Hepatocyte transplantation in man. *Cell transplantation*, 2(1):65–74, 1993.

[182] Mitsuo Miyazawa, Takahiro Torii, Yasuko Toshimitsu, Katsuya Okada, Isamu Koyama, and Yoshito Ikada. A tissue-engineered artificial bile duct grown to resemble the native bile duct. *American journal of transplantation*, 5(6):1541–1547, 2005.

[183] H. Mizuguchi, Z. Xu, A. Ishii-Watabe, E. Uchida, and T. Hayakawa. IRES-dependent second gene expression is significantly lower than cap-dependent first gene expression in a bicistronic vector. *Molecular Therapy: The Journal of the American Society of Gene Therapy*, 1(4):376–382, April 2000.

[184] Ali A Mokdad, Alan D Lopez, Saied Shahraz, Rafael Lozano, Ali H Mokdad, Jeff Stanaway, Christopher JL Murray, and Mohsen Naghavi. Liver cirrhosis mortality in 187 countries between 1980 and 2010: a systematic analysis. *BMC medicine*, 12(1):145, 2014.

[185] Roberto Montesano, Jean-Dominique Vassalli, A Baird, R Guillemin, and Lelio Orci. Basic fibroblast growth factor induces angiogenesis in vitro. *Proceedings of the National Academy of Sciences*, 83(19):7297–7301, 1986.

[186] Robert A Montgomery, Sommer E Gentry, William H Marks, Daniel S Warren, Janet Hiller, Julie Houp, Andrea A Zachary, J Keith Melancon, Warren R Maley, Hamid Rabb, et al. Domino paired kidney donation: a strategy to make best use of live non-directed donation. *The Lancet*, 368(9533):419–421, 2006.

[187] David J Mooney, Kaoru Sano, P Matthias Kaufmann, Karen Majahod, Betsy Schloo, Joseph P Vacanti, and Robert Langer. Long-term engraftment of hepatocytes transplanted on biodegradable polymer sponges. *Journal of Biomedical Materials Research: An Official Journal of The Society for Biomaterials and The Japanese Society for Biomaterials*, 37(3):413–420, 1997.

[188] DJ Mooney, S Park, PM Kaufmann, K Sano, K McNamara, JP Vacanti, and R Langer. Biodegradable sponges for hepatocyte transplantation. *Journal of biomedical materials research*, 29(8):959–965, 1995.

[189] Kristen T Morin and Robert T Tranquillo. In vitro models of angiogenesis and vasculogenesis in fibrin gel. *Experimental cell research*, 319(16):2409–2417, 2013.

[190] Keeley L Mui, Yong Ho Bae, Lin Gao, Shu-Lin Liu, Tina Xu, Glenn L Radice, Christopher S Chen, and Richard K Assoian. N-cadherin induction by ecm stiffness and fak overrides the spreading requirement for proliferation of vascular smooth muscle cells. *Cell Reports*, 10(9):1477–1486, 2015.

[191] Maurizio Muraca, Giorgio Gerunda, Daniele Neri, Maria-Teresa Vilei, Anna Granato, Paolo Feltracco, Muzio Meroni, Gianpiero Giron, and Alberto B Burlina. Hepatocyte transplantation as a treatment for glycogen storage disease type 1a. *The Lancet*, 359(9303):317–318, 2002.

[192] Menon KVN Murali AR. Acute Liver Failure.

[193] Sean V Murphy and Anthony Atala. 3d bioprinting of tissues and organs. *Nature biotechnology*, 32(8):773–785, 2014.

[194] Yoon Sung Nam, Joon Jin Yoon, Jae Gwan Lee, and Tae Gwan Park. Adhesion behaviours of hepatocytes cultured onto biodegradable polymer surface modified by alkali hydrolysis process. *Journal of Biomaterials Science, Polymer Edition*, 10(11):1145–1158, 1999.

[195] R M Namba, A A Cole, K B Bjudstad, and M J Mahoney. Development of porous peg hydrogels that enable efficient, uniform cell-seeding and permit early neural process extension. *Acta Biomateriala*, 5(6):1884–1897, 2009.

[196] National Data: Organ Procurement and Transplantation Network. National Data: Organ Procurement and Transplantation Network.

[197] Celeste M. Nelson and Mina J. Bissell. Modeling dynamic reciprocity: engineering three-dimensional culture models of breast architecture, function, and neoplastic transformation. *Seminars in Cancer Biology*, 15(5):342–352, October 2005.

[198] Dong Niu, Hong-Jiang Wei, Lin Lin, Haydy George, Tao Wang, I-Hsiu Lee, Hong-Ye Zhao, Yong Wang, Yinan Kan, Ellen Shrock, et al. Inactivation of porcine endogenous retrovirus in pigs using crispr-cas9. *Science*, 357(6357):1303–1307, 2017.

[199] M Oates, R Chen, M Duncan, and JA Hunt. The angiogenic potential of three-dimensional open porous synthetic matrix materials. *Biomaterials*, 28(25):3679–3686, 2007.

[200] Kohei Ogawa, Erin R Ochoa, Jeffrey Borenstein, Koichi Tanaka, and Joseph P Vacanti. The generation of functionally differentiated, three-dimensional hepatic tissue from two-dimensional sheets of progenitor small hepatocytes and nonparenchymal cells. *Transplantation*, 77(12):1783–1789, 2004.

[201] Satoshi Ogiso, Kentaro Yasuchika, Ken Fukumitsu, Takamichi Ishii, Hidenobu Kojima, Yuya Miyauchi, Ryoya Yamaoka, Junji Komori, Hokahiro Katayama, Takayuki Kawai, et al. Efficient recellularisation of decellularised whole-liver grafts using biliary tree and foetal hepatocytes. *Scientific reports*, 6:35887, 2016.

[202] Ogechi Ogoke, Janet Oluwole, and Natesh Parashurama. Bioengineering considerations in liver regenerative medicine. *Journal of Biological Engineering*, 11(1):46, 2017.

[203] J. G. O'Grady, S. W. Schalm, and R. Williams. Acute liver failure: redefining the syndromes. *Lancet (London, England)*, 342(8866):273–275, July 1993.

[204] Health Quality Ontario et al. Pancreas islet transplantation for patients with type 1 diabetes mellitus: a clinical evidence review. *Ontario health technology assessment series*, 15(16):1, 2015.

[205] Daniel Palmes and Hans-Ullrich Spiegel. Animal models of liver regeneration. *Biomaterials*, 25(9):1601–1611, 2004.

[206] Kyung Min Park and Sharon Gerecht. Hypoxia-inducible hydrogels. *Nature communications*, 5(1):1–12, 2014.

[207] Sunghee Estelle Park, Andrei Georgescu, and Dongeun Huh. Organoids-on-a-chip. *Science*, 364(6444):960–965, June 2019.

[208] Tae Gwan Park. Perfusion culture of hepatocytes within galactose-derivatized biodegradable poly (lactide-co-glycolide) scaffolds prepared by gas foaming of effervescent salts. *Journal of Biomedical Materials Research: An Official Journal of The Society for Biomaterials and The Japanese Society for Biomaterials*, 59(1):127–135, 2002.

[209] Weng Chuan Peng, Catriona Y Logan, Matt Fish, Teni Anbarchian, Francis Aguisanda, Adrián Álvarez-Varela, Peng Wu, Yinhua Jin, Junjie Zhu, Bin Li, et al. Inflammatory cytokine tnfα promotes the long-term expansion of primary hepatocytes in 3d culture. *Cell*, 175(6):1607–1619, 2018.

[210] NA Peppas, P Bures, WS Leobandung, and H Ichikawa. Hydrogels in pharmaceutical formulations. *European journal of pharmaceutics and biopharmaceutics*, 50(1):27–46, 2000.

[211] S Petronis, K-L Eckert, J Gold, and E Wintermantel. Microstructuring ceramic scaffolds for hepatocyte cell culture. *Journal of materials science: Materials in medicine*, 12(6):523–528, 2001.

[212] Gabriëlle G.M. Pinkse, Mathijs P. Voorhoeve, Mathieu Noteborn, Onno T Terpstra, Jan Anthonie Brujin, and Emilie De Heer. Hepatocyte survival depends on β1-integrin-mediated attachment of hepatocytes to hepatic extracellular matrix. *Liver International*, 24(3):218–226, 2004.

[213] K. P. Ponder, S. Gupta, F. Leland, G. Darlington, M. Finegold, J. DeMayo, F. D. Ledley, J. R. Chowdhury, and S. L. Woo. Mouse hepatocytes migrate to liver parenchyma and function indefinitely after intrasplenic transplantation. *Proceedings of the National Academy of Sciences*, 88(4):1217–1221, February 1991. Publisher: National Academy of Sciences Section: Research Article.

[214] Ivan K. H. Poon, Christopher D. Lucas, Adriano G. Rossi, and Kodi S. Ravichandran. Apoptotic cell clearance: basic biology and therapeutic potential. *Nature reviews. Immunology*, 14(3):166, March 2014. Publisher: NIH Public Access.

[215] V Racanelli and B Rehermann. The liver as an immunological organ. hepatology 43: S54–s62, 2006.

[216] Tony M Rahman and Humphrey J F Hodgson. Animal models of acute hepatic failure. *International Journal of Experimental Pathology*, 81:145–157, 2000.

[217] Colette S Ranucci, Ajay Kumar, Surendra P Batra, and Prabhas V Moghe. Control of hepatocyte function on collagen foams: sizing matrix pores toward selective induction of 2-d and 3-d cellular morphogenesis. *Biomaterials*, 21(8):783–793, 2000.

[218] Panduranga S Rao, Douglas E Schaubel, Mary K Guidinger, Kenneth A Andreoni, Robert A Wolfe, Robert M Merion, Friedrich K Port, and Randall S Sung. A comprehensive risk quantification score for deceased donor kidneys: the kidney donor risk index. *Transplantation*, 88(2):231–236, 2009.

[219] Alexander Revzin, Ryan J Russell, Vamsi K Yadavalli, Won-Gun Koh, Curt Deister, David D Hile, Michael B Mellott, and Michael V Pishko. Fabrication of poly (ethylene glycol) hydrogel microstructures using photolithography. *Langmuir*, 17(18):5440–5447, 2001.

[220] Jonathan A Rhim, Eric P Sandgren, Richard D Palmiter, and Ralph L Brinster. Complete reconstitution of mouse liver with xenogeneic hepatocytes. *Proceedings of the National Academy of Sciences*, 92(11):4942–4946, 1995.

[221] Thomas P Richardson, Martin C Peters, Alessandra B Ennett, and David J Mooney. Polymeric system for dual growth factor delivery. *Nature biotechnology*, 19(11):1029–1034, 2001.

[222] Laura Riolobos, Roli K Hirata, Cameron J Turtle, Pei-Rong Wang, German G Gornalusse, Maja Zavajlevski, Stanley R Riddell, and David W Russell. Hla engineering of human pluripotent stem cells. *Molecular Therapy*, 21(6):1232–1241, 2013.

[223] Fotios Sampaziotis, Miguel Cardoso De Brito, Pedro Madrigal, Alessandro Bertero, Kourosh Saeb-Parsy, Filipa AC Soares, Elisabeth Schrumpf, Espen Melum, Tom H Karlsen, J Andrew Bradley, et al. Cholangiocytes derived from human induced pluripotent stem cells for disease modeling and drug validation. *Nature biotechnology*, 33(8):845–852, 2015.

[224] Fotios Sampaziotis, Alexander W Justin, Olivia C Tysoe, Stephen Sawiak, Edmund M Godfrey, Sara S Upponi, Richard L Gieseck III, Miguel Cardoso De Brito, Natalie Lie Berntsen, María J Gómez-Vázquez, et al. Reconstruction of the mouse extrahepatic biliary tree using primary human extrahepatic cholangiocyte organoids. *Nature medicine*, 23(8):954, 2017.

[225] Arun J Sanyal, Naga Chalasani, Kris V Kowdley, Arthur McCullough, Anna Mae Diehl, Nathan M Bass, Brent A Neuschwander-Tetri, Joel E Lavine, James Tonascia, Aynur Unalp, et al. Pioglitazone, vitamin e, or placebo for nonalcoholic steatohepatitis. *New England Journal of Medicine*, 362(18):1675–1685, 2010.

[226] Igor M Sauer and Joerg C Gerlach. Modular extracorporeal liver support. *Artificial organs*, 26(8):703–706, 2002.

[227] Arnout G. Schepers, Hugo J. Snippert, Daniel E. Stange, Maaike van den Born, Johan H. van Es, Marc van de Wetering, and Hans Clevers. Lineage Tracing Reveals Lgr5+ Stem Cell Activity in Mouse Intestinal Adenomas. *Science*, 337(6095):730–735, August 2012.

[228] Johannes Schindelin, Ignacio Arganda-Carreras, Erwin Frise, Verena Kaynig, Mark Longair, Tobias Pietzsch, Stephan Preibisch, Curtis Rueden, Stephan Saalfeld, Benjamin Schmid, Jean-Yves Tinevez, Daniel James White, Volker Hartenstein, Kevin Eliceiri, Pavel Tomancak, and Albert Cardona. Fiji: an open-source platform for biological-image analysis. *Nature Methods*, 9(7):676–682, July 2012.

[229] Henk-Jan Schuurman. Regulatory aspects of clinical xenotransplantation. *International Journey of Surgery*, 23(B):312–321, 2015.

[230] RE Schwartz, HE Fleming, SR Khetani, and SN Bhatia. Pluripotent stem cell-derived hepatocyte-like cells. *Biotechnology advances*, 32(2):504–513, 2014.

[231] Per O Seglen. Preparation of isolated rat liver cells. *Methods in cell biology*, 13:29–83, 1976.

[232] Carlos E Semino, Joshua R Merok, Gracy G Crane, Georgia Panagiotakos, and Shuguang Zhang. Functional differentiation of hepatocyte-like spheroid structures from putative liver progenitor cells in three-dimensional peptide scaffolds. *Differentiation: REVIEW*, 71(4-5):262–270, 2003.

[233] Jing Shan, David J. Logan, David E. Root, Anne E. Carpenter, and Sangeeta N. Bhatia. High-Throughput Platform for Identifying Molecular Factors Involved in Phenotypic Stabilization of Primary Human Hepatocytes In Vitro. *Journal of Biomolecular Screening*, 21(9):897–911, October 2016.

[234] Jing Shan, Robert E. Schwartz, Nathan T. Ross, David J. Logan, David Thomas, Stephen A. Duncan, Trista E. North, Wolfram Goessling, Anne E. Carpenter, and Sangeeta N. Bhatia. Identification of small molecules for human hepatocyte expansion and iPS differentiation. *Nature Chemical Biology*, 9(8):514–520, August 2013.

[235] Keyue Shen, Samantha Luk, Jessica Elman, Ryan Murray, Shilpaa Mukundan, and Biju Parekkadan. Suicide Gene-Engineered Stromal Cells Reveal a Dynamic Regulation of Cancer Metastasis. *Scientific Reports*, 6:21239, February 2016.

[236] Leonard D Shultz, Bonnie L Lyons, Lisa M Burzenski, Bruce Gott, Xiaohua Chen, Stanely Chaleff, Malak Kotb, Stephen D Gillies, Marie King, Julie Mangada, Dale L Greiner, and Rupert Handgretinger. Human lymphoid and myeloid cell development in nod/ltsz-scid il2r gamma null mice engrafted with mobilized human hemopoietic stem cells. *Journal of Immunology*, 174(10):6477–489, 2005.

[237] Karim Si-Tayeb, Fallon K Noto, Masato Nagaoka, Jixuan Li, Michele A Battle, Christine Duris, Paula E North, Stephen Dalton, and Stephen A Duncan. Highly efficient generation of human hepatocyte–like cells from induced pluripotent stem cells. *Hepatology*, 51(1):297–305, 2010.

[238] Aleksander Skardal, Sean V Murphy, Mahesh Devarasetty, Ivy Mead, Hyun-Wook Kang, Young-Joon Seol, Yu Shrike Zhang, Su-Ryon Shin, Liang Zhao, Julio Aleman, et al. Multi-tissue interactions in an integrated three-tissue organ-on-a-chip platform. *Scientific reports*, 7(1):1–16, 2017.

[239] Mark A. Skylar-Scott, Sebastien G. M. Uzel, Lucy L. Nam, John H. Ahrens, Ryan L. Truby, Sarita Damaraju, and Jennifer A. Lewis. Biomanufacturing of organ-specific tissues with high cellular density and embedded vascular channels. *Science Advances*, 5(9):eaaw2459, September 2019. Publisher: American Association for the Advancement of Science Section: Research Article.

[240] Jonathan P Sleeman and Wilko Thiele. Tumor metastasis and the lymphatic vasculature. *International Journal of Cancer*, 125(12):2747–2756, 2009.

[241] Molly K Smith, Martin C Peters, Thomas P Richardson, Jessica C Garbern, and David J Mooney. Locally enhanced angiogenesis promotes transplanted cell survival. *Tissue engineering*, 10(1-2):63–71, 2004.

[242] Quinton Smith and Sharon Gerecht. Going with the flow: microfluidic platforms in vascular tissue engineering. *Current opinion in chemical engineering*, 3:42–50, 2014.

[243] Efienne M Sokal. Liver transplantation for inborn errors of liver metabolism. *Journal of inherited metabolic disease*, 29(2-3):426, 2006.

[244] Etienne M Sokal, Françoise Smets, Annick Bourgois, Lionel Van Maldergem, Jean-Paul Buts, Raymond Reding, Jean Bernard Otte, Veerle Evrard, Dominique Latinne, Marie Françoise Vincent, et al. Hepatocyte transplantation in a 4-year-old girl with

peroxisomal biogenesis disease: Technique, safety, and metabolic follow-up1. *Transplantation*, 76(4):735–738, 2003.

[245] H.H. Greco Song, Rowza T Rumma, C. Keith Ozaki, Elazar R Edelman, and Christopher S. Chen. Vascular Tissue Engineering: Progress, Challenges, and Clinical Promise. *Cell Stem Cell*, 22:340–354, 2018.

[246] Hyun-Ho Greco Song, Alex Lammers, Subramanian Sundaram, Logan Rubio, Amanda X Chen, Linqing Li, Jeroen Eyckmans, Sangeeta N Bhatia, and Christopher S Chen. Transient support from fibroblasts is sufficient to drive functional vascularization in engineered tissues. *Advanced Functional Materials*, page 2003777, 2020.

[247] Kwang Hoon Song, Christopher B Highley, Andrew Rouff, and Jason A Burdick. Complex 3d-printed microchannels within cell-degradable hydrogels. *Advanced Functional Materials*, 28(31):1801331, 2018.

[248] Zhihua Song, Jun Cai, Yanxia Liu, Dongxin Zhao, Jun Yong, Shuguang Duo, Xijun Song, Yushan Guo, Yang Zhao, Han Qin, et al. Efficient generation of hepatocyte-like cells from human induced pluripotent stem cells. *Cell research*, 19(11):1233–1242, 2009.

[249] Alejandro Soto-Gutierrez, Li Zhang, Chris Medberry, Ken Fukumitsu, Denver Faulk, Hongbin Jiang, Janet Reing, Roberto Gramignoli, Junji Komori, Mark Ross, et al. A whole-organ regenerative medicine approach for liver replacement. *Tissue Engineering Part C: Methods*, 17(6):677–686, 2011.

[250] Thomas R Spitzer, Megan Sykes, Nina Tolkoff-Rubin, Tatsuo Kawai, Steven L McAfee, Bimalangshu R Dey, Karen Ballen, Francis Delmonico, Susan Saidman, David H Sachs, et al. Long-term follow-up of recipients of combined human leukocyte antigen-matched bone marrow and kidney transplantation for multiple myeloma with end-stage renal disease. *Transplantation*, 91(6):672, 2011.

[251] Caroline J Springer, Ion Niculescu-Duvaz, et al. Prodrug-activating systems in suicide gene therapy. *The Journal of clinical investigation*, 105(9):1161–1167, 2000.

[252] Ben Z Stanger and Linda Greenbaum. The role of paracrine signals during liver regeneration. *Hepatology*, 56(4):1577–1579, 2012.

[253] Thomas E Starzl, Carl G Groth, Lawrence Brettschneider, Israel Penn, Vincent A Fulginiti, John B Moon, Herve Blanchard, Alfred J Martin Jr, and Ken A Porter. Orthotopic homotransplantation of the human liver. *Annals of surgery*, 168(3):392, 1968.

[254] Thomas Earl STARZL, TL Marchioro, KN Von Kaulla, G Hermann, RS Brittain, and WR Waddell. Homotransplantation of the liver in humans. *Surgery, gynecology & obstetrics*, 117:659, 1963.

[255] Kelly R Stevens, Jordan S Miller, Brandon L Blakely, Christopher S Chen, and Sangeeta N Bhatia. Degradable hydrogels derived from peg-diacrylamide for hepatic tissue engineering. *Journal of Biomedical Materials Research Part A*, 103(10):3331–3338, 2015.

[256] Kelly R. Stevens, Margaret A. Scull, Vyas Ramanan, Chelsea L. Fortin, Ritika R. Chaturvedi, Kristin A. Knouse, Jing W. Xiao, Canny Fung, Teodelinda Mirabella, Amanda X. Chen, Margaret G. McCue, Michael T. Yang, Heather E. Fleming, Kwanghun Chung, Ype P. de Jong, Christopher S. Chen, Charles M. Rice, and Sangeeta N. Bhatia. In situ expansion of engineered human liver tissue in a mouse model of chronic liver disease. *Science Translational Medicine*, 9(399):eaah5505, July 2017.

[257] KR Stevens, MD Ungrin, RE Schwartz, S Ng, B Carvalho, KS Christine, RR Chaturvedi, CY Li, PW Zandstra, CS Chen, and SN Bhatia. InVERT molding for scalable control of tissue microarchitecture. *Nature communications*, 4:1847, 2013.

[258] Karin C. Straathof, Martin A. Pulè, Patricia Yotnda, Gianpietro Dotti, Elio F. Vanin, Malcolm K. Brenner, Helen E. Heslop, David M. Spencer, and Cliona M. Rooney. An inducible caspase 9 safety switch for T-cell therapy. *Blood*, 105(11):4247–4254, June 2005.

[259] Amber N Stratman and George E Davis. Endothelial cell-pericyte interactions stimulate basement membrane matrix assembly: influence on vascular tube remodeling, maturation and stabilization. *Microscopy and microanalysis: the official journal of Microscopy Society of America, Microbeam Analysis Society, Microscopical Society of Canada*, 18(1):68, 2012.

[260] Ryo Sudo, Toshihiro Mitaka, Mariko Ikeda, and Kazuo Tanishita. Reconstruction of 3d stacked-up structures by rat small hepatocytes on microporous membranes. *The FASEB journal*, 19(12):1695–1697, 2005.

[261] E Sun, Y Gao, J Chen, X Wang, Z Chen, and Y Shi. Allograft tolerance induced by donor apoptotic lymphocytes requires phagocytosis in the recipient. *Cell Death and Differentiation*, 11:1258–1264, 2004.

[262] DE Sutherland, M Numata, AJ Matas, RL Simmons, and JS Najarian. Hepatocellular transplantation in acute liver failure. *Surgery*, 82(1):124–132, 1977.

[263] Brandon Swift*, Nathan D Pfeifer*, and Kim LR Brouwer. Sandwich-cultured hepatocytes: an in vitro model to evaluate hepatobiliary transporter-based drug interactions and hepatotoxicity. *Drug metabolism reviews*, 42(3):446–471, 2010.

[264] Kazutoshi Takahashi and Shinya Yamanaka. Induction of pluripotent stem cells from mouse embryonic and adult fibroblast cultures by defined factors. *cell*, 126(4):663–676, 2006.

[265] Takanori Takebe, Naoto Koike, Keisuke Sekine, Ryoji Fujiwara, Takeru Amiya, Yun-Wen Zheng, and Hideki Taniguchi. Engineering of human hepatic tissue with functional vascular networks. *Organogenesis*, 10(2):260–267, 2014.

[266] Takanori Takebe, Keisuke Sekine, Masahiro Enomura, Hiroyuki Koike, Masaki Kimura, Takunori Ogaeri, Ran-Ran Zhang, Yasuharu Ueno, Yun-Wen Zheng, Naoto Koike, Shinsuke Aoyama, Yasuhisa Adachi, and Hideki Taniguchi. Vascularized and functional human liver from an iPSC-derived organ bud transplant. *Nature*, 499(7459):481–484, July 2013. Number: 7459 Publisher: Nature Publishing Group.

[267] Takanori Takebe, Keisuke Sekine, Masaki Kimura, Emi Yoshizawa, Satoru Ayano, Masaru Koido, Shizuka Funayama, Noriko Nakanishi, Tomoko Hisai, Tatsuya Kobayashi, et al. Massive and reproducible production of liver buds entirely from human pluripotent stem cells. *Cell reports*, 21(10):2661–2670, 2017.

[268] Takanori Takebe and James M. Wells. Organoids by design. *Science*, 364(6444):956–959, June 2019.

[269] Antson Kiat Yee Tan, Kyle M Loh, and Lay Teng Ang. Evaluating the regenerative potential and functionality of human liver cells in mice. *Differentiation*, 98:25–34, 2017.

[270] Wei Tan and Tejal A Desai. Microfluidic patterning of cells in extracellular matrix biopolymers: effects of channel size, cell type, and matrix composition on pattern integrity. *Tissue engineering*, 9(2):255–267, 2003.

[271] Wei Tan and Tejal A Desai. Layer-by-layer microfluidics for biomimetic three-dimensional structures. *Biomaterials*, 25(7-8):1355–1364, 2004.

[272] Xu Tao, Li Shaolin, and Yu Yaoting. Preparation and culture of hepatocyte on gelatin microcarriers. *Journal of Biomedical Materials Research Part A: An Official Journal of The Society for Biomaterials, The Japanese Society for Biomaterials, and The Australian Society for Biomaterials and the Korean Society for Biomaterials*, 65(2):306–310, 2003.

[273] Daniel A Tatosian and Michael L Shuler. A novel system for evaluation of drug mixtures for potential efficacy in treating multidrug resistant cancers. *Biotechnology and bioengineering*, 103(1):187–198, 2009.

[274] A Joseph Tector, Richard S Mangus, Paul Chestovich, Rodrigo Vianna, Jonathan A Fridell, Martin L Milgrom, Carrie Sanders, and Paul Y Kwo. Use of extended criteria livers decreases wait time for liver transplantation without adversely impacting posttransplant survival. *Annals of surgery*, 244(3):439, 2006.

[275] Michael D Thompson and Satdarshan P S Monga. Wnt/beta-catenin signaling in liver health and disease. *Hepatology*, 45(5):1298–12305, 2007.

[276] Mark W. Tibbitt and Kristi S. Anseth. Hydrogels as extracellular matrix mimics for 3D cell culture. *Biotechnology and Bioengineering*, 103(4):655–663, 2009.

[277] Indira Tirado-Hurtado, Williams Fajardo, and Joseph A. Pinto. DNA Damage Inducible Transcript 4 Gene: The Switch of the Metabolism as Potential Target in Cancer. *Frontiers in Oncology*, 8, 2018. Publisher: Frontiers.

[278] Michael E Todhunter, Noel Y Jee, Alex J Hughes, Maxwell C Coyle, Alec Cerchiari, Justin Farlow, James C Garbe, Mark A LaBarge, Tejal A Desai, and Zev J Gartner. Programmed synthesis of 3D tissues. *Nature methods*, 12(10):975–981, October 2015.

[279] Hiroki Torikai, Andreas Reik, Frank Soldner, Edus H Warren, Carrie Yuen, Yuanyue Zhou, Denise L Crossland, Helen Huls, Nicholas Littman, Ziying Zhang, et al. Toward eliminating hla class i expression to generate universal cells from allogeneic donors. *Blood*, 122(8):1341–1349, 2013.

[280] Ryan L Truby and Jennifer A Lewis. Printing soft matter in three dimensions. *Nature*, 540(7633):371–378, 2016.

[281] Valerie Liu Tsang and Sangeeta N Bhatia. Three-dimensional tissue fabrication. *Advanced drug delivery reviews*, 56(11):1635–1647, 2004.

[282] Valerie Liu Tsang, Alice A Chen, Lisa M Cho, Kyle D Jadin, Robert L Sah, Solitaire DeLong, Jennifer L West, and Sangeeta N Bhatia. Fabrication of 3d hepatic tissues by additive photopatterning of cellular hydrogels. *The FASEB journal*, 21(3):790–801, 2007.

[283] Yosuke Tsuruga, Tohru Kiyono, Michiaki Matsushita, Tohru Takahashi, Hironori Kasai, and Satoru Todo. Establishment of immortalized human hepatocytes by introduction of hpv16 e6/e7 and htert as cell sources for liver cell-based therapy. *Cell transplantation*, 17(9):1083–1094, 2008.

[284] David Tuveson and Hans Clevers. Cancer modeling meets human organoid technology. *Science*, 364(6444):952–955, June 2019.

[285] C Udawatte and H Ripps. The spread of apoptosis through gap-junctional channels in BHK cells transfected with Cx32. *Apoptosis*, 10(5):1019–29, 2005.

[286] Okechukwu Ukairo, Chitra Kanchagar, Amanda Moore, Julianne Shi, Jeannemarie Gaffney, Simon Aoyama, Kelly Rose, Stacy Krzyzewski, Jack McGeehan, Melvin E. Andersen, Salman R. Khetani, and Edward L. Lecluyse. Long-term stability of primary rat hepatocytes in micropatterned cocultures. *Journal of Biochemical and Molecular Toxicology*, 27(3):204–212, March 2013.

[287] Gregory H. Underhill, Alice A. Chen, Dirk R. Albrecht, and Sangeeta N. Bhatia. Assessment of hepatocellular function within PEG hydrogels. *Biomaterials*, 28(2):256–270, January 2007.

[288] Basak E Uygun, Alejandro Soto-Gutierrez, Hiroshi Yagi, Maria-Louisa Izamis, Maria A Guzzardi, Carley Shulman, Jack Milwid, Naoya Kobayashi, Arno Tilles, Francois Berthiaume, et al. Organ reengineering through development of a transplantable recellularized liver graft using decellularized liver matrix. *Nature medicine*, 16(7):814–820, 2010.

[289] Joseph P Vacanti and Robert Langer. Tissue engineering: the design and fabrication of living replacement devices for surgical reconstruction and transplantation. *The lancet*, 354:S32–S34, 1999.

[290] M-P Van De Kerkhove, E Di Florio, V Scuderi, A Mancini, A Belli, A Bracco, M Dauri, G Tisone, G Di Nicuolo, P Amoroso, et al. Phase i clinical trial with the amc-bioartificial liver. *The International journal of artificial organs*, 25(10):950–959, 2002.

[291] Kwanchanok Viravaidya, Aaron Sin, and Michael L Shuler. Development of a microscale cell culture analog to probe naphthalene toxicity. *Biotechnology progress*, 20(1):316–323, 2004.

[292] Giovanni Vozzi, Christopher Flaim, Arti Ahluwalia, and Sangeeta Bhatia. Fabrication of plga scaffolds using soft lithography and microsyringe deposition. *Biomaterials*, 24(14):2533–2540, 2003.

[293] Kewei Wang and Bingliang Lin. Pathophysiological Significance of Hepatic Apoptosis, 2013.

[294] Xiaohong Wang, Yongnian Yan, Yuqiong Pan, Zhuo Xiong, Haixia Liu, Jie Cheng, Feng Liu, Feng Lin, Rendong Wu, Renji Zhang, et al. Generation of three-dimensional hepatocyte/gelatin structures with rapid prototyping system. *Tissue engineering*, 12(1):83–90, 2006.

[295] Valerie M. Weaver, Sophie Lelièvre, Johnathon N. Lakins, Micah A. Chrenek, Jonathan C.R. Jones, Filippo Giancotti, Zena Werb, and Mina J. Bissell. $\beta 4$ integrin-dependent formation of polarized three-dimensional architecture confers resistance to apoptosis in normal and malignant mammary epithelium. *Cancer cell*, 2(3):205–216, September 2002.

[296] Rebecca G Wells. Cellular sources of extracellular matrix in hepatic fibrosis. *Clinics in liver disease*, 12(4):759–768, 2008.

[297] Long-Ping Wen, Jimothy A. Fahrni, Sergiu Troie, Jun-Lin Guan, Kim Orth, and Glenn D. Rosen. Cleavage of Focal Adhesion Kinase by Caspases during Apoptosis. *Journal of Biological Chemistry*, 14(272):26056–26061, 1997.

[298] Russell H Wiesner. Patient selection in an era of donor liver shortage: current us policy. *Nature Clinical Practice Gastroenterology & Hepatology*, 2(1):24–30, 2005.

[299] Shigeki Yagyu, Valentina Hoyos, Francesca Del Bufalo, and Malcolm K Brenner. An Inducible Caspase-9 Suicide Gene to Improve the Safety of Therapy Using Human Induced Pluripotent Stem Cells. *Molecular Therapy*, 23(9):1475–1485, September 2015.

[300] Tsung Hua Yang, Hirotoshi Miyoshi, and Norio Ohshima. Novel cell immobilization method utilizing centrifugal force to achieve high-density hepatocyte culture in porous scaffold. *Journal of Biomedical Materials Research: An Official Journal of The Society for Biomaterials, The Japanese Society for Biomaterials, and The Australian Society for Biomaterials and the Korean Society for Biomaterials*, 55(3):379–386, 2001.

[301] Changqing Yi, Cheuk-Wing Li, Shenglin Ji, and Mengsu Yang. Microfluidics technology for manipulation and analysis of biological cells. *Analytica Chimica Acta*, 560(1):1–23, February 2006.

[302] Dean Yimlamia, Constantina Christodoulou, Giorgio G Galli, Kilangsungla Yanger, Brian Pepe-Mooney, Basanta Burugn, Kriti Shrestha, Patrick Cahan, Ben Z Stanger, and Fernando D Camargo. Hippo pathway activity influences liver cell fate. *Cell*, 157(6):1324–1338, 2014.

[303] Jianli Yin, Linfeng Yang, Lisha Mou, Kaili Dong, Jian Jiang, Shuai Xue, Ying Xu, Xinyi Wang, Ying Lu, and Haifeng Ye. A green tea–triggered genetic control system for treating diabetes in mice and monkeys. *Science translational medicine*, 11(515), 2019.

[304] Zobair M Younossi, Rohit Loomba, Mary E Rinella, Elisabetta Bugianesi, Giulio Marchesini, Brent A Neuschwander-Tetri, Lawrence Serfaty, Francesco Negro, Stephen H Caldwell, Vlad Ratziu, et al. Current and future therapeutic regimens

for nonalcoholic fatty liver disease and nonalcoholic steatohepatitis. *Hepatology*, 68(1):361–371, 2018.

[305] Chie Yuasa, Yumiko Tomita, Masayuki Shono, Kazunori Ishimura, and Akira Ichihara. Importance of cell aggregation for expression of liver functions and regeneration demonstrated with primary cultured hepatocytes. *Journal of cellular physiology*, 156(3):522–530, 1993.

[306] Ali Zarrinpar and Ronald W Busuttil. Liver transplantation: past, present and future. *Nature reviews Gastroenterology & hepatology*, 10(7):434, 2013.

[307] Qing Zhou, Dipali Patel, Timothy Kwa, Amranul Haque, Zimple Matharu, Gulnaz Stybayeva, Yandong Gao, Anna Mae Diehl, and Alexander Revzin. Liver injury-on-a-chip: microfluidic co-cultures with integrated biosensors for monitoring liver cell signaling during injury. *Lab on a Chip*, 15(23):4467–4478, 2015.

[308] Saiyong Zhu, Milad Rezvani, Jack Harbell, Aras N Mattis, Alan R Wolfe, Leslie Z Benet, Holger Willenbring, and Sheng Ding. Mouse liver repopulation with hepatocytes generated from human fibroblasts. *Nature*, 508(7494):93–97, 2014.